University of Southern Queensland

Faculty of Health, Engineering, and Sciences

Investigation into the Effect of Bonding Methods for 3D Printed Titanium in Scarf Ribbon Repairs with a Composite Parent

A dissertation submitted by

Nicholas Thomas Wall

In fulfilment of the requirements of

ENG4111 and ENG4112 Research Project

Towards the degree of

Bachelor of Engineering (Honours) – Mechanical

Submitted October 2020

Abstract

As material technology has continued improving, creating materials that are lighter, stronger, and more resistant to environmental conditions, their prevalence in all industries has also increased. This is no truer than in aviation which has gradually transitioned to polymer composites in order to minimise weight and consequently create some of the most advance transportation and weapons systems ever seen. The use of these materials is not without drawbacks, these mainly being cost, and the complex nature of failure and subsequent repair required. Because of these major factors, research into repair methods has come to the forefront of the industry with emphasis placed on the minimisation of costs associated with the repair processes as well as down-time experienced by the aircraft. The most dominant method used in such repair methods are scarf repair joints which are prepared in an autoclave system. In order to explore more portable and fast paced solutions, out-of-autoclave processes have become the main focus of repair techniques for research. The aim of this study was to identify associated effects and subsequent quality of bond created using the single vacuum bag debulking variant of out-of-autoclave processes utilising a set of basic testing criteria and comparable data taken from the literature.

Using appropriate sample preparation techniques, cure cycle selection and pre-experiment inspection, initial bond quality predictions were established based on visible porosity content and bond line observations. It was observed that cure cycle selection was definitively adequate for the double adhesive thickness samples while the results provide no clear indication of the adequacy for single adhesive samples. The double film adhesive honeycomb lattice scarf performed to the highest standard mechanically producing tensile strengths of 161.8 +/- 15.0 MPa, however displayed high levels of porosity (between 3% - 4%) which is not conducive to bond consolidation. Upon comparison to double vacuum bag debulking techniques, evidence suggested the quality of bond produced by the SVD system was of lower quality with regard to both porosity and resulting failure strength. The final observation was the thermal effect on the failure behaviour evident in the DIC videos taken of the failure event. These observations suggested evidence of a discontinuity caused by a mismatch in thermal properties of the materials.

Further studies into the reduction of porosity utilising DVD systems for dissimilar materials is required in order to establish a clear trend between porosity and resulting repair strength. An investigation into the catering of cure cycle for specific adhesive thicknesses as well as further mechanical testing would benefit the development of repair procedures specifically utilising SVD systems and offer insight into their suitability within the wider industry.

Limitations of Use

University of Southern Queensland

Faculty of Health, Engineering and Sciences

ENG4111/ENG4112 Research Project

The Council of the University of Southern Queensland, its Faculty of Health, Engineering & Sciences, and the staff of the University of Southern Queensland, do not accept any responsibility for the truth, accuracy or completeness of material contained within or associated with this dissertation.

Persons using all or any part of this material do so at their own risk, and not at the risk of the Council of the University of Southern Queensland, its Faculty of Health, Engineering & Sciences or the staff of the University of Southern Queensland.

This dissertation reports an educational exercise and has no purpose or validity beyond this exercise. The sole purpose of the course pair entitled "Research Project" is to contribute to the overall education within the student's chosen degree program. This document, the associated hardware, software, drawings, and other material set out in the associated appendices should not be used for any other purpose: if they are so used, it is entirely at the risk of the user.

Limitations of Use

Certification of Dissertation

University of Southern Queensland

Faculty of Health, Engineering and Sciences

ENG4111/ENG4112 Research Project

I certify that the ideas, designs and experimental work, results, analyses, and conclusions set out in this dissertation are entirely my own effort, except where otherwise indicated and acknowledged.

I further certify that the work is original and has not been previously submitted for assessment in any other course or institution, except where specifically stated.

Nicholas Thomas Wall

Sign: _____

15/10/2020

Acknowledgements

Table of Contents

List of Figures

List of Tables

1.   Introduction

1.1   Chapter Overview

This chapter will investigate and convey the current climate in aerospace repair technology and material applications within the industry. It will also initiate the concepts that will be developed in this project which aim to provide further recommendations on the reparative process of composite aircraft. The following research will provide context for the project by mapping appropriate aims and contextual information to support.

1.2   Research Background

Aircraft safety protocols and maintenance procedures are recognised as among the strictest of any industry globally. Because of these stringent guidelines, the cost of aircraft maintenance as well as repair times can be extremely high in the order of $3.1 million per aircraft with time periods of up to 4-6 months (IATA, 2014). These increased effects are rarely controlled by the maintenance team or the parent companies responsible for aircraft assets and instead are often controlled by contractors responsible for manufacturing spare/replacement components or by governing safety authorities. The monopoly held over this industry is rightfully held with the intent to ensure repairs conducted on aircraft are both legal and approved by safety authorities. This will almost always require the damaged components to be sent away for replacement or strict repair processes. This ensures the aircraft remains structurally sound and functionally safe for use. Unfortunately, this process causes increased downtime of the aircraft which also incurs an additional type of cost.

As stated by Li et al. (2017, pg 365) critical components used in aerospace applications are often required to be made of high strength steels and titanium alloys due to the dynamic nature of their operational life. This can directly influence their price for replacements and initial manufacture. A secondary result of the properties is their reduced critical crack size. Because of the unique characteristics (including failure characteristics) strict safety guidelines have been implemented to ensure the safe and enduring operation of these components. Often this will result in a part being replaced instead of manufactured due to the difficulty surrounding their repair.

As material technology has progressively developed, research results have produced improvements on existing substances discovering methods to make them lighter with more desirable mechanical properties. This has become an integral component of repair solutions in many industries.

A need was simultaneously identified and addressed as these refined materials became more prevalent in the aerospace sector, specifically the introduction of carbon fiber reinforced polymers (CFRP) as well as the existing prospect for natural fiber reinforced polymer composites. The increased tensile strength and shear strength (with the correct fibre orientation), and desirable physical properties provided by CFRPs enhanced the overall reliability and effectiveness of the parent system. This, in turn, extended the life span of components while also making the avenue for repair or replacement quicker due to the high precision manufacturing (Bhagwat et al. 2016).

Despite technological advances, increases in industry demand for profitability has influenced the need for decreased cost and downtime resulting in the conduct of research attempting to repair aircraft components 'in house'. This process change aims to eliminate the time hungry aspects of the current repair process. This will be targeted by opening avenues which would simplify the manufacture bonding process of repair patches used in such repairs as laps and scarf joints.
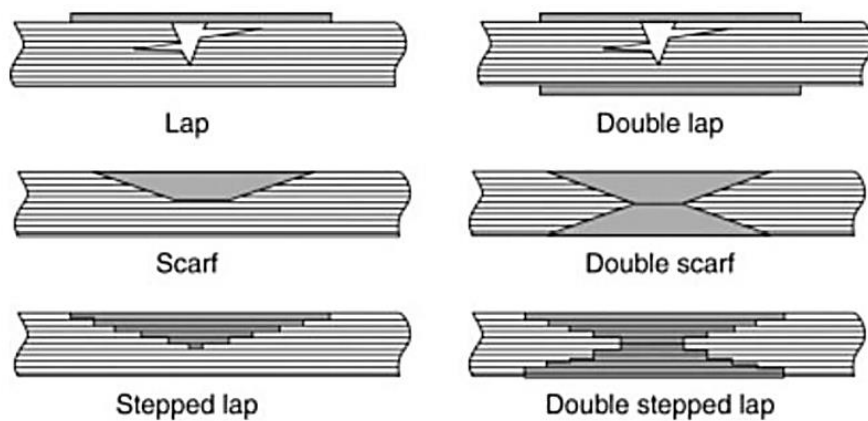
Figure 1: Scarf and Lap repair diagrams. (Fischer and Kracht, 2012)

When traditional repair materials are compared to new emerging material technology, clear benefits are highlighted by the research however, there are some draw backs to the advancements shown in this field, specifically surrounding out of autoclave processes. Some of these draw backs are not yet understood fully, and it is these points that this project will attempt to address. This specific investigation surrounds damage surface preparation and bonding techniques between additive manufactured components and composite parent structures. This will be explored throughout the following literature review.

1.3   Project Aim

The aim of this project was to assess the influence/effectiveness of vac bag only out of autoclave (OOA) processes of 3D printed titanium in scarf ribbon aircraft repairs. The scope is limited to assessing the quality of a cured film adhesive compared to a similar standard of results of an adhesive paste. Both scenarios investigate the bonding of a 3D printed titanium 'patch' to a specific composite parent component.

1.4   Project Objectives

To appropriately address the project aim, a set of objectives will be used to ensure the accuracy and relevancy of this dissertation is maintained. These objectives are listed below and are closely related to those found in Appendix A.

1. Conduct an appropriate review of existing literature surrounding adhesive methods and properties of 3D printed titanium in order to develop a sound foundational knowledge.

2. Identify properties to be evaluated which will shape both the inspection techniques and the design of the overall experiment including governing parameters.

3. Using a combination of guidance from the project supervisor and a review of previous research, assess project methodologies to maintain effective sample manufacture and assessments.

4. Using the identified available facilities; produce sample specimens demonstrating correct surface preparation and adhesion processes.

5. Demonstrate effective use of testing facilities producing consistent results. Determine the relationship between results, sample preparation (including adhesive method) and common defects identified for the given adhesive method.

6. Qualitatively analyse and dissect the results of the project including a discussion regarding the accuracy and validity within the current climate of autoclave technology.

Additional Research Scope (time permitting):

7. Compare and contrast results with previously conducted projects in the same area of study and offer a logical progression/recommendation on further studies to be conducted on composite scarf ribbon repairs.

8. Conduct testing using an alternate method of data collection. Specifically, the addition of an embedded sensor in the adhesive layer for more accurate and insightful results.

1.5   Chapter Summary

As identified in the subject of material technology, specifically surrounding the out of autoclave process, there is potential large-scale application within a broad array of industries. The most notable of these being the aviation industry. As these processes are relatively new and have not been fully or functionally tested there are grey areas in current industry knowledge which need to be addressed in order to make them viable options for use within the industry. This will result in a further increase in cost and time saving methods. This project will offer insight into the out of autoclave process. Specifically, the application of composite scarf ribbon repair using additive manufacturing (3D printed titanium). The results intend to inform of the quality and validity of the use of such a process in comparison to traditional autoclave repairs.

2. Literature Review

2.1 Chapter Overview

This chapter will identify and highlight the current processes and knowledge gaps surrounding material technology research in the field of out of autoclave methods. This research will then form the basis of the governing variables moving into the experimental component of the project. In order to achieve this a logical sequence of topics will be researched. This will start with the review of CFRPs, scarf repair techniques, and out of autoclave processes before moving into adhesives, bonding defects and their effects. Lastly, the testing methods and equipment used in both mechanical and bond morphology analysis will conclude the literature review.

2.2 Carbon Fiber Reinforced Polymer

Carbon fiber reinforced polymers are a composite material consisting of an epoxy resin which is impregnated with a carbon fiber matrix system prior to being cured. Within the system the epoxy resin offers ductility while the carbon fibers create an increased rigidity, strength and stiffness to the material. (*Mouritz, 2012*) As CFRP is an anisotropic material, it is considered to have directional strength properties dictated by the layout and proportion of carbon fibers within the polymer. (*Corum, Battiste, Liu, Ruggles, 2000*)

This material has shown more desirable physical properties including decreased weight and a greater corrosion resistance to traditional metals and alloys while also possessing a dramatic increase in strength and fatigue limits as well. (*Chawla, 2013*) It is due to these resulting properties that these materials have become ever more prevalent in industries such as aerospace and high-end automobile racing. This is evident when examining aircraft such as the airbus A350 XWB and the Boeing 787 Dreamliner which both boast weight ratios comprised of over 50% CFRP. (*EADS, 2016*) (*Boeing, 2006*)

Due to the directional behaviour displayed by individual layers of CFRP, a system was developed in order to counteract this effect. This involves the specific selection and manufacture of thin sheets of CFRP which have been controlled to produce fibers orientated in a single direction. These sheets offer highly increased properties in a specific direction. These sheets are then layered on top of one another using a selection of different orientations which counteracts the anisotropic characteristics. Although there is a slight increase in weight, the improvement in mechanical properties outweighs any negatives caused by this.
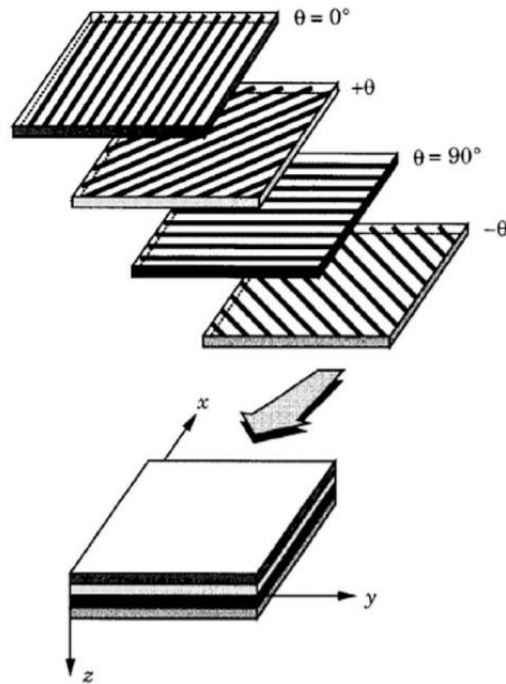
Figure 2: Layering of differently orientated CFRP sheets. (Tawfik, Lehata, Elhewy and Elsayed, 2016)

Although the manufacture of CFRP products is considered to be up to 4.5 times more energy intensive than traditional steel. The benefits of the materials properties are far more valuable in high end industries seeking to advance their own technology and push the theoretical boundaries currently present in their respective fields. (*Das, 2011*) The manufacture process has changed greatly with out of autoclave presenting as a new emerging method for the material production. This will be evaluated in depth later on in this chapter however it is important to note that this process has been developed out of the demand for more portable and commercialised methods of producing composite products.

2.3   Additive Manufacturing (3D printed Titanium)

3D printing has opened created a new avenue of approach in the realm of manufacturing. In the search for customisable and portable systems which can be used to produce solutions of varying complexity and component design, additive manufacturing presented as a front runner.

Additive Manufacturing (AM) is a unique approach to industrial production which has played a pivotal role in the movement from analog to digital processes. The nature of AM provides the opportunity for individual parts to be manufactured at a high speed for trial or direct operator use while maintaining relatively low material waste. The various methods for AM to occur usually involve a similar sequence of events. These generic steps are; the design of the component using a CAD software, the use of this

finalized CAD file to generate a file compatible with the manufacturing software, file manipulation to account for the 'tool path' which details the layers of the design as well as the individual path of the tool, the machine setup, the physical build, excess material removal, post-build processing and the application of the product (*Gibson, Rosen and Stucker, 2010*). Intuitively the nature of strictly adding material means that material waste is minimised (being almost zero). This helps reduce costs while also increasing the ease of manufacture for both individual and sets of products.

Though there are several ways for AM to occur the only difference between them is the material or energy type which facilitates the actual addition of material. These can broadly be categorised as one of seven types; VAT Photopolymerization, Material Jetting, Binder Jetting, Material Extrusion, Powder Bed Fusion, Sheet Lamination and Directed Energy Deposition (*Gibson, Rosen and Stucker, 2010*). Due to the limited scope of the project and accompanied available resources, only the Powder Bed Fusion method will be investigated in this literature review.

Although the term Additive Manufacturing generally refers to the process of strictly adding material to produce a final product, each method utilises an alternate method to achieve this. Powder Bed Fusion is a term used to collectively describe the specific processes which, for the vast majority, originated as Selective Laser Sintering (SLS). As processes and equipment used in this method became more advanced, additional methods of the powder bed fusion family emerged, each modifying the base SLS model in one or more ways to improve upon the previous process. (*Gibson, Rosen and Stucker, 2010*). A pertinent improvement to powder bed fusion is the ability to produce components using metal and metal alloy powders.

The physical process for the manufacture of products is broadly described as; a mechanism which 'spreads' a powder of a desired material evenly over a work plane (surface of operation). This powder is then directly acted upon using a form of laser and heater combination which fuses the powdered particles to form a solid. Following the formation of the solid for this layer the spreading mechanism then distributes another layer and the process is repeated layer by layer until the end product is created. Some key points of this process is that the thinner each layer is, the more accurate the final product will be in comparison to the CAD file. Additionally, it is important to mention that due to the instantaneous moment of melting to change the powder into a solid, there will be some form of unpredictable flow which creates an uneven thickness of the solid material (although this is unnoticeable to the naked eye). (*Gibson, Rosen and Stucker, 2010*).

This process has been visually detailed in the figure below.
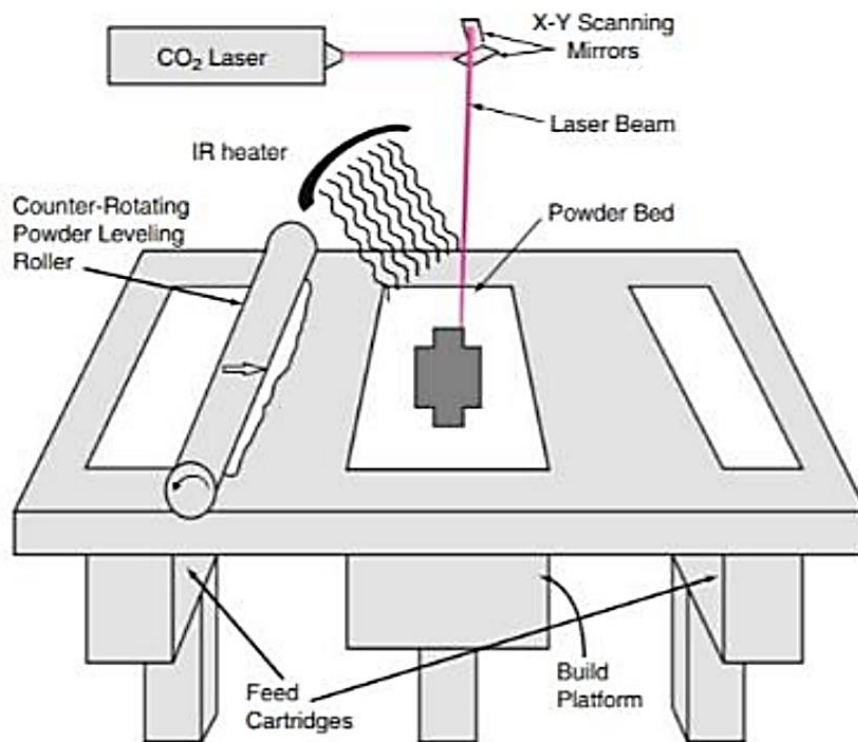
Figure 3: Schematic of SLS Process (Gibson et al, 2010)

This process has proven to be an instrumental component in rapid prototyping (RP) and, with additional enhancements allowing metal alloys to be utilised, opened the window of opportunity to many industries including the aerospace sector. The technology has been particularly useful in creating unique and tailorable components such as repair patches for the integration into damaged structures. Although not a proven or mainstream method, this avenue shows great promise and is one of the reasons for this project's demand.

The material which is most applicable to the aerospace industry is the use of a titanium alloy due to its similar mechanical and thermal properties when compared to traditional composite materials used in aircraft structures. (*Donachie, 2000*) The specific alloy is known as Ti-6Al-4V also called TC4 or Ti64 and the properties can be seen in the figure below.

	Density, g/cm³	Young's Modulus, GPa	Shear Modulus, GPa	Bulk Modulus, GPa	Poisson's Ratio	Yield Stress, MPa (Tensile)	Ultimate Stress, MPa (Tensile)	Hardness, Rockwell C	Uniform Elongation, %
Min	4.429	104	40	96.8	0.31	880	900	36 (Typical)	5
Max	4.512	113	45	153	0.37	920	950	--	18

Table 1: Physical and Mechanical Properties of Ti-6Al-4V (cartech,2017)

The use of this material in an AM environment depends solely on the machine available as each machine model is specifically tailored to individual materials. The correct machine selection ensures an accurate and consistent part is produced in a desirable operating environment (this includes the operating space capable of vacuum sealing, heat treatment characteristics and excellent laser accuracy). This is particularly pertinent when considering the available facility which uses the Renishaw RenAM500Q; a machine utilised for the identical properties required to produce a component of this material with high accuracy and the ability to monitor any deviations as a result of laser input, splatter, gas flow and the physical sample design. An example of the print quality is shown in the figure below.

Compact scarf design 1   Compact scarf design 2   Compact scarf design 3
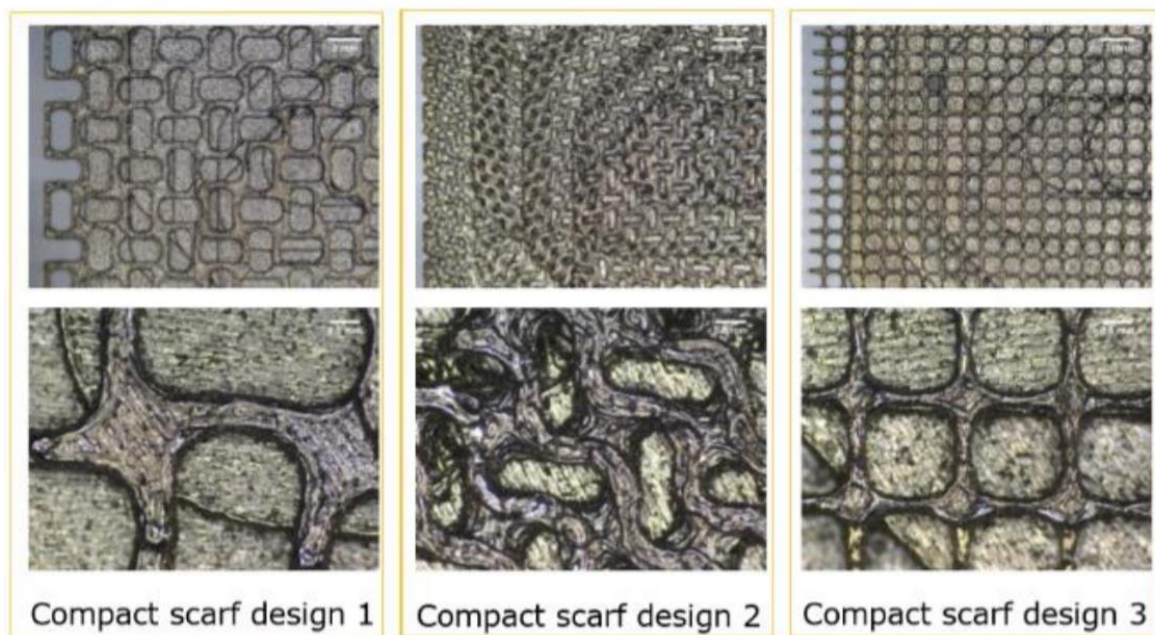
Figure 4: Print Quality of RenAM500Q for the Centre of Future Materials USQ (ABR-AMM Slideshow ,2020)

2.4   Scarf Ribbon Repairs

For as long as aircraft have existed, so too have accidents and damage incidents to the aircraft in question. As time progressed and these aircraft attempted longer voyages at higher altitudes, the consequences of wear on the aircraft as well as catastrophic failures of components became increasingly dire. In order to continually push the limits of aviation, the complexity of aircraft structure increased and so too did the method required to repair damages caused by wear and tear or isolated incidents.

The initial method used to repair damage was relatively cosmetic, only attempting to fill damaged sections with somewhat useless material and then proceed to brace the existing parent structure

using mechanically fastened struts. This has since been developed to cater for the component type which has been damaged, the size of the damaged area and the type of damage experienced.

The most advanced however reliable, method is known as a bonded scarf repair. This repair type has been developed from a method known as a stepped lap repair. The only difference is the surface preparation of the damaged area being repaired. As the name suggests, the stepped lap consists of incremental steps which are machined out of the damaged area prior to an adhesive being applied between the area and a smooth faced component matching the machined void. The component should be prepared in such a way that the surface aligns flush with the outer surface of the parent structure. The only difference between the aforementioned stepped lap and the scarf repair is that the damaged area is machined at a constant gradient matching that of the repair component to be fitted. It provides a uniform surface to apply adhesive, consequently resulting in a uniform adhesive thickness. This method gives greater ease to control parameters such as the scarf gradient and adhesive thickness while also decreasing defect occurrence.

Restoring a damaged component via bonded scarf repair is vastly more cost effective than the current procedure used to address the same issue within the industry. Current procedure dictates that the damaged component be sent to a contracted company to be repaired if possible, in all other cases the component must be completely scrapped, and a replacement ordered for all future use. This lengthy process usually results in premium costs incurred from the contractor with additional costs due to operational down time (*Saeed, 2015*). This is particularly important to civilian airline companies as their profits will begin to decrease. Additionally, it may also play a large role in the military sector as equipment is often labelled as unusable for extended periods of time while deployed in high conflict areas around the world. This can potentially endanger the life of many service men and women who rely on such equipment.

When the damaged component is sent away, the majority of contractors conducting the repair will select the bonded scarf due to its conducive bonding behaviour and high percentage of strength recovery as detailed by Fischer and Kracht (*2012*). This specific repair joint type has been accepted as the most reliable method for almost 30 years. It had predominantly been implemented due to its superior stiffness, strength and aerodynamic surface characteristics (as well as the ability to tailor the section) (*Wang and Gunnion, 2008)*.

The predominant application for bonded scarf joints is structural components or those which require flawless aerodynamic performance. This bond type will be investigated in this report. Forms of scarf repairs can vary however, the use of a 3D printed titanium patch and corresponding adhesive which is then cured in the prepared damage section will be used for this study. Due to the uniform properties of the 3D printed titanium, orientation of the patch is irrelevant and any distinct discrepancies in performance will occur due to the adhesive variances.
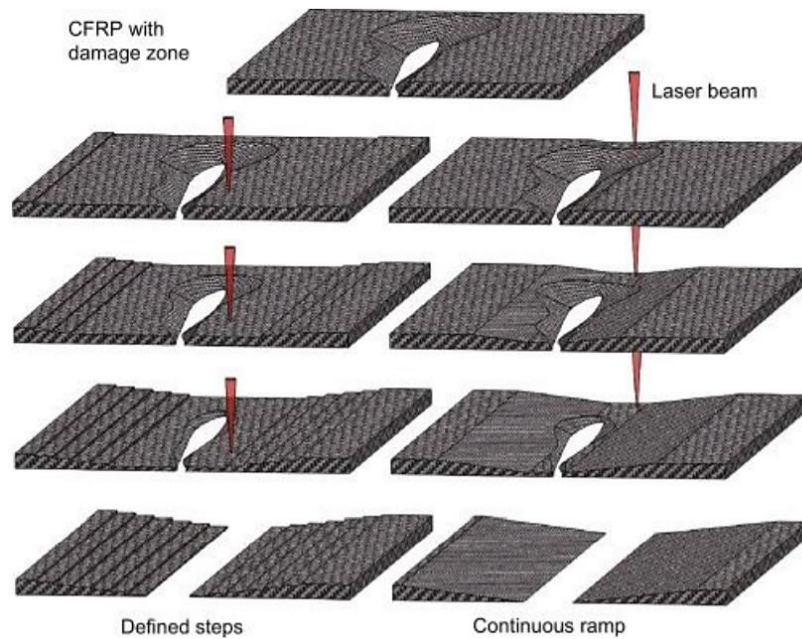
Figure 5: 3D Scarf Schematics. (Jaschke and Dittmar, 2018)

As shown above, the 3D scarf is often extremely complex and in the aspect of testing can prove to be extremely costly in terms of both materials and time. The image depicts a simplification of the 3D problem into what is known as a 2D scarf. The 2D scarf has been shown to be an extremely useful tool which produces accurate and useful results in both mechanical testing and bond assessment.
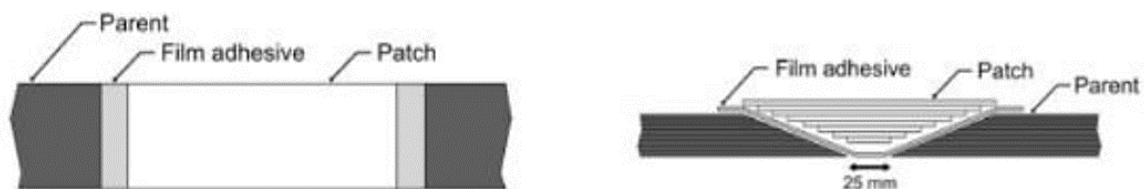
Figure 6: 2D Scarf Schematic. (Chong, Liu, Subramanian, Ng, Tay, Wang and Feih, 2018)

The same text which contains figure 6 also references previously conducted studies which state that a 2D repair will display between 50-70% of the parent specimen. This method will be most desirable

in producing more test samples for less overall material as well as allowing experimental parameters to be controlled with greater ease. Therefore, because an accurate correlation can be drawn between a 2D test and its parent 3D design, as well as the ease of production and repeatability of the 2D configuration, it has been identified and selected for investigation in this project.

2.5   Autoclave and Out of Autoclave Process

In the process of establishing an effective bond between composite components, an appropriate cure cycle is used within either an autoclave or a vacuum bag debulking set up. This cure cycle often accounts for the need to 'set' both adhesives and composite components, and as such dictates the equipment required to achieve this. For example, when considering a B-stage cured composite, the final cure will 'set' both the adhesive and the composite itself requiring maximum accuracy in both temperature and pressure to ensure defect avoidance. This process is achieved by applying high pressure at a predetermined elevated temperature in order to create a chemical reaction for the desired length of time. (*May, 1987*) In order to accomplish this, the right selection of equipment must occur however, the availability and end result (of the repair) must also be considered to ensure that the repair patch is not disproportionately 'over-engineered'.

Generally, the autoclave is considered the most accurate and reliable with the double vacuum bag and single vac-bag, second and third, respectively. This order is a result of the ability of the physical infrastructure present in each set of equipment. In the case of an aircraft repair, the parent structure is already considered as a fully cured component, but both the adhesive and repair patch can require additional curing after application to the damage site. The repair requiring final cure of both adhesive and patch is known as an in-situ co-cured configuration and configuration requiring the final cure of only the adhesive is simply an in-situ cure configuration.

As stated in the previous sub-chapter, 3D printed titanium optimally displays uniform properties and is designed to be used in its manufactured state with minimal changes to both physical and mechanical characteristics throughout the bonding process. Therefore, this report will focus on in-situ cure configurations as the repair patch does not exist as a B-stage cure prior to application. Additionally the use of a 3D printed patch has been selected due to the absence of bulky equipment and the ease it will create for repair processes, using an autoclave process is counterintuitive to this point and consequently this indicates the need for an investigation into out of autoclave (OOA) processes which will be conducted in this project.

Due to the porous state of 3D printed titanium which has been manufactured using powder bed technology, the effect of vacuum bag debulking will be somewhat negligible between single and double vac-bag (DVB) methods. The double vac-bag process is traditionally used to remove volatiles and consolidate fibres of composite materials, however the effect incurred in adhesive curing is not considered to be proportionately advantageous. The comparison of patch curing is shown below and serves as a correlation rather than a direct representation of adhesive properties using multiple cure methods.

Process		Porosity (%)	Tensile modulus (GPa)	Tensile strength (MPa)	Flexural modulus (GPa)	Flexural strength (MPa)	Interlaminar shear strength (MPa)
Patch only	Hotbonding	0.5 ± 0.1	44 ± 2	580 ± 47	34 ± 1	681 ± 27	65 ± 3
	DVD	0.2 ± 0.1	45 ± 2	615 ± 39	37 ± 1	745 ± 10	63 ± 2
	Autoclave	0.0 ± 0.0	45 ± 1	658 ± 19	40 ± 2	746 ± 29	67 ± 2

Table 2: Mechanical and Physical Property Comparison for Various Manufacturing methods (Chong et al, 2018)

Single vac-bag debulking (SVD) is recognized to only be capable of producing pressures of up to 1atm (*Centea and Hubert, 2011*) which intuitively will result in an increase in porosity within the adhesive, and as per Feng et al. (*2019*), an increase in each percentage of porosity between 0% and 4% will result in a 9% decrease in interlaminar strength. However, this process is expected to only slightly increase porosity due to the already high porous nature of the printed patch. The physical set up of an SVD system is represented below. The only difference incorporated in the DVD set-up is the presence of a rigid outer box which encases the entire system in order to achieve the secondary 'vacuum bag'.
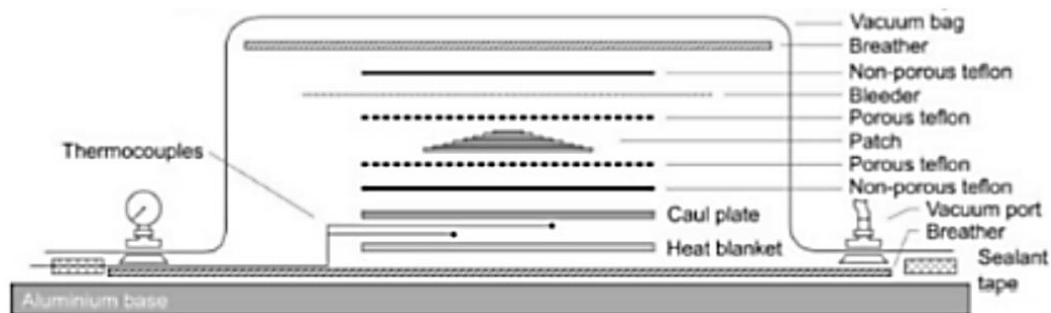
Figure 7: SVD configuration (edited image from Chong et al (2018).)

The next logical element to consider in SVD methods is the cure cycle which is to be utilised for adhesive consolidation within the repair. Rudawska and Czarnota (2013) state that there are three distinct types of cures: cold cures, single stage cures and two stage cures. Cold cures traditionally take a much longer time to occur than the single and two stage cures. Single stage cures, although considered equally as effective as two stage cures, take an increased level of accuracy for temperature control. This increased accuracy is required during the lowering of temperature from the elevated cure holding temperature down to ambient conditions in order to ensure the absence of shrinkage stresses which lower the cohesive strength of the joint. (*Adams et al, 1992*)

Preu and Mengel (*2007*) state that two stage cures traditionally involve an initial cure solidifying at ambient temperature with an adequate applied pressure for a period of time depending on the adhesive type and reactivity which will result in an adhesive at 60-70% of its final strength. The final cure then indicates an elevated temperature of between 50 and 100 degrees Celsius for the adherend with no pressure applied. As well as being significantly faster, the elevated temperature generally facilitates the production of an adhesive with greater thermal and chemical strength which are all desirable properties in aircraft repairs.

2.6   Adhesive Methods and Surface Preparation

As mentioned previously, the bonded scarf repair is most frequently implemented utilising an adhesive which is cured using either a hotbonding, autoclave or OOA (usually DVD) process. For the purposes of this report only OOA process will be investigated for the adhesive film. The behaviour of the adhesive can be strongly dependent on the cure cycle used to 'set' the adhesive in place. Although not entirely aligned with the processes for manufacturing, the differences in material characteristics are exemplified by Chong in the text *'Out-of-autoclave scarf repair of interlayer toughened carbon fibre composites using double vacuum debulking of patch', Composites Part A: Applied Science and Manufacturing, vol. 107' (2018).* These cure cycles are usually given as a recommendation from the manufacturer and can vary significantly from supplier to supplier.

Adhesive films are an extremely popular form of bonding utilised in the repair of aerospace components. This is predominantly due to the ability to control key parameters in the bonding process which consequently result in a bond with much more desirable characteristics that possess a higher reliability. The adhesive thickness is tailored to the repair while also being relatively simple to shape and apply in order to compliment both the dimensions of the damaged section and the physical requirements of the repaired section.

For scenarios requiring less serious overhauls of damaged sections or where the key equipment for a high temperature, vac bag curing process is unavailable, epoxy paste adhesives have proven to be useful as an alternate adhesive method. Many adhesive producers identified the demand and developed high quality products to address the necessity for aviation adhesives.

The key aspect to consider when selecting an adhesive is the resulting flexural characteristics and strength of the finalized bond. This report will investigate the use of two alternate adhesion methods being a film adhesive and an epoxy paste adhesive. Using the previously mentioned key aspects, the selections of FM 300-2 film adhesive and LOCTITE EA 9394 AERO (also known as Hysol EA 9394) epoxy paste adhesive have been selected for investigation and comparison.

As per the technical process bulletin from LOCTITE, the epoxy paste produces outstanding mechanical properties and does not require an elevated temperature or vacuum environment to cure. Conversely the FM 300-2 fil adhesive will require a facility to bond however, it can be expected that the results are more desirable despite the additional effort being committed to the process. However different the materials appear; they are both extremely applicable in the aerospace sector displaying properties which are conducive to effective performance within the industry.

In both adhesive cases, the surface preparation has proven to be an extremely important factor to ensuring optimal performance of the bond (*Katnam et al, 2013*). Techniques vary, each possessing distinct advantages and disadvantages. Most common techniques used are routing, drilling, milling, grinding and sanding. These can be done by hand or using a robot/automated machine. The purpose of this report is to investigate repair techniques that do not require bulky industrial machinery therefore the work which is completed by hand is much more applicable and will be evaluated. The difference in techniques can be seen in the image below.
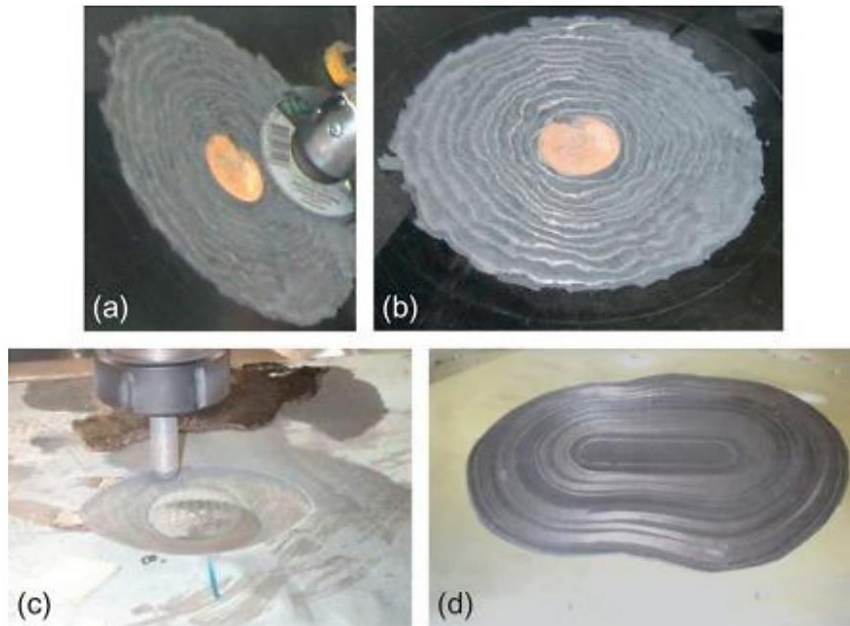
Figure 8: a) Scarf made by manual grinding, b) surface profile from manual grinding, c) robotic machining, and d) surface profile from robotic machining. (Wang and Duong, 2016)

Despite the lack of facilities, due to the increasing portable nature and affordable cost of CNC machines the robotic machining method should be considered moving forward in studies within this field. These machines offer a level of precision which is near impossible to match with hand tools and can provide even greater control over bond parameters. (*Wang and Duong, 2016*)

2.7   Bonding Defects/Failure Mechanisms

At every stage of the repair process, the chosen repair method must be evaluated in terms of its failure mechanisms and contributing defects which are associated with them. The importance of this evaluation is evident when examining the quality of the end repair product. Failure mechanisms directly influence the materials behaviour around the failure incident. The shear strength, and resistance to peel stress are impacted heavily with the rising level of defects such as porosity, incorrect adhesive thickness, moisture content, bond line stress and incorrect cure cycling. These will be investigated individually in the following sub-sections.

It is important to identify the behaviour of a scarf prior to assessing the defects and failure mechanisms, this may help identify and predict prior failure events early or help prepare for their possible occurrence. Gunnion and Wang (*2009*) have detailed equations describing the adhesive shear stress experienced for circular scarf repairs. Although useful to examine these will not be directly

critical to this study. It is important to note that the maximum allowable stress is dependent on scarf and adhesive strength.

$$\tau_{max} = \frac{\sigma_{applied}}{2}\sin(2\alpha)$$	$$\alpha = \frac{1}{2}\sin^{-1}(\frac{2\tau_{avg}}{\sigma_{xx}})$$
Maximum adhesive shear stress	*Scarf angle corresponding to maximum shear stress*

Table 3: Equations detailing characteristics of a cicular scarf repair (Gunnion and Wang, 2009)

2.7.1   Porosity

Although a relatively easily identified issue, porosity or more specifically the void content of both cured material and cured adhesives, prove to be a leading factor in the degradation of bond quality. Voids are found to promote crack initiation and/or propagation with studies referencing the common rule that every 1% increase in void content per volumetric unit will result in between 4 and 6% decrease in shear strength. In order to best avoid these imperfections strict guidelines have been provided as the result of numerous studies which outline strategies regarding void minimisation and elimination.

The three key components identified as critical to success for void elimination involve the correct use of the cure cycle, the elimination of gases and other volatiles (conducted using a vacuum) and the correct pre-adhesion preparation for moisture elimination.

As stated in a number of studies these steps have been detailed as: 1) Air must be evacuated using a vacuum, ensuring adequate time for gases to be removed while also ensuring the resin is able to fill the 'gaps' left by the evacuated gas; 2) Pressure must be adequate and constant during the cure to prevent and suppress the growth of volatiles in vaporisation; and, 3) Resin remains in the voids to 'fill' and 'set' requiring a low resin viscosity and high pressure. (*Fahrang, 2016*)

Studies have also shown that the need for moisture elimination is vital in reducing void content within the final product. It had been discovered that moisture absorption counterintuitively produced no additional voids and instead the increase in porosity percentage was directly correlated to the humidity during the material preparation. This further supports the previously mentioned second step in the aforementioned process.

2.7.2 Bond Line Characteristics

Gunnion and Wang (*2009*) describes the resultant stress distribution of a circular scarf, interestingly the distribution had a uniform x direction resultant mirrored on both the x and y axis. This provides the unique opportunity to predict and model this behaviour. The minimum stress experienced was in the out-of-plane direction, which is as predicted due to the force resultant. The most significant stresses occurred at regions of fiber termination allowing for stress concentrations to build at points of lower resistive strength. However, concerning this may seem, further studies have proven the techniques effectiveness compared to its predecessor the external patch repair.

A consideration which has an influential role in shaping the bond line stress behaviour is the adhesive thickness. Although technical guidelines have not been specified and are difficult to find, a general rule is that the length of the scarf is 20 to 120 times the adhesive thickness. This is obviously dependent on the scarf angle, adhesive type (including viscosity) and the porosity of the adherend. The adhesive must be capable of filling porous voids while not excessively adding to the thickness of the bond interface which could detrimentally affect the performance of the bonded component.

2.7.3 Cure Issues

Although an obvious issue, the result of an uneven or inadequate cure can cause decreased mechanical properties like that displayed in B-stage cured components being only 60-70% of the final desired strength. The uneven cure can create stress concentrations in areas of inadequate resistive strength. Conversely an incorrect cure can facilitate the early or unwanted occurrence of peeling or peeling stresses. Despite being a possibility, the adaptation of a bonded scarf repair from an external patch has almost completely eliminated the occurrence of peeling and peeling failures in comparison to the older method. In order to avoid the mentioned defects and failure mechanisms it is often desirable to utilise various avenues of testing and inspections which will be explored in the following section.

2.8 Testing Equipment and Techniques

2.8.1 Non-Destructive Testing

Prior to each stage of sample preparation, it is vital to assess the material in its current state in order to determine the appropriate actions moving forward. This includes but is not limited to the inspection of both visible and microscopic damage, defects from manufacturing or material preparation and any

material irregularities. This is particularly important when considering the difference in properties between the parent structure and the repair patch. (*Katnam et al, 2013*)

Although non-destructive methods such as ultrasonic testing and micro-CT scanning will not be utilised in this project, it is important to note that the use of them in the assessment of the material is key in both detecting and preventing catastrophic failures in the repair structure. Despite the lack of facilities to carry out non-destructive testing, these avenues should be utilised where possible in future studies.

2.8.2   Destructive Testing

This form of testing is designed to compliment the non-destructive aspect. Rather than measuring the materials composition and microstructure it assesses the mechanical properties providing results which intend to reinforce the findings presented in the non-destructive tests. These can include tensile and compressive tests, flexural and shear tests, and assessments of the final microstructure after mechanical tests are conducted (including methods such as digital image correlation).

2.8.2.1 Optical Microscopy

This aspect of destructive testing involves the production of test samples under regular testing conditions however prior to a physical examination occurring the specimen is 'sliced' longitudinally before having its profile polished to reveal the physical appearance of the material and corresponding bondline. The typical equipment involved in the process is a cutting and polishing machine used to prepare the specimen followed by an optical microscope (also called a light microscope) used to view the material profile and lastly a micrograph which is utilised to capture images of the viewed profile.

The most important properties which this method aims to identify are defects and deformities in the pre-preg material, titanium component and adhesive layer. These include void presence, misalignment and adhesion between both parent and repair components.

2.8.2.2 Tensile and Compressive Testing

Tensile and compressive testing are extremely common tests predominantly utilised for assessing either mechanical or behavioral properties of a specified material or system of materials. ASTM D8131 defines the process for assessing tensile properties of tapered composite materials. Although only 50% of the test sample will contain composite material, this standard remains applicable to this study and will be used to define the experiment parameters including number of tests, their size and physical variables.

2.8.2.3 Flexural and Shear Testing

Although not incredibly pertinent to this immediate study, the assessment of flexural and shear properties is important to the broader subject of aerospace materials and material compatibility (specifically between parent structures and repair material). Loading conditions in aircraft are complex and extremely dynamic and as such should be considered in detail prior to commissioning new repair techniques. Although test standards such as ASTM D5379, D790 and 6272 are utilised widely in studies, (including *Chong et al.* (*2018*)) these tests are incredibly vast in variability and as such can have multiple studies solely devoted to their conduct and results. However, the applicability of considerations used in these studies are valid and will be considered comprehensively for this study.

2.8.2.4 Digital Image Correlation

Although analysing small segments of a test sample with optical microscopy is beneficial, traditionally the only large-scale examination conducted during the experiment would yield a single value being the tensile strength. Although useful the value depicts a narrow result pertaining to the mechanical properties of the material with no regard for failure or loading behaviour of the entire system. This overall system behaviour can be observed using multiple segments of optical microscopy or alternatively, through a process known as digital image correlation.

According to Mobasher (2016), Digital Image Correlation (DIC) is a noncontact, optical, full-field deformation observation approach. This process was progressively adopted following its initial use and has now become a prominent method for the evaluation of both composites and reinforced concrete. DIC is conducted by specifying an area of interest (AOI) and dividing it into an evenly spaced grid which is used to track the deformation of local positions. During the destructive testing, a video recording device with the correct resolution accuracy is used to track each subset of points in terms of its position and then compared to its original position to provide a deformation behaviour prior to failure. This has been visually represented in the figure below. Mobasher (*2016*) also details the possibility to differentiate and smooth displacement fields in order to derive strain fields.
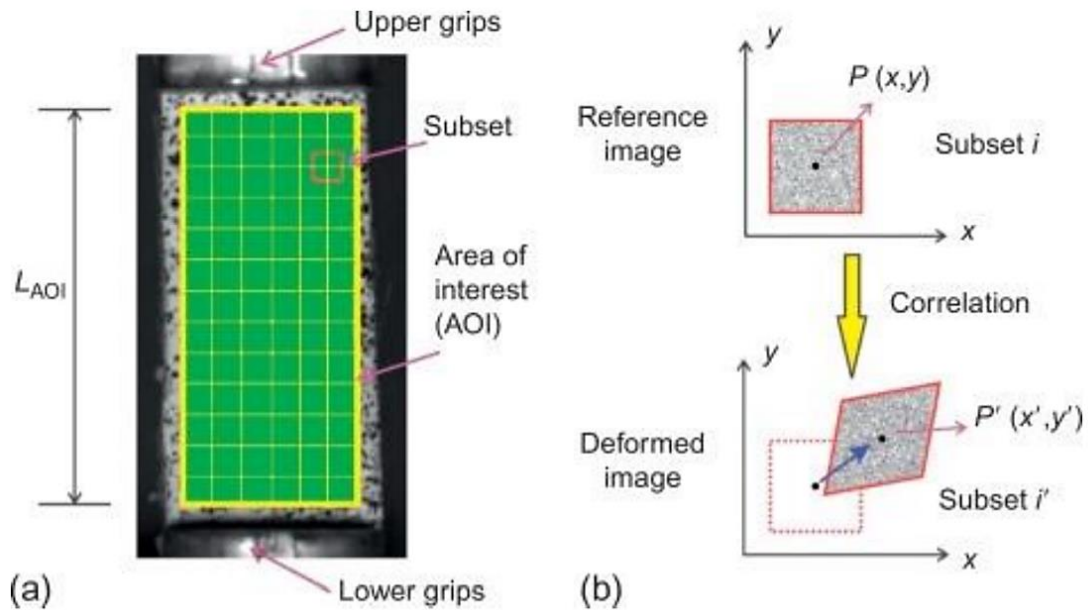
Figure 9: (a) Area of interest and subset reference; (b) schematic representation of an element in the subset prior and pose deformation (Mobasher, 2016)

2.9 Identified Area of Study (Gap in Research)

Research surrounding the scarf repair joints, specifically bonded scarf repairs, have been studied extensively as shown in reports from various authors including Jaschke et al. (*2018*) and Chong et al. (*2018*). Its key to note the conditions and experiment parameters which were used in these studies as there are clear areas that could be improved or further investigated. These reports utilised a B-stage cured pre-preg which required the use of a DVD system in order to consolidate the bonded repair. Although useful when regarding the aerospace maintenance industry, this may not be the ideal route for investigation and eventual application. Considering SVD systems, far less studies have been conducted. I believe this is because the use of an alternative material which is dissimilar to the parent component has not been highlighted as a viable solution yet. This is because additive manufacturing technology has only improved to the current standard in recent history and prior to this point, these materials would not be adequate for use in such a strict field.

It's also important to note that the vast majority of studies including Gunnion and Wang (*2009*), Fahrang (*2016*) and Chong et al. (*2018*) investigated either the behaviour of the adherend or the theoretical behaviour of the bond line with little emphasis and investigation on the adhesive itself. This is evident in the majority of studies conducted on bonded scarf repairs and even more so when considering the bonding of dissimilar materials (of which I failed to source any studies on). This

appears as a glaring gap in knowledge, giving way to further studies to be conducted, specifically benefiting the aviation sector.

The adhesives used in all studies with B-stage cured adherends are a film adhesive requiring curing in conjunction with the adherend. Very few studies have investigated the difference in various adhesives when utilised in a scarf bond, which is why this has been highlighted for specific use in an aerospace application.

Fahrang has highlighted clear steps required for the elimination of porosity in his 2016 report. Emphasized in numerous investigations are the moisture effects or volatile effects on resulting porosity. These studies considered the adhesive consolidation without considering key mechanical properties on the structure. These reports also investigated single materials and not bonded units. Preu and Mengel (*2007*) are an exception to this, investigating the effect of the cure cycle on both adherend and adhesive.

As an overview, limited studies have been conducted on bonded scarf repairs focusing on adhesive parameters and corresponding behaviour with no immediate obvious studies conducted in this area between two dissimilar materials. Additionally, there is an evident lack of studies conducted on the effect of both adhesive type and the cure cycle. This is where the foundation of this investigation has been created. This report will focus on the effects of adhesive type and cure cycle for the bonding of dissimilar materials (specifically additive manufactured repair patch) using a SVD system.

2.10   Chapter Summary

This chapter aimed to investigate the requirements pertinent to bonded scarf repairs. This included reviewing relevant standards and guidelines used to conduct an accurate experiment while producing results that are viable. These processes have also been assessed for their applicability and influence on aerospace applications of bonded scarf repairs. It focused on failure mechanisms, production techniques and testing/evaluation methods. A significant amount of focus was placed on adherend assessment and parameters surrounding their handling in the bonding process. The vast majority of literature had neglected the effect of adhesive type and cure cycle, and no study was found to have investigated these points in an SVD system of bonded dissimilar materials. To influence and contribute to the improvement of repairs in the aerospace industry this particular field of repair method should be explored.

3.   Methodology

3.1   Chapter Overview

A requirement of any useful study is accuracy, reliability, and repeatability of results. This is only achieved through the detailed and comprehensive planning of the experimental methodology in order to establish a basis for the guidelines to be followed for the experiment. The purpose of this chapter is to create the aforementioned methodology using appropriately selected research questions and hypotheses in order to produce desirable and insightful recommendations.

3.2   Research Type

It is a widely known fact that experiments are conducted in order to answer one or more questions of importance. The experiments conducted are designed in such a way that they produce data that can be analysed in order to provide some form of evidence or a direct answer to the question(s) at hand. There are many types of research ranging from exploratory to comparative research however, the two common categories considered are qualitative and quantitative. Although no research is strictly qualitative or quantitative as there are elements of both in every study, it is particularly pertinent for this study to remain predominantly qualitative in order to produce results which closely correlate to the physical measurements of an expanded 3-dimensional study. Qualitative experiments require the use of research questions which shape an overarching hypothesis and the conduct of the experiment. This will be provided in the following sections of this chapter.

3.3   Research Focus

Research conducted in this study will be focused and guided utilising an appropriate selection and further development of the scope. This will encompass the aims, as well as proposed research questions to be answered providing conclusions for the project objectives outlined in the introduction of this report.

3.3.1   Aim

Section 2.9 details the research that had been conducted in the field of bonded scarf repair and parameter optimization however little detail was placed on adhesive parameters and their effect on the final bonded joint. This has given rise to the need for research to be conducted into the behaviour

and processes surrounding adhesives in bonded scarf repairs of dissimilar materials using a SVD system. This need has stemmed from a demand in technology improvements for aircraft repair techniques and an evident lack of research currently existing in this field.

The vast majority of studies were creating a standard data set for later comparison of further studies due to the lack of information surrounding the area. They often compared soft and hard patch approaches, varying different parameters between the two types which in turn, created an impractical level of difference for an accurate comparison to be conducted. This is a particularly useful point to mention as it plays a key role in the shaping of this report's study.

This report will aim to establish a baseline for the testing of joints containing two dissimilar materials which will then be qualitatively compared to similar processes conducted on hard patch repairs utilising similar parent and adherend materials. It is also important to conduct a comparison of the difference between SVD and DVD systems in the context of hard patch bonded scarf repair joints. Recognising these points, this dissertation aims to investigate the effect of adhesive type and vacuum debulking system on final joint morphology and the mechanical and material properties of an in-situ scarf joint between two dissimilar materials.

3.3.2   Scope

Key considerations to factor into the project scope include equipment availability, time constraints, additional pressure due to the social impact of *COVID-19* and the need to produce viable and accurate analysis of the experiment. Concepts relate directly to the objectives observed in sections 1.3, 1.4, and 2.9. As stated in the Introduction the scope of this project is:

"To investigate and compare the final repair quality and mechanical behaviour of multiple types of adhesive and the effect of cure cycle used in a single vacuum bag system for bonded scarf repairs between two dissimilar materials."

3.3.3   Research Questions

To maintain effective time management for the duration of the project and ensure objectives are met with little deviation, the following research questions have been developed.

3.3.3.1 Research Question 1

With regard to porosity and bond consolidation, does the SVD system produce an adequate quality of bonded scarf in comparison to previously conducted DVD processes?

Is the single selected cure cycle effective for adhesion of both adhesive thicknesses?

Are the scarf repair strengths adequate in comparison to prior conducted composite-composite co-cured scarf repairs?

Does the introduction of dissimilar material present any thermal mismatch creating discontinuity in failure behaviours?

3.4   Experimental Objectives

As mentioned in the *Focus* and *Scope* sections of this chapter, guidelines must be followed to facilitate the effective production of results which will answer or contribute to the answers of the previously identified research questions. In order to achieve this, specific experiments will be utilised, these have been selected and developed from the *Material Testing* section of chapter 2 – Literature Review.

3.4.1   Non-Destructive Method

The specific non-destructive experimental method that will be utilised is microscopy. This will be used to evaluate the porosity and void percentage of the adhesive itself, as well as investigating the interface between the porous titanium component and the adhesive. This will directly address research question 1 and will also offer insight into research questions 2 – 4.

3.4.2   Destructive Methods

As previously conducted in both experiment for scholarly articles and USQ projects, ASTM D8131 will be strictly adhered to for tensile testing of the samples. This will validate the results of the experiments through their accuracy and consistency. The use of DIC will be incorporated into testing of all samples to gain insight into the behaviour prior to failure, including strain and displacement of local nodes in the samples. Post-experiment photography will be used to document results for further evaluation and discussion.

3.5 Chapter Summary

In this chapter the methodology has been specified to facilitate the fulfillment of this project's objectives, ultimately concluding with a process to bridge the identified knowledge gaps which were specified in the literature review. Research aims and key research questions have been proposed in direct servitude of the overarching project goal, ensuring accuracy and effectiveness of the study. The methods for achieving the project objectives and assessing the repair quality of various adhesives used in dissimilar bonded scarf repair materials in an SVD have been identified according to available resources and will be detailed in the following chapter.

4. Experiment Outline

4.1 Overview

The purpose of this chapter is to define the procedure used for specimen fabrication and experimental testing of the material. This will include highlighting the steps taken for adhesion, scarf preparation, and the testing techniques utilised during the material assessment (both destructive and non-destructive). All points will attempt to be correlated directly to the aforementioned research questions.

4.2 3D Printed Titanium Component

For this experiment the 3D printed titanium component was outsourced to an external facility. The samples were prepared using a Renishaw 3D printer. The 3D printing machine model is a RenAM500Q, selected due to its high accuracy and ability to monitor any deviations as a result of laser input, splatter and gas flow. The machine produced a model using the alloy; Ti-6Al-4V also known as TC4 or Ti64.

Various samples were available for use, in order to create a baseline, the solid scarf was selected with an additional porous honeycomb sample utilised to vary the adhesive thickness for testing.

The method utilised for component fabrication is identical to that described in the literature review of this dissertation. Using a powder form of the alloy, layers of powder would be spread across the enclosed work area before concentrated lasers would melt the powder forming individual layers of solid alloy material. This process would repeat until all the total layers formed created the desired specimen thickness. Due to the extremely high accuracy and desirable finish, the material required no further processing before use in this experiment.

4.3 Composite Panel and Handling

As stipulated in the literature review, the most important aspect of specimen fabrication is the appropriate handling of components both prior to, and during adhesion. This will aide in mitigating against contamination which would otherwise result in decreased quality of specimens for testing (Gunnion and Wang, 2009). The most crucial contaminate to consider is moisture which as previously mentioned could decrease sheer strength of the material by 4% - 6% for every 1% increase in porosity.

As the film adhesive is stored frozen, it should be left in ambient workspace conditions to defrost. This will ideally minimise the remaining moisture residue from the adhesive and limit the transfer to the composite panel. All storage of composite panels should be limited to dry ambient areas in order to control possible ingress into the material resulting in compromised specimens.

4.4 Sample Preparation and Fabrication

Due to the relatively complete nature of both the parent composite panels and the 3D printed Ti64 scarf components it was deemed necessary to utilise single vacuum bag debulking only for the curing of the adhesive film in all cases. To ensure results were standardized all samples were cured simultaneously in the same vacuum bag. The layup and curing procedures are stipulated in the following sub-chapters. It is important to note the requirement for PPE to be worn for all preparatory and testing phases of the experiment. The PPE for the workshop is steel capped boots, a laboratory jacket and safety glasses while the specific PPE for chemical handling and sanding tasks is as per the workshop PPE list with the additions of latex gloves and a cupped particulate respirator mask (in accordance with AS/NZS 1716:2012).
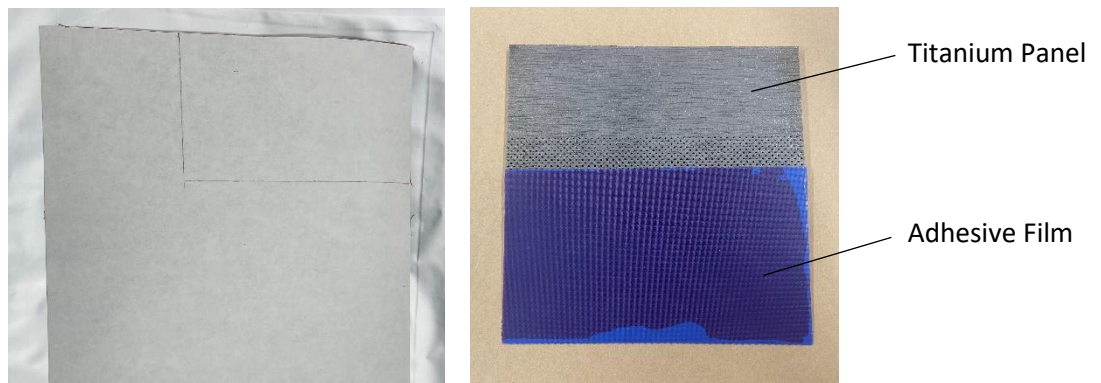
4.4.1 Sample Surface Preparation

In alignment with previous DSTG projects conducted by USQ undergraduate students scarf surface preparation remained the same for all composite panels. The steps specified are:

1. Sand the scarf surface with 400 grit aluminum oxide paper while under running water to wash any excess particles from the surface.
2. Using fine fibre cloths, wipe the surface with methyl-ethyl-ketone based mould cleaner until particles cannot be visibly seen on the cloth. It is important to ensure the cloth does not catch on the panel edges resulting in individual fibres remaining on the sample causing contamination.
3. Conduct break water test using distilled water. If the surface is prepared correctly water beads should form and not spread on (or wet) the surface. Dry the surface using a dry fine fibre cloth.
4. Place the prepared panels in a vacuum oven for an hour at 100℃. This will ensure both the panels and surface are dry and free from contaminants for adhesive bonding.
5. Remove from oven and place in clean and controlled workspace to cool prior to adhesion.

4.4.2   Adhesive Preparation and Application

The adhesive film to be utilised is FM300-2 (Appendix C). Because this material is stored in a frozen state it is extremely brittle. It is important to carefully remove it from the freezer and place in a clean workspace to defrost in ambient conditions. This will avoid brittle fracture of each piece of film. The film has the capability of curing at ambient temperatures and cannot be refrozen once defrosted it is therefore important that the material is used relatively quickly once defrosted.

Once the surface of the panels is prepared and the adhesive film has defrosted, the scarfed components can be placed together temporarily, and the area of the contacted surfaces measured to ensure complete adhesive coverage is achieved. Using the measured dimensions, a matching piece of the film adhesive may be cut and applied to either the composite or Ti64 scarfed component. The remaining component can be applied to the adhesive ensuring both scarfed surfaces are entirely covered by adhesive.

Figure 10: (Left) Adhesive film marked to size
(Right) Adhesive film applied to Ti64 component

For preparation of the double adhesive sample, two identical pieces of the film adhesive may be cut, and each applied to opposite surfaces of the bonded pair. These two pieces are to be aligned and attached matching the two corresponding film adhesive strips to one another. Due to the difficulty maintaining alignment this step should be conducted prior to placement on the bagging apparatus for curing of the adhesive.
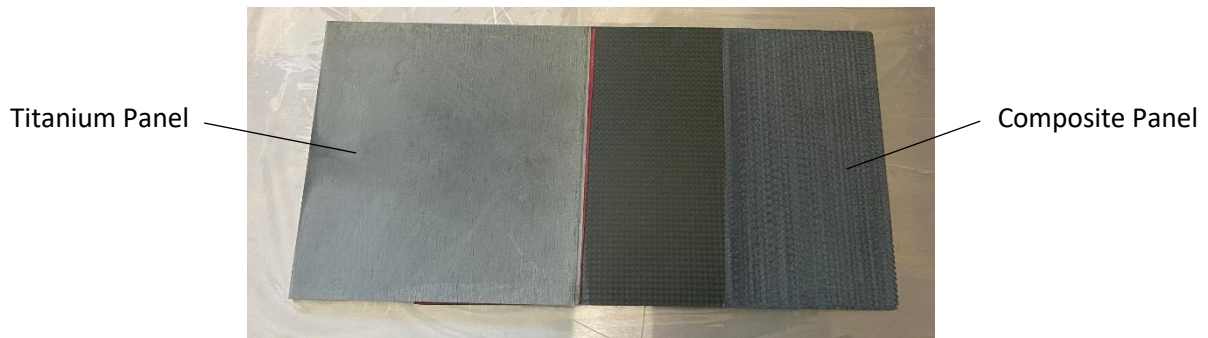
Titanium Panel   Composite Panel

Figure 11: Composite panel and Ti64 component attached via un-cured film adhesive

4.4.3 Bagging Procedure

Before the adhesive cure can occur, the bagging apparatus must be assembled correctly in conjunction with the heating elements which will facilitate the correct cure conditions for the experiment. The first step, as should be considered for all stages of the experiment, is to establish a clean and safe workspace. Following this the appropriate materials should be gathered. The materials required are:

- Vacuum bag (nylon material)
- Breather apparatus (polyester sheet)
- Sealant tape
- Tooling plate
- Release film (non-perforated)
- Optional caul plate (used for surface finish needs)
- Heating elements and associated components (including computer-controlled system)
- Vacuum source and associated components (including vacuum port and hosing)

A diagram of a single vacuum bag set-up is depicted below in Figure 12. As highlighted in the literature review a caul plate is used to produce ideal surface finishes or to produce desirable results for in-situ scenarios. When in use the caul plate can be located between the release film and breather.

Figure 12: SVB bagging apparatus diagram

For this experiment the tooling surface is a stainless-steel bench due to its thermal properties and cleanliness. Using a microfibre cloth and surface cleaner, clean the tooling plate until all visible contaminants have been removed. This may require multiple passes to ensure cleanliness. Once deemed clean the area should be left for 5 minutes to dry before a final wipe down using a clean and dry aircraft grade wipe.

Once the surface has been prepared, place a non-perforated release film on the surface followed by the panels and another film over the top to prevent the adhesive from bonding to both the tooling plate surface and the vacuum bag. The panels and the plastic film should then be fixed using strong magnets to ensure no movement can occur during the curing process. This is shown in the two images below.
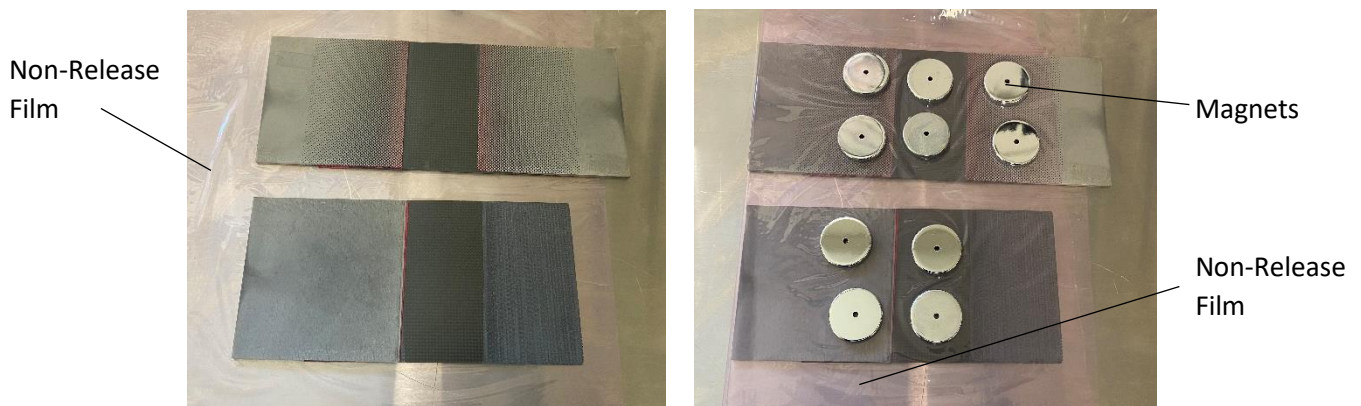

Figure 13: (Left) The panel and base non-release film placed on the tooling plate
(Right) The panels, non-release films and magnets holding the assembly in place

The next step is to attach the thermocouples and upper layers of the vacuum bag. Using tape to fix the thermocouples it is vital to place them as close to the bond line as possible as shown in Figure 14. This will ensure accurate temperatures are communicated to the computer program which will control the output of the heating pad in accordance with the cure cycle.
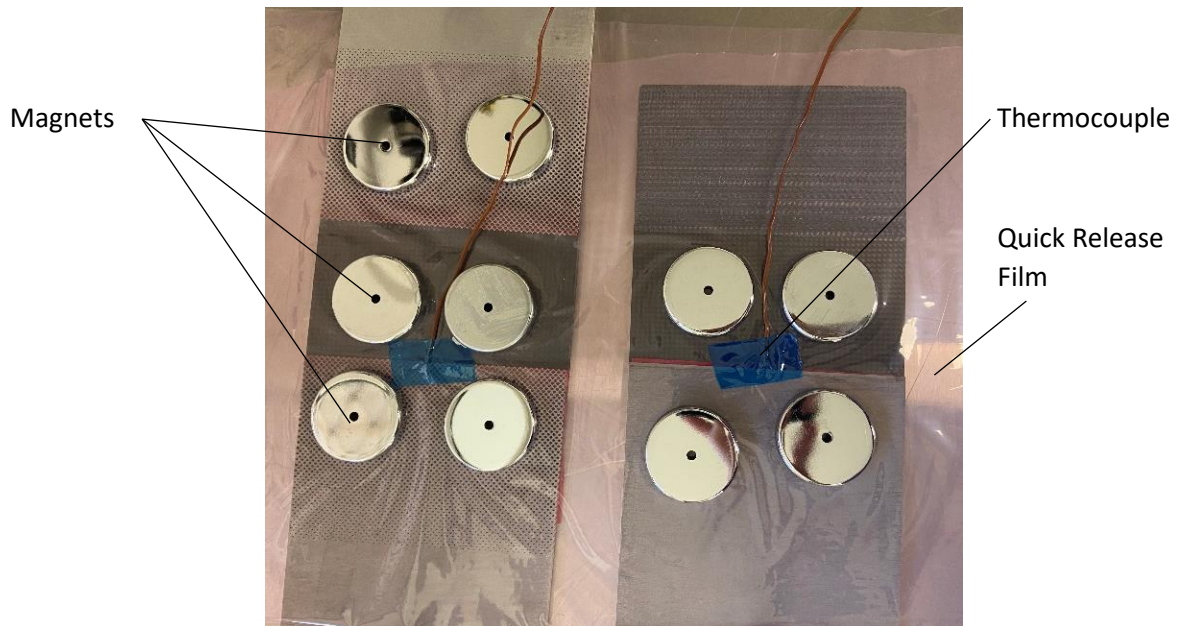
Figure 14: Thermocouple fixed to assembled scarf and SVB components along adhesive bond lines which are to be cured

Following this, the sealant tape should be fixed to the tooling plate surface. This seal quality established with the tooling surface will directly affect the vacuum during curing. Therefore, it is important to ensure any possibly areas of interest are appropriately addressed to mitigate against air infiltration. These areas are the corners and the entry point for the thermocouple wires. This is demonstrated in Figure 15.
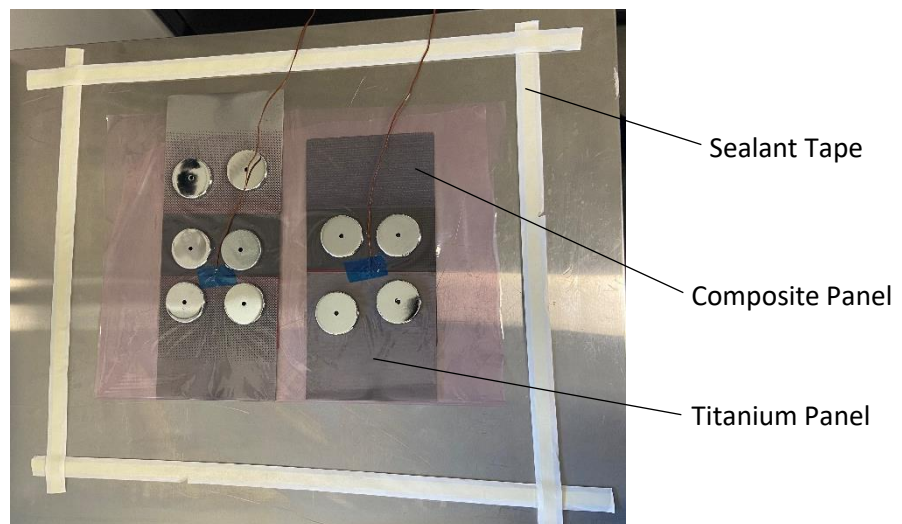

Figure 15: Sealant tape arrangement surrounding the fixed specimens for curing

The final step for the bagging procedure is to apply the breather fabric and the vacuum bag. As depicted in Figure 16, the breather fabric is placed over the entire area of interest (the specimens). This is then followed by the vacuum bag which is attached via the sealant tape. The vacuum bag should have a vacuum port to allow the evacuation of air to occur in the desired manner. The apparatus set up prior to operation and during vacuum operation is shown in Figure 17 below.
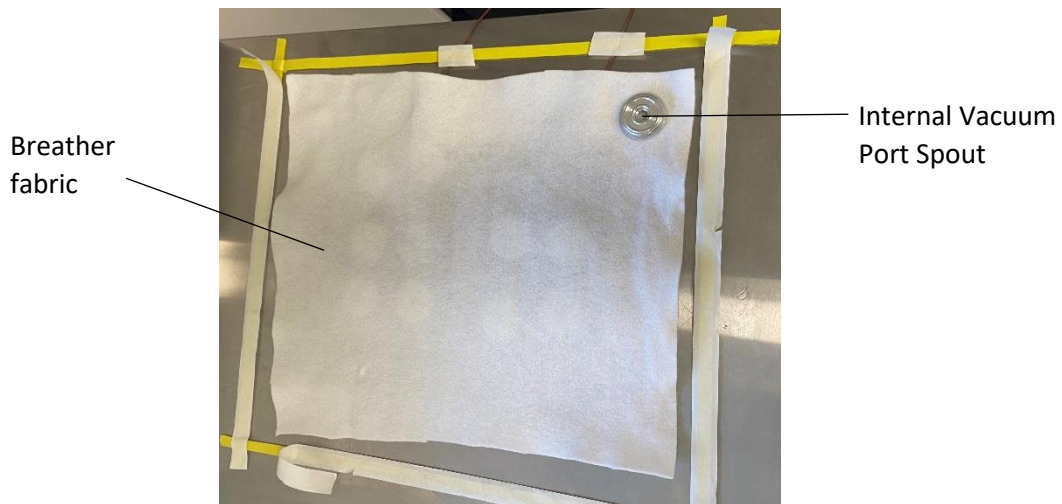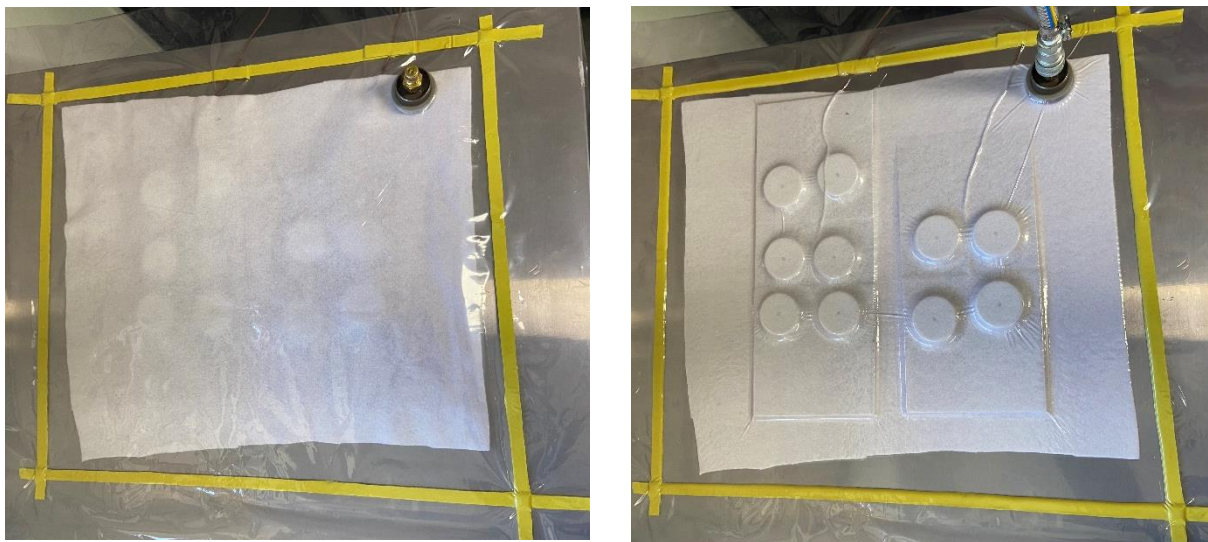

Breather fabric

Internal Vacuum Port Spout

Figure 16: Breather fabric placed over the desired bagging area of interest

Figure 17: (Left) Vacuum bag applied to apparatus prior to operation
(Right) Vacuum bag assembly during vacuum operation

As observed in Figure 17, minimal "creasing" except where thermocouple wires are present, indicates a tight and effective seal which will produce a strong vacuum conducive to effective cure conditions. Images regarding the vacuum source equipment, computer controlled curing equipment and entire laboratory workspace can be found in Appendix L.

4.4.4   Cure Cycle

Prior to the cure cycle occurring the heating pad must be placed appropriately with reference to the thermocouples which will be recording the temperature throughout the cure. Figure 18 depicts the placement of the heating pad which fully covers the specimens during the cure cycle.
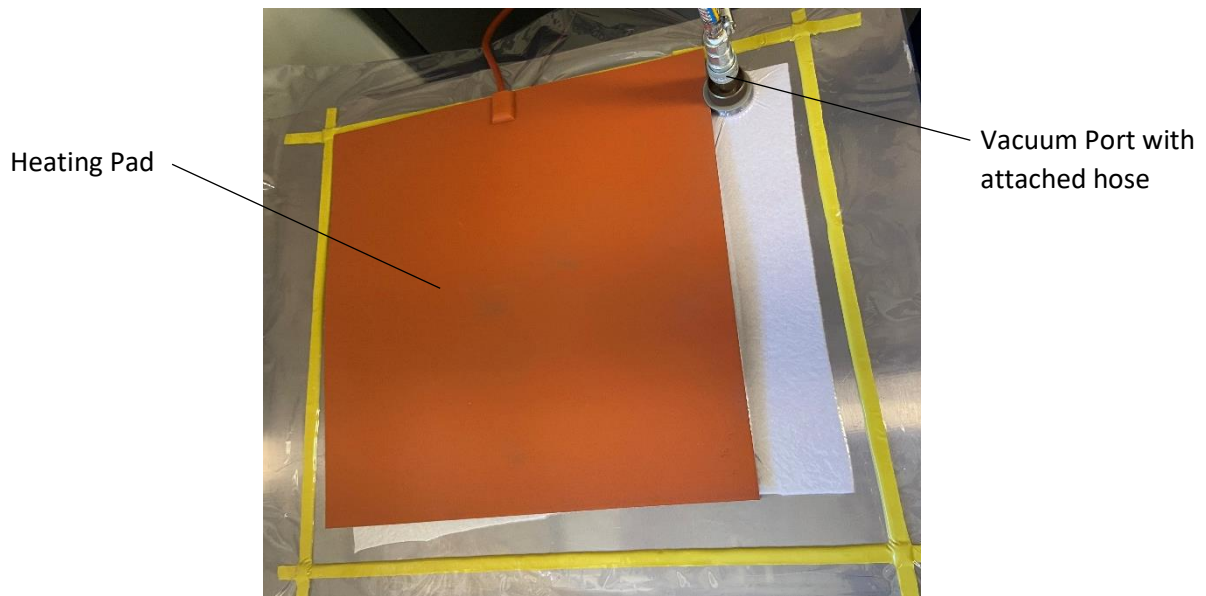
Heating Pad

Vacuum Port with attached hose

Figure 18: Heating pad placed over the bagging apparatus

Additional nylon material as well as a heavy glass cover has been placed over the heating pad to create a conducive and reasonably well insulated environment while also adding stability to the assembled apparatus. This has been shown in Figure 19 below.
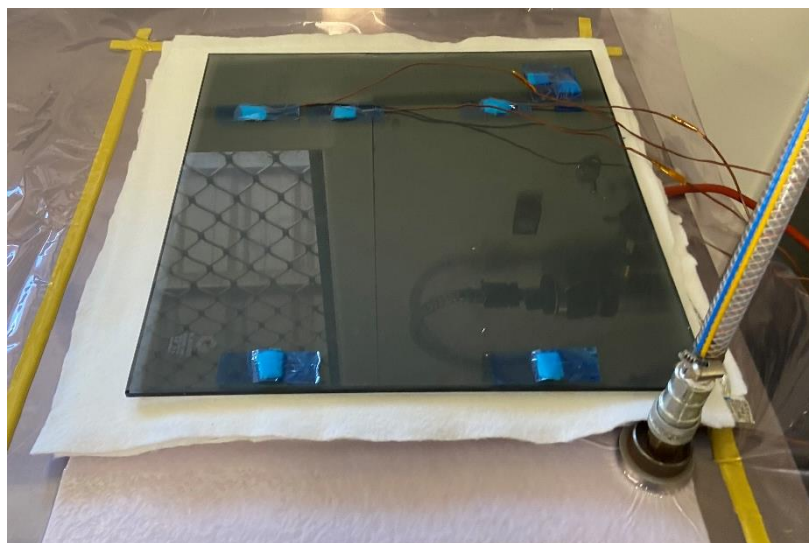
Figure 19: Fully assembled bagging and heating apparatus prepared for cure

FM300-2 is an adhesive designed to cure using out-of-autoclave methods such as SVD or DVD apparatus. It is designed to cure at 121℃ with a ramping rate of 1.7℃/min. The process for curing was specified by the supplier. The stages of the cure are given below:

1. Engage vacuum inside the vacuum bag
2. Initial ramp from ambient temperature to 121℃ at a rate of 1.7℃/min
3. Hold at 121℃ for a period of 90 minutes
4. Heating element return to ambient temperature
5. Vacuum released

4.4.5   Individual Specimen Preparation

Once the panels are cured the individual specimens were cut using a waterjet. It was outsourced to the Z4 HES Workshop at the USQ Toowoomba Campus. The specific piece of equipment that conducted the cutting was a Matcam V-Series Waterjet using a KTM Neoline 40i intensifier. This specific machine cuts at 60,000 psi and uses 80 grit garnet as the abrasive. Due to the nature of the waterjet cutting technique the edges of the samples aligned with the Ti64 component outline (in line with the honeycomb design where applicable). This pattern along the edges has the potential to create stress concentrations due to the decreased cross-sectional area at the indented points along the side however this will be inspected upon completion of testing to corroborate the theories accuracy.

Following this process each panel's bond line was assessed for its alignment to the opposite panel (to ensure it remains flush). Those that were not flush were subsequently deemed unacceptable and were then sanded to be as close to flush as possible (remaining cognisant that the Ti64 is an extremely resistant material). An example of the unacceptable bond overlap is depicted in Figure 20 below. It is then proceeded by a correctly sanded joint which has been deemed acceptable for this experiment in Figure 21.
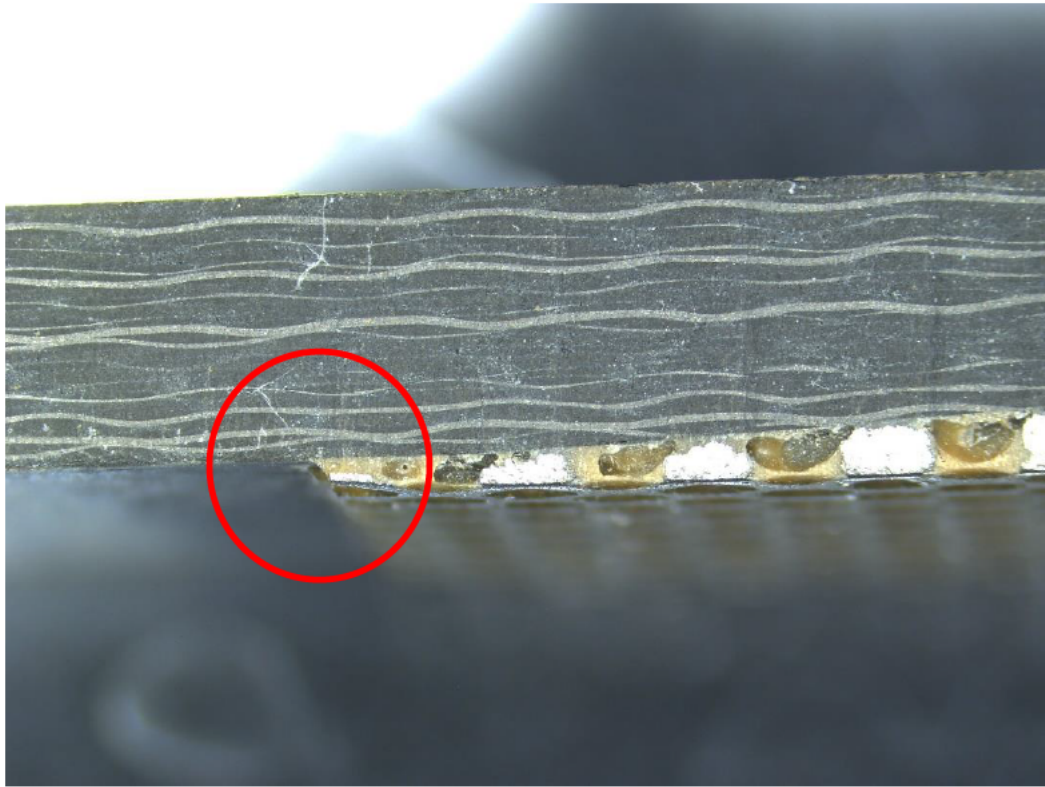
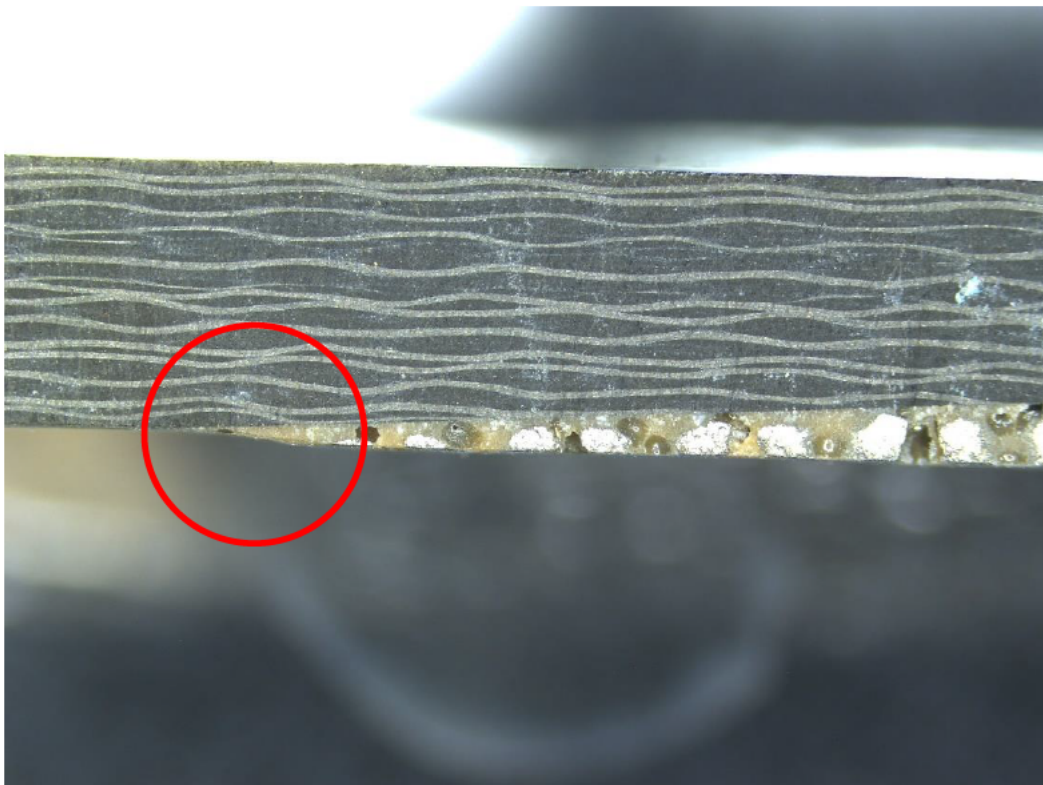*Figure 20: Unprepared overlap deemed unacceptable for testing*

Figure 21: Sanded bond-line deemed acceptable for testing

4.4.6   Specimen Storage

Due to the susceptibility of the composite material to moisture ingress and subsequent compromise it is vital, for all periods while preparation and fabrication are not occurring, to store specimens and materials in dry ambient conditions. This is particularly difficult to sustain when considering the possibility of volatile environmental conditions however should be maintained by monitoring the condition of samples daily.

4.5   Tensile Testing & Direct Image Correlation

Destructive testing, being tensile testing recorded via digital image correlation was determined as the optimal method to deduce answers to Research Questions 3, 4 and 5. This was achieved utilising a 100kN MTS Insight testing rig. The waterjet-cut specimens were numbered for traceability of results and reference to their original position within the panel. This was done to examine the behaviour of the specimens during loading and at the point of failure with the intent of examining a potential relationship between bond quality and mechanical performance.

Figure 22: Diagram of tensile testing and DIC rig setup (annotated)

In order to utilise the tensile testing rig shown above, the following steps were used to ensure adequate data sets were recorded:

1. Set up the digital image correlation apparatus pointing at the correct area of interest for the experiment (see Figure 22)
2. Utilising the focus and lighting tools on the apparatus ensure the image of the experiment is clearly visible on the screen of the attached computer
3. Adjust the 100kN MTS Insight rig grips to the correct height for the panel length
4. Set the loading rate of the rig to 1mm/min
5. Insert specimen into the loading rig and tighten the grips adequately to avoid slipping
6. Start the DIC recording
7. Start the testing using the 100kN MTS rig
8. Once completed the recording can be stopped and saved
9. Reset the testing rig software and remove the broken sample for examination
10. Repeat steps 5 to 9 for all remaining specimens

Once all specimens have been tested the resulting electronic files can be saved to an external storage device for further investigation. It is important to maintain two or more copies in the instance of lost or corrupt files occurring.

4.6   Microscopy Examination

The microscopic photographing of specimens occurs both before and after tensile testing has been conducted. The pre-experiment examination included the assessment of specimen dimensions in order to ascertain the average cross-sectional area. A series of photographs of the bonded interface also occurred in order to determine the percentage of porosity visible which would provide a general average of the porosity for that particular sample type (i.e. solid scarf, single adhesive honeycomb scar and double adhesive honeycomb scarf).

The microscopic examination conducted after testing was used to determine failure mechanisms through the interpretation of the scarf surface after failure had occurred. This investigation in conjunction with the pre-experiment analysis of the bond interface will offer insights to the answers to Research Questions 1, 2 and 5. This will ideally be combined with results given from the digital image correlation to determine the failure behaviour, failure mechanisms and bond quality for each specimen type.

4.7   Chapter Summary

Throughout this chapter the procedures selected and undertaken, aimed to bridge the identified knowledge gaps through the fulfilment of the aforementioned research questions. As highlighted numerous times in the literature review, special care must be taken to ensure contamination is prevented or mitigated against. The care taken in numerous stages of the experiment is clearly documented in this chapter. Although some stages were not within the experiment's direct control (outsourced components/machining etc.) the relative level of accuracy was maintained from the onset and throughout. The proceeding chapters will present the results, their interpretation, and a qualitative discussion of them.

5. Results

5.1 Chapter Overview

The images taken during pre-experiment inspection, the mechanical testing results, the post-experiment inspection images and digital image correlation have been portrayed and interpreted in this chapter. These results have then been compared to prior experimental testing of composite to composite bonded scarf joints as well as double vacuum bag procedure experiments in order to draw similarities or lack thereof between the different data sets. These comparisons will also be used to build a case around their validity.

In order to assess the standardization of sample size, physical measurements were taken prior to mechanical testing. These measurements were also used to assess the validity of results. Appendix H, I, J and K contain all recorded data including images and data sets from mechanical testing.

5.2 Sample Sizing

Due to the machining of elements being reasonably accurate and out of control of the experiment, the widths of the different sample types were cut at equal spacing according to the overall panel widths. The outsourced waterjet cutting divided the overall width into five equal segments to create individual specimens. The resulting specimen widths are given in Table 4 below. The thickness of each specimen has also been shown in Table 5. These measurements were taken using a set of calibrated digital Vernier calipers.

Sample	Average Width (mm)
Solid Sample	29.010
Honeycomb Pattern (single adhesive)	28.982
Honeycomb Pattern (double adhesive)	28.751

Table 4: Average widths of different sample types

Sample	Specimen Adhesive Thickness (mm)	Specimen Overall Thickness (mm)	Average Overall Thickness (mm)	Std Dev (mm)
1	0.2655	5.238		
2	0.3882	5.341		
3	0.3657	5.359	5.4572	0.0163
4	0.3341	5.382		
5	0.3296	5.366		
6	0.3060	5.355		
7	0.3205	5.361		
8	0.3160	5.350	5.3592	0.0117
9	0.3183	5.381		
10	0.2235 (outlier)	5.349		
11	0.6421 (cure issue)	5.328		
12	0.6501 (cure issue)	5.423		
13	0.5417	5.369	5.3682	0.0400
14	0.5440	5.391		
15	0.5424	5.430		

Table 5: Individual specimen thicknesses

The adhesive thicknesses tabulated above were measured using microscopic images to assess the thinnest adhesive point along the interface. This was conducted to best mitigate against the varying effects caused by the rough surface of the Ti64 components. The results displayed above align with the nominal thickness of the film adhesive being 0.41mm. The changes in thickness are believed to be a direct correlation between volatile percentage and the quality of adhesive consolidation. Specimen 11 and 12 produced only partially cured products which is believed to have caused the large adhesive thickness measurements displayed in Table 5. This fact should be considered while reviewing the tensile testing results.

Table 5 also expresses the overall thickness of each specimen. In accordance with the theorised behaviour of the adhesive during curing, the avenues of evacuation for volatiles is maximized at the edges of the panel sets (scarf design type). It is also important to note that for the honeycomb design scarf joints, the relative difference across the panels were significantly smaller (taking into account the effect of double adhesive on the final set of specimens) which is in line with the theory that a porous plate provides more readily accessible avenues of evacuation across the panel length.

Specific anomalies being specimen 1 and 10 were located in the same orientation to the heating pads and vacuum port, this is believed to have caused an effect known as resin starving. This effect causes the resin to be drawn out of the edge during curing which reduces the volume of adhesive in that location causing a thinner adhesive layer. This has the potential to obscure the final results of the experiment.

5.3   Pre-Experiment Microscopy

In order to generate a general estimate of porosity for each individual panel the bond-line was examined from both sides and averaged to determine the void volume percentage found within the cured adhesive film.

To determine the void density, the area of voids identified in the microscopic images of each panel's profile was recorded and averaged across both sides. Although this does not give a perfect indication of void content it is the closest that can be achieved without using non-invasive techniques such as ultrasonic or x-ray imaging. A segment of a specimen has been depicted in both Figure 22 and Figure 23 for reference.
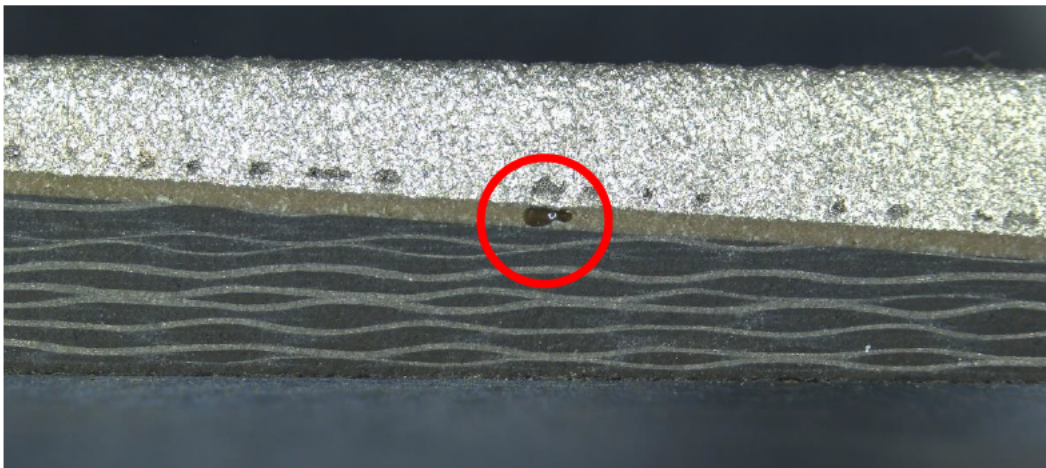
Figure 23: Microscopic image taken depicting a void in the adhesive of the solid sample scarf after curing has occurred (void highlighted using red circle)
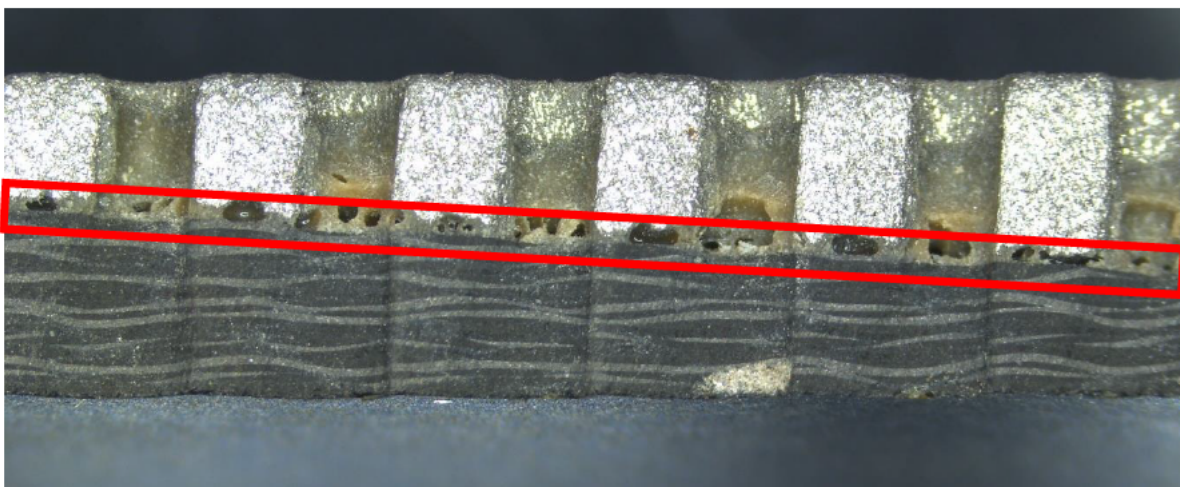
Figure 24: Microscopic image taken depicting the numerous voids in the adhesive interface of a honeycomb single adhesive film sample after curing (voids located inside the honeycomb pores are not of importance for investigation)

As shown in the images above, the void size can be calculated and the total area of all the voids combined can be used to determine the average void percentage of each of the specimens. This process has been recorded in Table 6 with the accompanying results. For the honeycomb specimens it is vital not to record voids which are located in the pores of the Ti64 components as they are not adhering the scarf joint together. This is relatively easy to identify with the resolution of the images available for examination.

Sample	Bond-Line Area (mm^2)	Void Area Side 1 (mm^2)	Void Area Side 2 (mm^2)	Average Void %
1	23.124	0.7692	1.1062	4.055
2	34.057	1.5498	0.6790	3.272
3	32.185	1.1020	1.0929	3.410
4	28.983	0.8103	0.7260	2.650
5	28.484	0.4615	1.2403	2.987
6	25.875	1.8914	0.8378	5.274
7	27.573	1.7029	1.1896	5.245
8	27.034	1.6507	1.1332	5.149
9	27.205	1.6601	1.0707	5.019
10	19.310	1.2132	0.9519	5.606
11	55.169	Uncured specimen		
12	55.831	Partial/Uncured specimen		
13	46.613	0.2105	0.1056	0.339
14	47.491	0.0260	0.0669	0.098
15	47.346	N/A	0.3938	0.832

Table 6: Individual specimen adhesive void percentage

Table 6 provides valuable information which trends can be drawn from. However, before delving into these trends it is important to note the clear issue surrounding specimen 11 and 12. These samples did not cure correctly and as a result the voids did not form correctly. This produced a void percentage of 0% which intuitively is not correct for this scenario. This narrowed the pool of specimens for the solid sample scarf joint to 3 results.

Interestingly the double film adhesive (samples 1-5) produced consistently lower void percentages when compared to the single adhesive film despite having a thicker adhesive interface. This is believed to be a result of the location of the samples in relation to both the heat pad and vacuum port during the curing process.

Contrary to the original hypothesis, the solid scarf samples produced extremely low void percentages despite having far less avenues of evacuation for volatiles. This unusual result is believed to be caused by the panel positioning in relation to the vacuum port (as it was closest to the port). However, this

positioning also meant that the edge of the panel was much closer to the edge of the heat pad causing inadequate temperature control resulting in the uncured segment being specimen 11 and 12.

Examining each specimen type it is evident that the edges produced a much more readily accessible avenue of evacuation for the volatiles, which in turn produced a lover void density in the adhesive. This affect was somewhat counteracted due to the aforementioned resin starving cases which cause a decrease in adhesive thickness. The decrease in thickness of the adhesive meant that whatever increased benefit was experienced due to the decreased void density was somewhat counterbalanced cue to the limited volume of adhesive available.

5.4   Tensile Testing

Tensile testing was conducted on 14 of the 15 specimens listed in Table 5. Specimen 11 did not cure correctly and therefore the bond failed during the apparatus set up for tensile testing. Prior to testing it was also identified that specimens were displaying effects caused by water ingress at the base of the composite panel. This is believed to have been caused by humid weather however due to their length it did not impede on the testing area of the specimens and therefore was not considered to impact the results. The results shown are indicative of the listed thicknesses and widths given in Table 4 and Table 5. The strengths of each sample are given below in Table 6.

Sample	Cross-Sectional Area (m^2)	Force (N)	Tensile Strength (MPa)
1	0.000156348	28150.275	180.049
2	0.000156434	26476.354	169.249
3	0.000156952	25324.057	161.349
4	0.000157613	25044.012	158.896
5	0.000157153	21913.963	139.443
6	0.000155199	13753.031	88.615
7	0.000155373	14938.824	96.148
8	0.000155054	18273.340	117.851
9	0.000155952	16924.881	108.526
10	0.000155025	12990.564	83.797
11	N/A	N/A	N/A
12	0.000154420	16912.410	109.522
13	0.000155755	19388.730	124.482
14	0.000156393	20734.027	132.576
15	0.000157524	19794.430	125.660

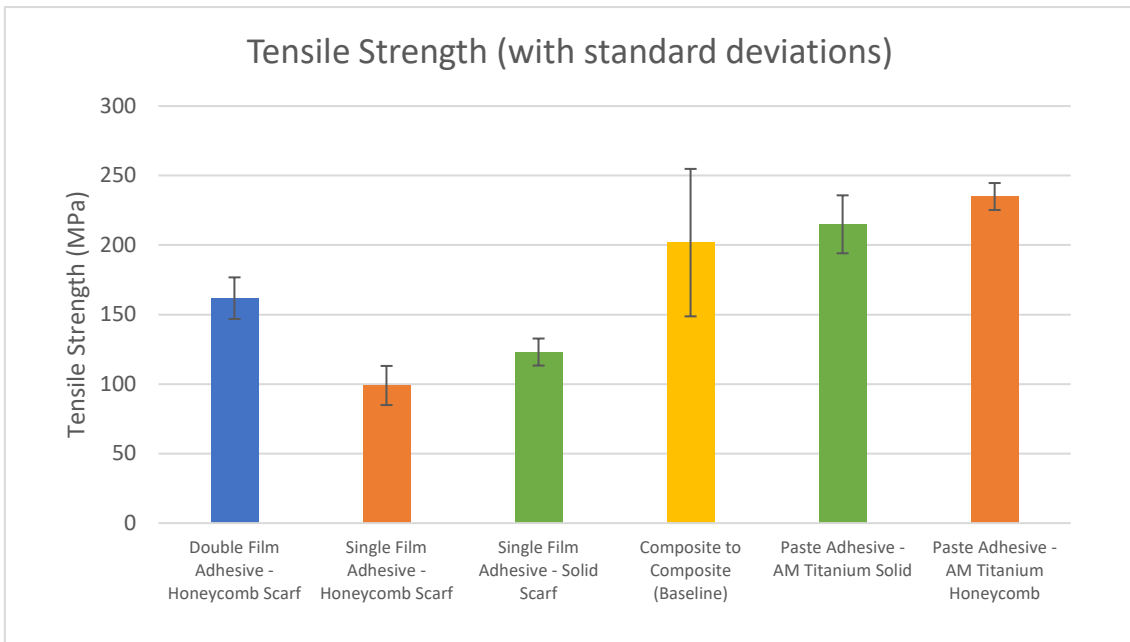*Table 7: Individual specimen cross-sectional areas and strengths*

Figure 25: Categorised specimens' tensile strength with standard deviations
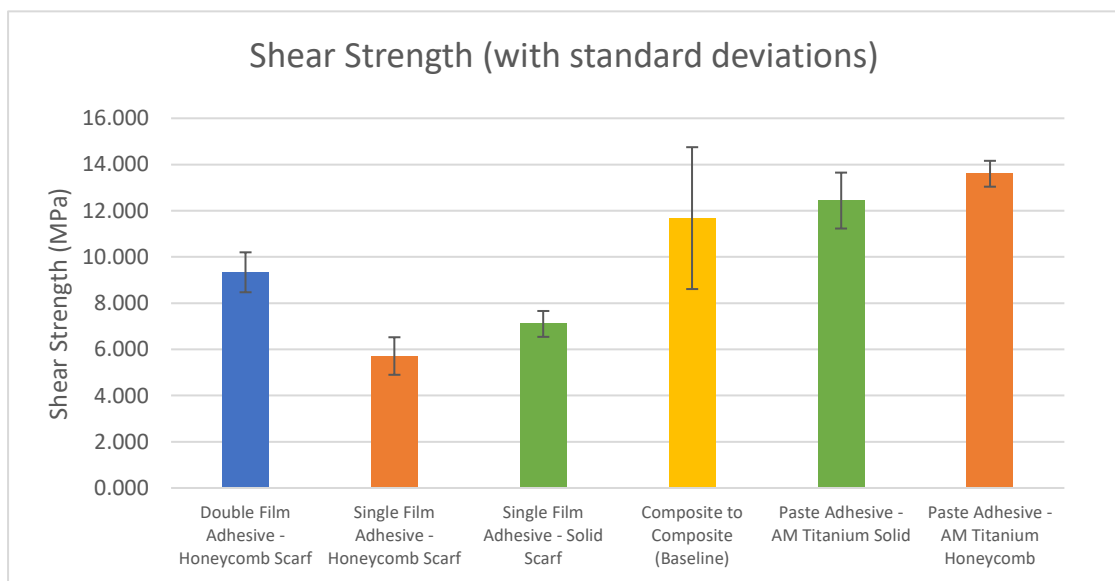

Figure 26: Categorised specimens' shear strength with standard deviations

Figure 25 and 26 depict the tensile strength and shear strength respectively for each of the tested scarf types with the addition of the paste adhesive results which were recorded by Assoc Prof Xuesen Zeng from USQ in an alternate investigation previously conducted. These additional results have been included to conduct a comparison and determine whether or not the film adhesive substitute is a viable option. From the figures above it is evident that the double adhesive honeycomb scarf joint displayed a higher strength than its single film adhesive counterparts despite its larger thickness which is often associated with high porosity and subsequent lowered bond quality.

This initial theory is believed to have been negated by the increased "traction" or gripping area inside the titanium honeycomb patch pores which allowed the increased volume of adhesive to meld the two materials together with an overall more consolidated bond.

The most evident result displayed in the tables is the significantly lower results displayed by the coupons tested in this experiment in comparison to those tested by Assoc Prof Xuesen Zeng previously. It is important to note the clear fluctuations in the baseline results which give rise to the possibility that the double film adhesive result could be comparable with the lower end of these results (standard deviation displayed for the composite to composite testing). The improvement seen in the experiments conducted specifically for this investigation was the controlled results producing decreased variability. This resulting smaller standard deviation intuitively indicates that the figures are more reliable despite being less desirable. Additionally, the failures seen in the film adhesive were at a much higher strain, possibly eluding to a more elastic failure mode.

Comparatively the void percentages could be correlated with the strengths for the honeycomb scarfs however the minimised porosity level found in the solid scarf produced a result that was between the honeycomb scarf tests. It is believed that the solid scarf produced accurate void results for the geometry of the test coupons however the honeycomb scarfs experienced what is known as "pull out". Pull out occurs when adhesive leaks through the designed pores of a panel. Intuitively this would provide many evacuation avenues for volatiles to exit the bond line however it also draws adhesive out of the bond line as well. Counterintuitively this also gives the opportunity for voids to form despite volatiles contained in the bond being minimised.

Defects identified in the initial microscopy were noted to be corroborated with the identified failure mechanisms using both DIC and post experiment inspection. Both of these topics will be discussed in the following sub-chapters.

5.5   Digital Image Correlation

The use of digital image correlation provides a more detailed view of the failure event allowing individual frames to be inspected while also providing figures regarding the strain of the coupon being tested (this is done through surface strain mapping). This "*frame-by-frame*" inspection can provide insights into the failure mechanisms by corroborating evidence found in the post experiment inspection with that given in the DIC.

Each DIC recording was reviewed with the key frame of interest for each experiment evaluated for significant features which could have an explanation for, or an impact on, the failure event. These key frames have been provided in Appendix J. Important features which were identified in the review have been displayed in the subsequent figures to provide context for the tabulated results in Table 8.

The following image demonstrates how the DIC calculates the strain of the specimen using strain mapping across the entire area of interest. The mapping has highlighted areas of high stress (red zones). These could also correspond to stress causing features which could induce premature failure or indicate bonding defects.
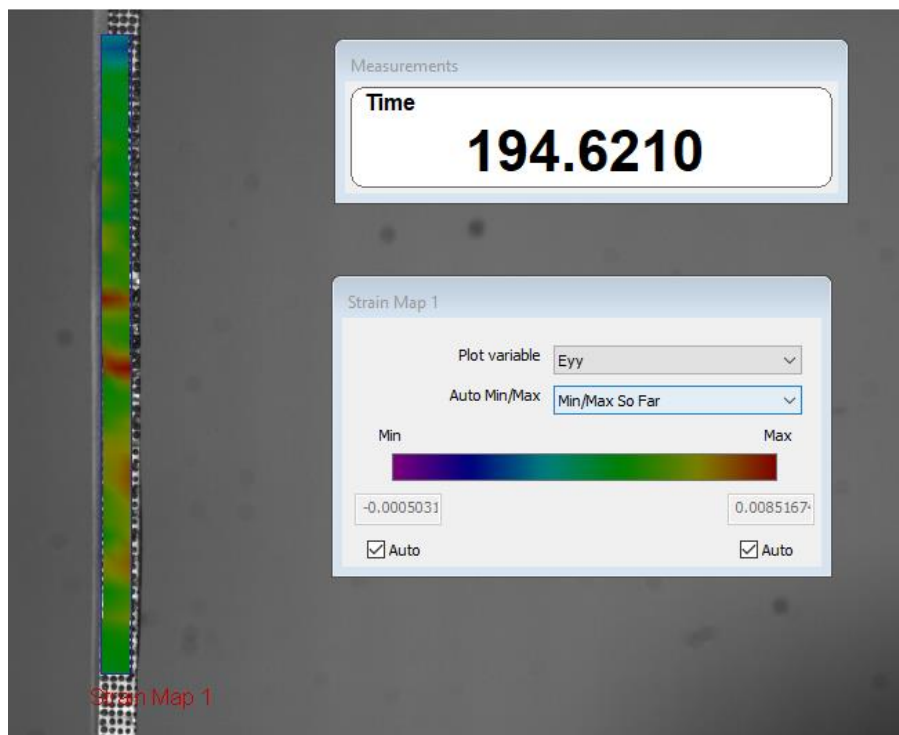
Figure 27: DIC strain mapping of specimen 1

Evaluating the DIC video recordings provides information for the single 2D side which is being recorded. The only useful information which could be drawn from review of such a video (exclusive of the strain measurements) was any evident fracture events, such as material fracture, or initial point of failure for the specimen. All other failure information could only be drawn from a post-test inspection.

The following image depicts the composite (left) fracture while the remaining failure below this point can be grouped generally into either a cohesive or adhesive failure (including the interface). This failure event evidently was the initiation point of the coupon failure indicating a possible stress fracture or residual stress in the materials caused by a thermal mismatch.
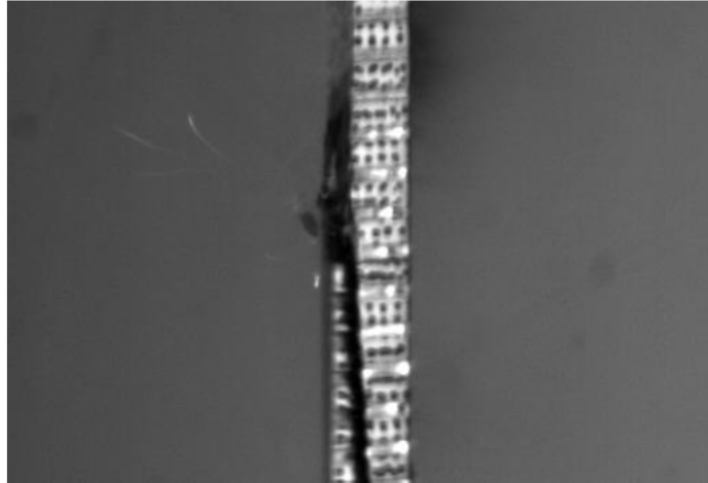
Figure 28: Composite Fracture at the time of failure, fracture projectiles can be seen to the left of the sample

The main point which was evident when evaluating the DIC video recordings was the high stress concentrations found in the indented sides created by the honeycomb pattern which had also been applied to the composite during the waterjet cutting stage of the sample preparation. Evidence of these concentrations can be seen in the following image set as darkened points which highlight the bond line on the 2D surface. It is also noteworthy to mention this was only experienced by the honeycomb scarf as the solid scarf displayed no signs of increased stress or strain prior to the failure event.
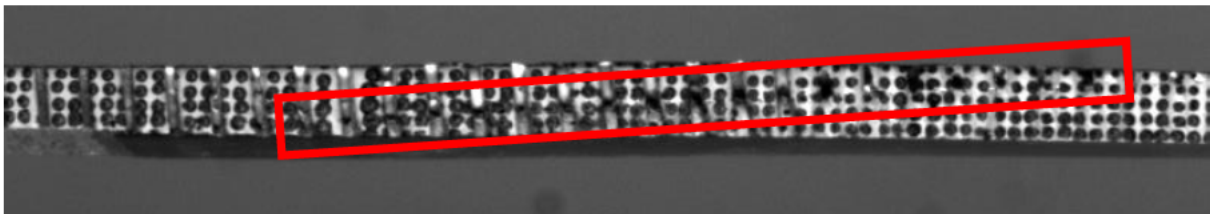
Figure 29: Stress concentration pattern visible as darkened points on the bond line (double film adhesive honeycomb scarf)
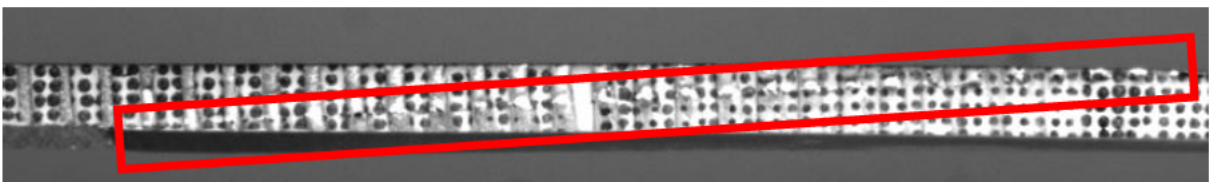
Figure 30: Stress concentration pattern visible as light points on the bond line (single film adhesive honeycomb scarf)

The following table details the failure characteristics of each sample as dictated by the DIC images and strain measurements.

Specimen	Failure Strain (%)	Failure point (Stress)	Additional Notes
1	2.331	through composite tip	The specimen displayed evidence of stress concentrations halfway down the specimen.
2	2.388	through composite tip	Specimen displayed stress concentrations in the honeycomb outline along bond line.
3	2.123	through both tips	Specimen failed through composite tip with a stress concentration shown at the titanium tip.
4	2.301	through composite tip	N/A
5	1.899	through both tips	Fracture of both titanium and composite ends occurred however titanium tip only partially fractured.
6	1.141	centre of specimen	Centre of specimen initiated the failure however the composite tip still fractured.
7	1.248	midsection of bond line	Failure initiated towards the titanium tip however failure through the composite tip occurred.
8	1.639	at titanium tip	Failure initiated at titanium tip which propagated along bond line before fracturing at composite tip.
9	1.501	through titanium tip	Initiated at titanium tip with fracture through the titanium tip and propagation along the bond line.
10	0.999	at titanium tip	Initiated at titanium tip with partial fracture occurring and failure propagating along the bond line.
11	N/A (premature failure)		
12	1.259	at titanium tip	Failure occurred at the titanium tip with simultaneous propagation up the bond and fracture of the composite tip.
13	1.811	at titanium tip	Failure occurred at the titanium tip, noticeable substrate failure or an exchange of bond interface failure can be witnessed before a fracture through the titanium tip occurs.
14	1.822	separation of titanium tip	Initial separation of the titanium tip occurs very prematurely to the specimen failure event, this concentration propagates along the bond line with the simultaneous major failure of the midsection of the composite scarf.
15	1.503	at titanium tip	Initial failure occurs at the titanium tip with the similar secondary events at specimen 14 being the propagation and subsequent major failure of the composite midsection.

Table 8: DIC data for failure events of all tested specimens

The data tabulated in Table 8 will be corroborated using the post-experiment inspection via microscopy in the following sub-chapter to infer the correct failure mechanism is determined.

The video recordings showed a peculiar behaviour of all specimens before and during the mechanical testing. This behavioral feature was the noticeable twisting or torque of the unloaded coupons. This potentially indicates varying levels of residual stress due to the thermal mismatch between the composite and the titanium or potentially between the adhesive and the parent materials. It is noteworthy to mention that the degree of twisting which is depicted in the videos can generally be grouped at distinct degrees of severity using the class of bond and scarf pattern.

The most severe twisting was experienced by the double adhesive honeycomb scarf followed by the single adhesive honeycomb scarf and lastly the single adhesive solid scarf showed little signs of twisting or torque in the samples. This twisted form may have contributed to the fracture experienced at the composite tip for both the single and double adhesive honeycomb scarfs as this appeared to be a common theme throughout the failures. This could be credited to the lower shear strength of the composite when compared to the titanium material or potentially indicating a failure of the material before the bond which would intuitively indicate a bond with high quality consolidation.

5.6   Thermal Stress Comparison

It is evident from the data in the previous chapters that the film adhesive has performed to a lower standard than previous studies which used a paste adhesive for bonding. This is counterintuitive when considering the significantly higher level of control on the variables for the film adhesive and the conditions surrounding each respective adhesive type. This decreased performance may be explained due to the dissimilar materials and their corresponding mismatched properties, specifically the coefficient of thermal expansion (CTE).

During the curing stage of specimen preparation both materials are subject to a raised temperature for an extended period of time. Intuitively each material will react differently (given that the CTE are different for both material) which has the possibility to create residual stress in the specimen structure and influence the results when cooled to ambient temperature.

Depending on the method of manufacture, the accuracy of production and the layup design of the fibres found within the composite the coefficient of thermal expansion can range from $-0.3\text{x}10^{-6}/℃$ to $-1.2\text{x}10^{-6}/℃$ (Nippon Steel, (Unknown)). As per the AZO Materials (2020) online resource library, titanium alloy (Ti6Al4V) has a CTE ranging from $8.7\text{x}10^{-6}/℃$ to $9.1\text{x}10^{-6}/℃$. Due to the inability to create a perfect material with extremely precise properties both ranges must be considered when evaluating the thermal stress between them.

In order to reconcile the difference in results from the mechanical testing and possibly provide greater insight into the failure behaviour of the specimens the thermal stress will be calculated for the different material properties. Two specific thermal stress scenarios will be considered, these will provide a range of possible outcomes which could have influenced the mechanical testing of the specimens.

Firstly, the largest magnitude of coefficient thermal expansion values (largest difference between the values which will provide the upper boundary for possible thermal stress) and then the smallest values (smallest difference will provide the lower boundary for thermal stress). An important observation to note is the different behaviour expected by both materials. The composite will expand as temperature decreases due to the negative coefficient while the titanium will contract due to its positive coefficient. These opposing behaviours will create stress within the bond as the temperature changes in order to maintain contact with both material interfaces.

In both scenarios the environmental conditions remain the same. These being a rise from ambient air conditions up to 121 degrees Celsius followed by a return to ambient air conditions. From we can take the initial air condition as 121 degrees Celsius with the final temperature being approximately 20 degrees Celsius. This is because the bond is not formed until it has been exposed to a 121-degree temperature for an extended amount of time.

Because residual stress cannot be directly measured it must be calculated using thermal strain which is causally related to the coefficient of thermal expansion through the equation shown in Figure 31. The following sub chapters will explore the aforementioned scenarios through the use of the equations in Figure 31.

$$E = {}^{\sigma}/_{\varepsilon} \qquad (1)$$

$$\varepsilon = {}^{dL}/_{L} \qquad (2)$$

$$ {}^{dL}/_{L} = \alpha * DT \qquad (3)$$

Figure 31: Relationship of equations between residual stress and thermal strain

Where E is the modulus of elasticity, ε is the strain, σ is the stress, L is the original characteristic length, dL is the change in length, α is the coefficient of thermal expansion and dT is the change in temperature.

5.6.1   Thermal Stress Upper Boundary Scenario

Considering the stress of each material and combining the magnitudes will provide the theoretical estimate of the total residual thermal stress on the bond interface. In this specific scenario the coefficient of thermal expansion for both the composite material and titanium alloy are given as; -1.2x10⁻⁶/℃ and 9.1x10⁻⁶/℃, respectively, and the estimated modulus of elasticity are 135 GPa for the composite and 110 GPa for the titanium alloy.

From Figure 31, if equation 3 is substituted into equation 2 and the new equation 2 is then substituted into equation 1 the following relation can be drawn for the residual stress:

$$\sigma = E * \alpha * DT \qquad (4)$$

Figure 32: Direct relation between stress and thermal strain

Using equation 4 from Figure 32 above.

Residual stress of the composite:

$$\sigma = 135 * 10^9 * -1.2 * 10^{-6} * (121 - 20)$$
$$\sigma = -16.362 \, MPa$$

Residual stress of the titanium alloy:

$$\sigma = 110 * 10^9 * 9.1 * 10^{-6} * (121 - 20)$$
$$\sigma = 101.101 \, MPa$$

Therefore, the total residual stress is the composite stress subtracted from the titanium residual stress giving a final result of 117.463 MPa of total residual stress within the bonded structure interface.

5.6.2   Thermal Stress Lower Boundary Scenario

Considering the stress of each material and combining the magnitudes will provide the theoretical estimate of the total residual thermal stress on the bond interface. In this specific scenario the coefficient of thermal expansion for both the composite material and titanium alloy are given as; -0.3x10⁻⁶/℃ and 8.7x10⁻⁶/℃, respectively, and the estimated modulus of elasticity are 135 GPa for the composite and 110 GPa for the titanium alloy.

Using equation 4 from Figure 32 above.

Residual stress of the composite:

$$\sigma = 135 * 10^9 * -0.3 * 10^{-6} * (121 - 20)$$
$$\sigma = -4.090 \, MPa$$

Residual stress of the titanium alloy:

$$\sigma = 110 * 10^9 * 8.7 \ * \ 10^{-6} * (121 - 20)$$
$$\sigma = 96.657 \ MPa$$

Therefore, the total residual stress is the composite stress subtracted from the titanium residual stress giving a final result of 100.747 MPa of total residual stress within the bonded structure interface.

5.6.3   Thermal Stress Summary

From the previous theoretical calculations, we can see a range between 100.75 MPa and 117.46 MPa of stress which could potentially influence the mechanical performance of the bonded scarf joints. It is important to note these calculations will align more closely with the solid scarf scenario due to the geometry and behaviour during expansion and contraction. The honeycomb pattern will expand both outwardly and into the honeycomb pores while the solid scarf will only expand outwardly as there is no internal space to consume during the expansion phase. Although the magnitude of expansion will remain the same due to the material properties, the localised direction and subsequent affects will vary slightly. Due to this fact it can be assumed that the residual stress will remain somewhat similar between the two titanium designs however the effect that the residual thermal stress has on the failure mechanisms will vary significantly.

Due to the geometry of the scarf joins and the 2-dimensional strain due to thermal changes, the effect of the calculated stress range will predominantly reduce the tensile strength rather than the shear strength of the materials. Figure 25 displays a decreased performance of around 40 MPa for the double film adhesive, 100 MPa for the single film adhesive and 75 MPa for the single film solid scarf samples in comparison to the composite to composite baseline results. This is counterintuitive when considering the increased control over variables in the bonding and sample preparation process when using a film adhesive. However, factoring an increase of between 100.75 MPa and 117.46 MPa for the residual thermal stress in the tensile directions indicates these figures are much more closely aligned being equal to or greater than the previously mentioned baseline.

Although the thermal stress offers insights into the reason for decreased mechanical performance there are a large number of other factors influencing the results which cannot be determined without further experimentation and investigation. Thermal influence and behaviour may also play a role in the failure mechanisms of certain samples. This will be investigated in subsequent chapters.

5.7   Post-Experiment Inspection (Failure Mechanisms)

Surface inspection via microscopy is a useful tool which can help corroborate theorised failure mechanisms which have been eluded to in the previous sub-sections of this chapter. Through the appropriate failure mechanism identification, the strength of the bond and subsequent bond quality can be validated. Surface observations were made which identify the underlying failure mechanisms for each sample. These were compared to the literature to validate the assumptions made on each inspection.

As eluded to in the previous sub-chapter there are multiple failure modes and mechanisms. The main categories are adhesive failure, cohesive failure, combination failure being both adhesive and cohesive failure, fracture of the material and finally substrate failure. Figure 33 provides a visual representation of these failures (excluding material fracture) and what occurs within the samples.
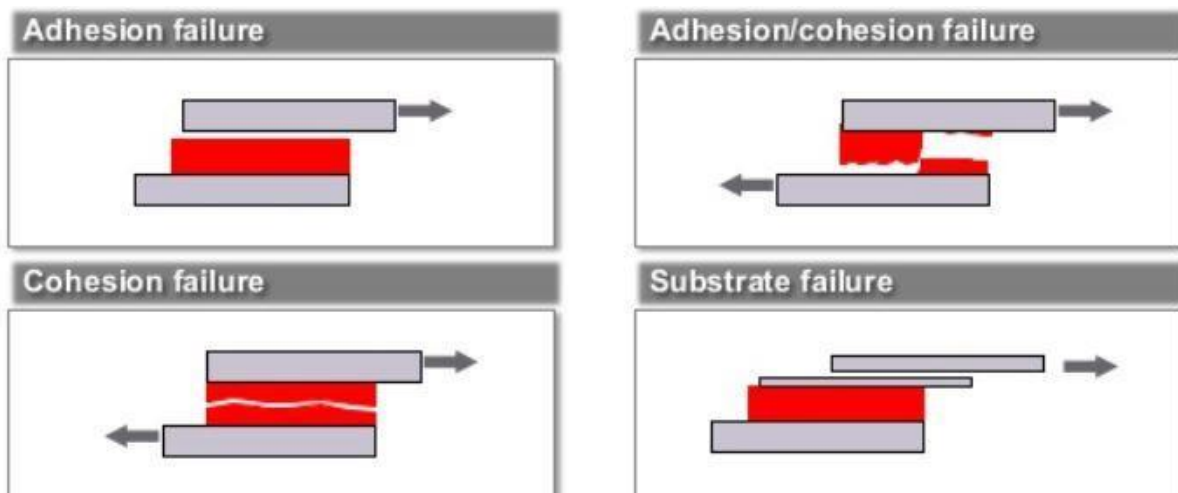
Figure 33: (top left): Adhesive failure, (top right): Adhesive and Cohesive combination failure, (bottom left): Cohesive failure, and (bottom right): Failure of the material substrate. (Brown, (2018)).

Figure 34 and Figure 35 highlight the key regions of failure using visual inspection of both a honeycomb and solid scarf testing coupon. On initial inspection it appears that both samples display a high amount of adhesive failure combined with material fracture which is indicative of a low-quality bond due to the lack of cohesive failure.
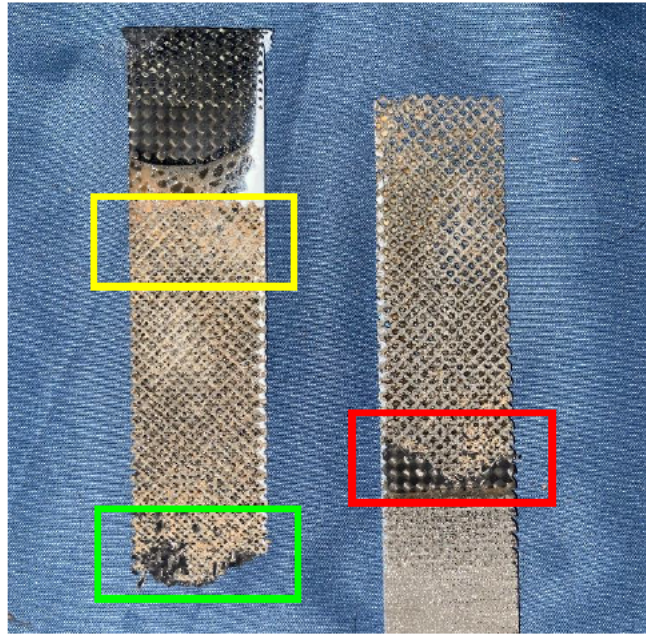
Figure 34: Initial failure mechanisms identified during post-experiment inspection of double film adhesive AM titanium honeycomb scarf, (yellow box): Adhesive failure, (red box): Combination adhesive and , and (green box): Composite fracture.
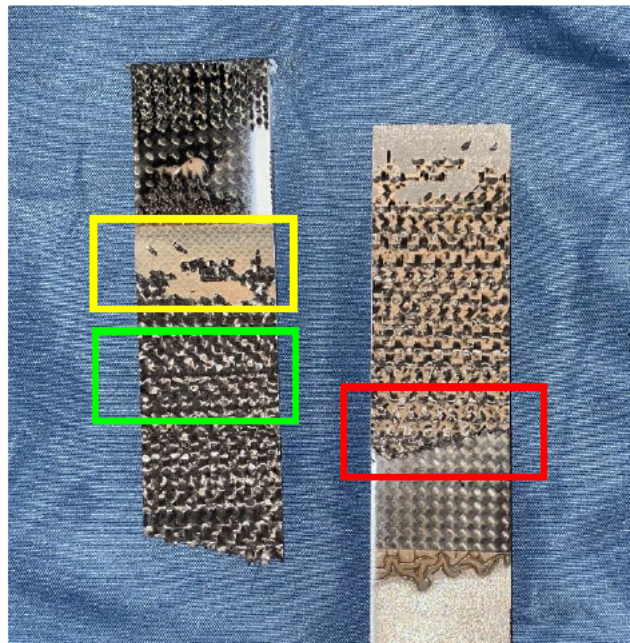
Figure 35: Initial failure observations of single adhesive solid scarf. (yellow box): Adhesive failure on titanium interface, (green box): Adhesive failure on composite interface, and (red box): Composite fracture.

Upon microscopic inspection these regions which were initially thought to have no evidence of cohesive failure actually show quite different observations than found at the outset. Further inspections will be investigated in the following figures.
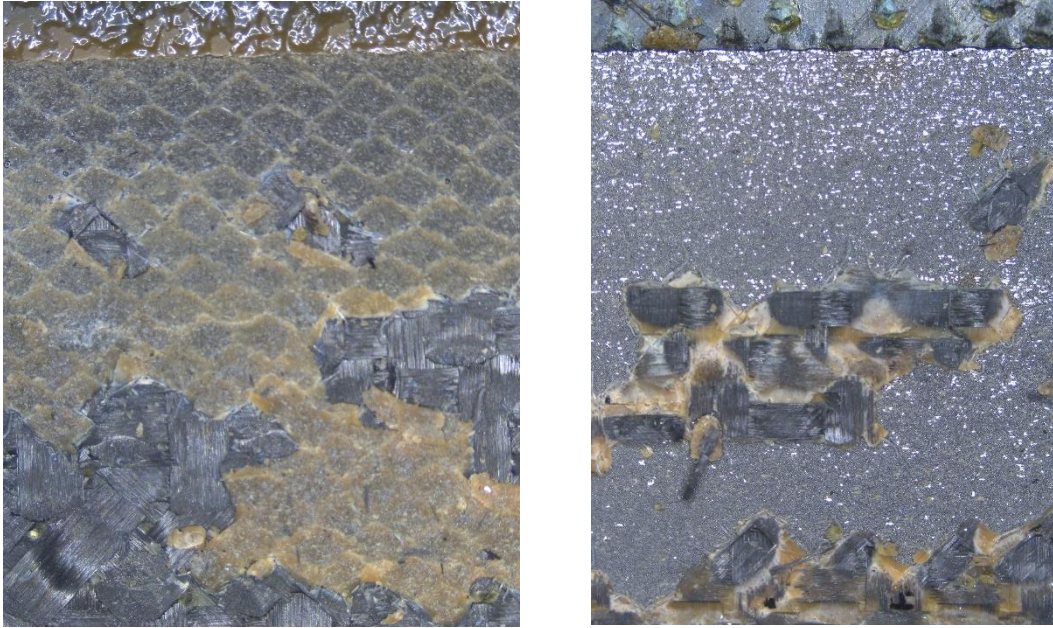
Figure 36: Failure observations for solid scarf sample. Left) Combination of adhesive failure along both material interfaces. Right) Failure of adhesive with evidence of composite substrate failure

As shown in Figure 36, the adhesive has failed along the titanium interface as well as through the composite substrate with no sign of cohesive failure occurring. Upon closer inspection a yellow sheen can be observed on the composite surface which indicates a successful bond however, in this instance the bond was found to be of lower quality with signs that it was predominantly unsuccessful. Conversely the bond failure seemed to transfer between the different material interfaces throughout the sample. This may be a result of the residual stress caused by thermal expansion and contraction or simply an inadequate cure.

An additional observation to be drawn from Figure 36 is the porosity throughout the adhesive which appears to be somewhat aligned with the originally calculated content for solid scarf samples. This observation affirms the calculations as correct with further evidence drawn from the specimen images examined from Appendix K.
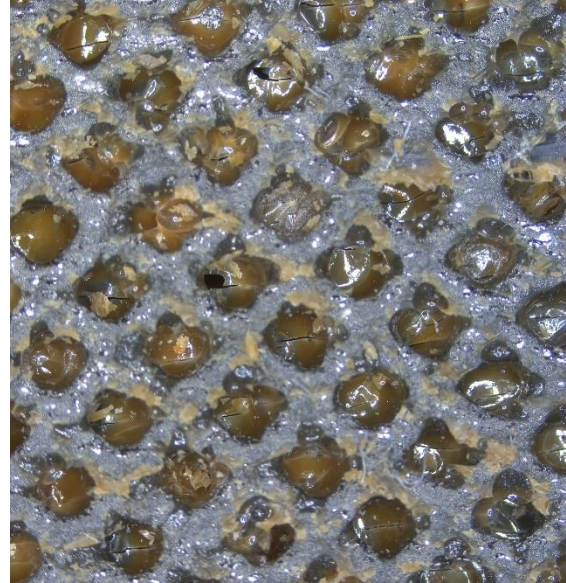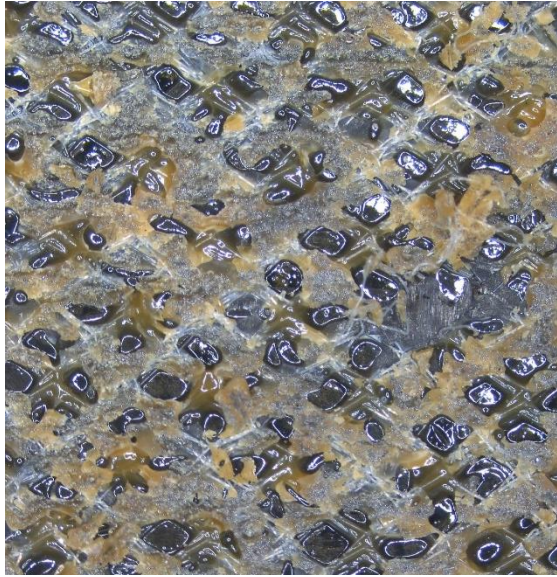
Figure 37: Failure observations for double adhesive honeycomb scarf sample. Left) Cohesive failure with evidence of adhesive failure. Right) Adhesive failure on titanium surface with evidence of cohesive failure.

Comparatively Figure 37 clearly displays much more evident signs of cohesive failure than Figure 36 as seen with the relatively uniform yellow sheen/particles displayed across both surfaces above. Both observations above indicate a successful bond to a varying degree. The porosity for this sample is much more difficult to observe due to the relatively intact sections of adhesive found in the honeycomb pore sections. Alternatively, the volume of adhesive found in the honeycomb pore sections is higher than anticipated which could indicate a decreased amount of adhesive which has been left to physically bond the two surfaces together. This could potentially hinder mechanical performance while inducing premature failure.
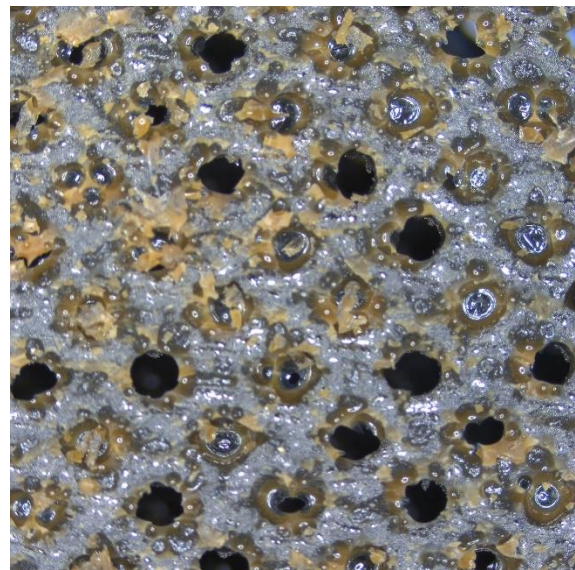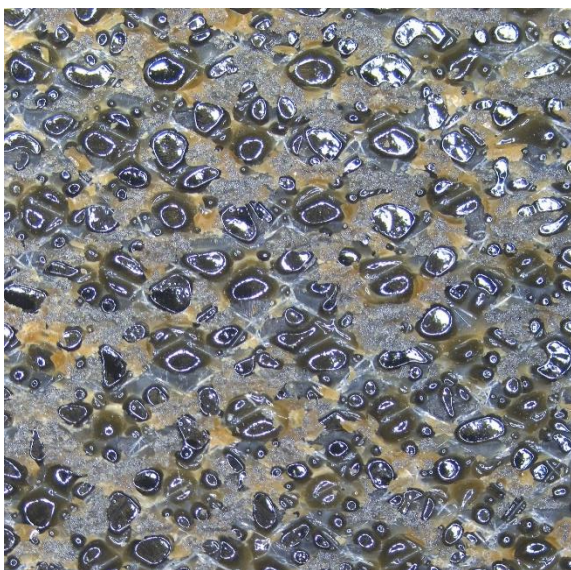
Figure 38: Failure observations for single adhesive honeycomb scarf sample. Left) Adhesive and cohesive failure with evidence of high porosity. Right) Cohesive failure with evidence of adhesive failure along surface interface of titanium

The somewhat similar visual representations of both Figure 37 and Figure 38 are very misleading. On initial inspection it may seem evident that the images display the same failure mechanisms, however on closer inspection it is observed that the single adhesive version actually contains a much lower cohesive failure area percentage and far more adhesive failure than it's double film adhesive counterpart. This also coincides with the increased void content which is also evident in the left-hand representation of Figure 38.

While the image on the right side of Figure 38 may appear to contain a large amount of cohesive failure indicated by the yellow particles surrounding the honeycomb pores, this is actually an indication of adhesive failure occurring through the very porous areas surrounding the honeycomb lattice pattern. As stated in previous chapters this correlates closely with the phenomena known as "pull out" which is when the adhesive is pulled through the honeycomb lattice during curing.

Using Figures 36, 37 and 38 as a guide the entire set of specimens were assessed for the dominant failure mechanism. This assessment was conducted through the use of visual inspection, microscopic imagery and regular photography combined with the digital image correlation results. For a comparison of failure mechanism and resulting failure strength the tensile testing results have also been included in Table 9.

Specimen	Dominant Failure Mechanism	Failure Strength
1	Cohesive failure with features of adhesive failure	180.049 MPa
2	Cohesive and adhesive failure with titanium fracture	169.249 MPa
3	Cohesive failure with minimal adhesive failure	161.349 MPa
4	Cohesive failure with features of composite material fracture	158.896 MPa
5	Cohesive and adhesive failure with composite fracture	139.443 MPa
6	Combination of Adhesive (30%) and Cohesive (70%) failure	88.615 MPa
7	Combination of Adhesive (50%) and Cohesive (50%) failure	96.148 MPa
8	Combination of adhesive (40%) and Cohesive (55%) failure with titanium fracture at scarf tip	117.851 MPa
9	Almost identical failure as specimen 8	108.526 MPa
10	Combination of Adhesive (50%) and Cohesive (50%) failure	83.797 MPa
11	Premature failure, with features of porous areas and uneven application of adhesive.	
12	Adhesive failure with significant composite substrate failure	109.522 MPa
13	Minor adhesive failure on titanium interface (10%), comprehensive composite substrate failure (85%) and minor composite fracture (5%)	124.482 MPa
14	Substrate failure of the composite with major fracture of the composite scarf	132.576 MPa
15	Minor adhesive failure on titanium interface (5%), comprehensive composite substrate failure (80%) and major composite fracture (15%)	125.660 MPa

Table 9: Failure mechanisms identified for each test coupon after mechanical testing

Table 9 provides an evident correlation between the dominant failure mechanism and resulting failure strength when considering the different adhesive thicknesses however does not offer the same insights when evaluating the difference between titanium scarf lattice types. Evaluating the double adhesive specimens (1 – 5) there is a clear increased failure strength with these test coupons displaying an overwhelmingly unambiguous failure mechanism, cohesive failure of the adhesive.

Despite the major failure mechanism of the single adhesive honeycomb lattice scarf being cohesive failure, the increased percentage of adhesive failure has reduced the failure strength by a considerable margin. The halving of cohesive failure area has reduced the failure strength by almost 40% in this case.

In the case of the single film adhesive solid scarf sample set the dominant failure mechanism was substrate failure of the composite material with a much higher frequency of composite fracture. Despite The comparison of samples with identical adhesive thicknesses and different titanium scarf lattice structure (single film honeycomb and single film solid scarf) offers a vague correlation between failure mechanism and failure strength. However, the same comparison provides much more detailed correlation about the affect of geometry and thermal stresses which could help improve the sample preparation stage of the experiment.

The major substrate failure experienced by all solid scarf samples indicate a bond which exceeds the strength of the substrate itself, this could be due to manufacturing defects however this is unlikely as the failure strength of the double adhesive samples was much greater with no substrate failure evident in post testing inspection. The most likely cause of this is due to the localised thermal stress which is not experienced in the honeycomb scarf due to the lattice structure expanding in a much smaller magnitude (around individual lattice pores). Although the substrate failed it still achieved a marginally greater failure strength than the single film alternative being the honeycomb lattice scarf.

From these results it can be observed that the use of additional adhesive provides opportunities for cohesive failure to occur more superlatively across the samples which in turn produce higher failure strengths. Additionally, the use of a honeycomb lattice aids the scarf's ability to disperse residual thermal stress in the adhesive which conversely causes solid samples to fail along the substrate rather than the adhesive. This will cause an increase of the failure strength but only due to the specific material properties associated with the failed material substrate.

A final observation to be drawn from Table 9 is the outlying sample being specimen 11. This test coupon failed prematurely prior to mechanical testing. This is believed to have occurred due to an inadequate cure identified in a pre-testing examination. The untested specimen showed evidence of

a red adhesive rather than a yellow adhesive bond interface. This clearly indicates an inadequate cure as the adhesive is red prior to the cure process and subsequently changes colour after curing is achieved. This poor bond is a direct result of the location of this specimen within the curing apparatus during the cure cycle causing the specimen to not achieve adequate temperatures which are conducive to a successful bond. Evidence of the prematurely failed bond can be found in Appendix K.

5.7 Chapter Summary

Through the successful demonstration of the methodology to achieve the aforementioned research question, plausible results were recorded and analysed for both theoretical and practical experiments. All achieved results and associated defects could be explained through analysis, the application of the methodology or other phenomena. While all result trends and correlations could be explained, the explored associated list of effects is not exhaustive but instead just the major effects which fall within the scope of this investigation. The results displayed in this chapter will be discussed in the subsequent chapter which intends to provide evidence and answers to the research questions proposed in this study.

6. Discussion

6.1 Chapter Overview

This chapter will explore the results found in the previous chapter in order to attempt most aptly to answer the research questions specified in Chapter 3. This result discussion will focus on the relationship between porosity, bond consolidation, adhesive variables and resulting strength. It will also draw effects from residual thermal stress and appropriate use of the methodology during sample preparation.

6.2 Research Question 1 Discussion

With regard to porosity and bond consolidation, does the SVD system produce an adequate quality of bonded scarf in comparison to previously conducted DVD processes?

The distinction of a successful bond from an unsuccessful bond can be credited to the void percentage observed in the bond line, adequate sample preparation and desirable failure strength observed in final testing of samples. As attempted in numerous previous studies, for the case of autoclave processed for bond curing, the ideal void percentage is 0%. OOA processes are a smaller version of the same technology which attempts similar quality bonds in order to achieve comparable resulting strengths. As stated by Feng et al. (2019) for each 1% increase in void percentage between 0% and 4% there is a 9% decrease of interlaminar strength.

The resulting void percentage for the solid scarf fell between 0% and 1% while the double film adhesive and single film adhesive honeycomb lattice scarf achieved roughly 4% and 5.5% respectively. This intuitively indicates the honeycomb lattice creates an inferior quality of bond in the case of the SVB system. The additional consideration of the failure strength of each sample type indicates a reduced quality of bond as the failure strengths produced are up to half the magnitude of the results produced by comparable DVD processes.

These clear indicators provide evidence that the quality of bond produced by SVD systems in this investigation are of lower quality in comparison to the bonds produced by DVD processes however the potential for other factors to be responsible for these decreased performance indicators is possible and as such, further investigations are recommended.

6.3   Research Question 2 Discussion

Is the single selected cure cycle effective for adhesion of both adhesive thicknesses?

As stated in the Research Question 1 Discussion, the metric used to assess the quality of a bond relies heavily on void percentage, failure strength and subsequent failure mechanisms observed after testing. Comparing the void percentages reveals that, for the honeycomb lattice scarf (which keeps all variables the same except for adhesive thickness), the double adhesive thickness actually achieved a much more desirable porosity percentage of around 1.5% of the total bond interface area less than its single adhesive counterpart. Although the void percentages were not desirable in comparison to the comparable DVD processes (being <0.1%) they displayed somewhat reasonable results considering the geometry of the titanium scarf.

An additional insight which can be taken directly from Research Question 1 Discussion is the failure strength comparison between the single and double adhesive honeycomb scarf against similar studies which have previously been conducted. When factoring in the residual thermal stress, the double adhesive actually displays an increased mechanical performance in comparison to the previous study baseline while the single adhesive does not achieve comparable results.

The final observation to consider from the results is the failure mechanism of the two adhesive types found through post-experiment inspection. The dominant cause of double adhesive failure was cohesive failure of the adhesive while the single adhesive failure had a much larger percentage of adhesive failure in the case of the honeycomb scarf and a somewhat inconclusive adhesive quality result being substrate failure in the solid scarf specimens.

These observations lead to the conclusion that the single selected cure cycle is effective for the double adhesive thickness but not effective for both adhesive thicknesses. However this cannot be definitively expressed as the results provide inconclusive evidence for single adhesive bond quality and as such would require further studies to be conducted possibly incorporating a larger range of adhesive thicknesses for solid scarf designs or potentially introduction of more alternative lattice structures.

6.4 Research Question 3 Discussion

Are the scarf repair strengths adequate in comparison to prior conducted composite-composite co-cured scarf repairs?

The comparison between the baseline and the experimental results has been shown in numerous instances throughout this investigation however when considering adequacy or "*fit for use*" the method of sample production should also be considered. With regard to explicit tensile strength found via direct mechanical testing we can see that the resulting strength is of lower magnitude than that of the baseline however that does not necessarily indicate that the repair strength is inadequate.

The most likely instance of adequate performance in the three sample types of this investigation is clearly the double film adhesive honeycomb scarf due to the failure behaviour and failure strength observed in testing. In line with Feng et al. (2019) the failure strength was around a 40% decrease from the baseline which is indicative of a porosity content percentage of around 4%, similar to that observed in the tested samples.

Additionally, considering the somewhat simpler set up and subsequent cure process surrounding the SVD system provides further reasoning as to why the scarf repair strength is adequate in comparison to the composite-composite co-cured scarf.

Despite these observations, the failure strengths are not adequate in comparison to the composite-composite co-cured scarf however are remarkably close to consideration for greater adequacy. A specific look at controlling both the porosity content and residual thermal stress would minimise or even reverse the failure strength decrease observed as a result of these effects.

6.5 Research Question 4 Discussion

Does the introduction of dissimilar material present any thermal mismatch creating discontinuity in failure behaviours?

Due to the inability to observe any definitive thermal strain or ensuing effects caused by a thermal behaviour mismatch, the failure strengths and failure mechanisms had to be correlated with theoretical calculations for residual thermal stress. This intuitively cannot provide conclusive answers to this question. Despite this, the resulting correlations found have been overwhelmingly promising and offer valuable insight into the failure behaviour and any potential thermal effects which may have caused them.

From the literature review an increase in failure strength was expected from the film adhesive due to the ability to both refine and control certain variables of the adhesive, including reduced porosity, constant adhesive thickness, temperature control of the cure cycle and sample preparation. The decreased failure strength can partially be accounted for due to the increase in porosity as previously stated however this does not create a clear margin of increased performance. This lowered performance from the expected result could be accounted for due to residual stress experienced from a thermal mismatch of the materials which is created after curing of the adhesive has occurred.

Calculations indicated a range between 100 MPa and 117 MPa of potential residual stress within each sample. Consequently, the strength of the samples tested are between 60 MPa and 120 MPa less than the baseline results. Factoring the theoretical thermal stress in conjunction with the loss of performance due to porosity would align much more closely with the originally predicted performance of this adhesive type.

The final observation to be drawn is the clear warping of samples after the cure cycle was conducted. In the DIC videography, it is evident that the samples have experienced deformation due to a temperature change. Although this is not definitive evidence of a thermal mismatch it does provide conducive evidence contributing to such a situation.

Overall, for the evidence given in this investigation, it can be said that a thermal material mismatch has induced a discontinuity in failure behaviours being failure strength and visual observation of the circumstances of the failure event.

6.6   Additional Insights

In addition to the observational points highlighted in the answers to the aforementioned research questions, results were produced which have little evidence of effects which were within the scope of this investigation. However, the trends or theoretical explanations to these results offer interesting insights into material behaviours, cure process quality and phenomena associated with the scarf and adhesive types.

As identified in the methodology, the geometry of both the scarf samples in conjunction with the apparatus size and orientation can play a strong role in the final bond quality produced. The location of the honeycomb lattice scarfs was seen to be closer to the centre of the heating pad while the solid scarf was orientated in such a way that it was more exposed to the ambient air. Despite having a

thermocouple directly on the bond-line, the side surface of the panel experienced significant temperature differences and failed to create a successful bond.

From this observation it can be stated that the DVD system, specifically referring to the apparatus and physical geometry, provides a more effective method for curing.

As identified in the results chapter, a phenomenon known as pull-out was observed in the honeycomb lattice structure. This phenomenon was actually experienced differently for each adhesive thickness. The double adhesive was theorised to have a higher chance for introduction of volatiles and a subsequent higher final void content however the pull-out of the double adhesive is believed to have also drawn the vast majority of volatiles out through the multitude of evacuation avenues. Despite drawing out a large percentage of the adhesive layer, the accompanying reduction in void content seems to have dramatically increased the mechanical performance of the double adhesive samples in comparison to the single adhesive samples.

This begs the conclusion that with the optimised adhesive thickness, the pull-out effect can actually be utilised to aid with reduced porosity and subsequent increased mechanical performance.

The final insight to be drawn from the results presented in this investigation is the comparatively different thermal behaviour of the solid scarf samples and the honeycomb lattice scarf samples. As viewed in the DIC and expressed by Pasternak et al. (2019) the localised effects of smaller structures can create thermal strains in multiple directions rather than the traditional "outward" expansion predicted for a single solid structure. Results indicated a clearly different failure mechanism between the different geometric scarf types with additional changes in the mechanical strengths.

It cannot be definitively stated that the thermal effects of different geometric scarfs are responsible for these changes however it is evident that discontinuity exists, and this is most likely due to the alternate thermal behaviours expected from these panel types.

6.7   Chapter Summary

This chapter has discussed observations drawn from the results in order to adequately answer the proposed research questions for the investigation. The observations have been interpreted to draw trends and insightful evaluations from the work conducted. Any research questions which were not able to be fully or conclusively answered were identified and the recommended further investigations were consequently expressed.

7. Conclusion and Recommendations

7.1 Dissertation Conclusion

The aim of this project was to assess the influence and effectiveness of SVB OOA processes for the preparation and resulting adhesion of 3D printed titanium in scarf ribbon repairs. This assessment was limited to a comparison with the quality of a cured film adhesive compared to a similar standard of results of an adhesive paste. Both scenarios did investigate the bonding of a 3D printed titanium 'patch' to a specific composite parent component.

This assessment and subsequent comparison were achieved through the experiment objectives identified in Chapter 1.4, as well as the research questions as previously mentioned from Chapter 3.3.3. As identified in Chapter 2.9 of the literature review, the majority of prior research studies conducted focused on the adherend behaviour or the theoretical behaviour of the bond line with very sparse emphasis on the adhesive itself. This area of study was nonexistent when investigating adhesive bonded dissimilar materials which is where the requirement for this study was borne.

Due to the absent presence of data and investigations surrounding this field of research, basic approaches and theoretical calculations were identified for use in this study combined with observations drawn from the literature were used to gather relevant results and gain an understanding of the characteristics both before and during testing. From these results the following observations were taken:

- The quality of bond produced by SVD systems are of lower quality in comparison to the bonds produced by DVD processes with respect to porosity, bond consolidation and resulting failure strength.
- Through the assessment of failure mechanisms and failure strength, the selected cure cycle is effective for the double adhesive thickness but inconclusive for the single adhesive thickness.
- The results produced by the SVD OOA system for adhesion of dissimilar materials were not adequate when compared to existing composite-composite co-cured scarf data regarding defect percentage and mechanical properties.
- Lastly, a discontinuity in failure behaviours was observed around the failure event as a result of a thermal material mismatch. This suggesting that selection of an alternate cure cycle with lower temperature differences could produce improved qualities.

Although additional research will contribute data to further improve the accuracy of assumptions or observations identified in this research, recommendations from current findings are:

The optimisation of bond adhesion occurs with the use of DVD systems in place of SVD processes where possible; cure cycles should be assessed and catered for different thicknesses; the use of dissimilar materials is ideal for small temperature changes as this will minimise discontinuities that will influence failure properties of the samples.

7.2 Recommended Further Experiments/Investigations

Despite the quality of work produced for the duration of this investigation, due to time constraints caused by the COVID 19 pandemic, the study was limited and could be further advanced through additional recommended investigations. These recommendations are:

- A repeated experiment with the film adhesive utilising expanded sample sizes which would help reinforce the findings from this investigation regarding porosity and failure behaviours;
- An additional repeat of the film adhesive experiment utilising DVD processes to address and attempt to reduce the high porosity content identified in this investigation;
- Refinement of cure cycle, which is catered for individual scarf characteristics, possibly using kinetics modelling as investigated in prior studies;
- A study to investigate flexural aspects of the repair which would provide greater insights into industry suitability for an aviation application
- Utilising the most promising 2D specimens to model and test more complex geometries or 3D patches.

The conduct of these additional investigations will improve the accuracy of results for this technology type and provide clarity on the suitability of the process for physical use in the aviation industry or wider material technology applications.

8.   References

Li Q, Djugum R, Sun S, Walker K, Choi J and Brandt M. 2017, "Repair and manufacturing of military aircraft components by additive manufacturing technology", 17th Australian International Aerospace Congress, viewed 10 October 2019, Conference Paper.

Fischer F and Kracht D. 2012, "Laser-based repair for carbon fiber reinforced composites", Machining Technology for Composite Materials, viewed 10 October 2019, https://www.sciencedirect.com/topics/engineering/aircraft-repair.

Singamneni S, Yifan LV, Hewitt A, Chalk R, Thomas W, et al. 2019, "Additive Manufacturing for the Aircraft Industry: A Review", Journal of Aeronautics and Aerospace Engineering, viewed 10 October 2019, Journal Article.

Battles B. 2003, "Maintenance Costs: Significant but Tricky", Aviation Pros, viewed 13 October 2019, https://www.aviationpros.com/aircraft/maintenanceproviders/mro/article/10387195/aircraft-maintenance-costs-significant-but-tricky

Liu R, Wang Z, Sparks T, Liou F, Newkirk J. 2017, "Aerospace applications of laser additive manufacturing", Laser additive Manufacturing P 351-371, viewed 13 October 2019, https://www.sciencedirect.com/science/article/pii/B9780081004333000130

Mason K. 2006, "Autoclave Quality Outside the Autoclave?", Composites World, viewed 14 October 2019, https://www.compositesworld.com/articles/autoclave-qualityoutside-the-autoclave

Alexander R. 2000, "Repairing Composite Surfaces", EEA Sport Aviation, viewed 15October 2019, https://www.eaa.org/eaa/aircraft-building/building-your-aircraft/whileyoure-building/building-articles/composite/repairing-composite-surfaces

Kramer, P., Friedersdorf, F., Williams, K. S., Jackson, D.A., Schultz, K.A., Sweitzer, T. 2018, 'Effect of mechanical stress and environmental conditions on degradation of aerospace coatings that guard against atmospheric corrosion', Corrosion Conference and Expo, Conference Paper.

Nicolaus, M., Möhwald, K., Maier, H.J. 2017, 'A Combined Brazing and Aluminizing Process for Repairing Turbine Blades by Thermal Spraying Using the Coating System NiCrSi / NiCoCrAlY / Al', Volume 26, Issue 7, pp 1659-1668.

Kim, G., Sterkenburg, R., 2017, 'Manufacturing or repairing composite parts and components using laser scanning technology', 32nd Technical Conference of the American Society for Composites, Volume 1, pp 66-77.

Khan, S.M.A., Es-Saheb, M., Mohsin, M.E.A., 2017, 'Fatigue life enhancement of cracked aerospace grade aluminium repaired with bonded composite patch: Experimental study' Volume 56, pp 1873-1878.

Chowdhury, N.M., Chiu, W.K., Wang, J., Chang, P., 2016, 'Experimental and finite element studies of bolted, bonded and hybrid step lap joints of thick carbon fibre/epoxy panels used in aircraft structures', Volume 100, pp 68-77

Saeed, K., Abid, M., 2015, 'Crack growth performance of aluminium plates repaired with composite and metallic patches under fatigue loading', 4th International Conference on Aerospace Science and Engineering. Article number 7489504.

Ružek, R., Doubrava, R., Raška, J., 2015, 'Wing repair using an adhesively bonded boron composite patch - Design and verification', Volume 6, Issue 2, pp 259-278.

Muda, M.K.H., Mustapha, F., Mohd Aris, K.D., Sultan, M.T.H., 2014, 'Fabrication technique for bio-composite patch repair on laminated structures of CFRP plate', Volume 564, pp 366-371.

Chowdhury, N., Chiu, W.K., Wang, J., 2014, 'Review on the fatigue of composite hybrid joints used in aircraft structures', Volume 891-892, pp 1591-1596.

IATA and MCTF, *Airline Maintenance Cost Executive Commentary—An Exclusive Benchmark Analysis of Maintenance Cost Task Force (MCTF) FY 2013*, IATA, 2014.

Katnam, K.B., Da Silva, L.F.M., Young, T.M., 2013, 'Bonded repair of composite aircraft structures: A review of scientific challenges and opportunities', Volume 61, pp 2642.

Wang C, Gunnion A, 2008, "On the design methodology of scarf repairs to composite laminates", Composites Science and Technology, viewed 15 October 2019, Journal article.

Adams, RD, Coppendale, J, Mallick, V and Al-Hamdan, H. 1992. The effect of temperature on the strength of adhesive joint. *Int. J. Adhes. Adhes.*, 12: 185–190.

Cagle, CHV. 1977. *Kleje i klejenie [Adhesives and gluing]*, Warszawa: WNT.

Preu, H and Mengel, M. 2007. Experimental and theoretical study of fast curing adhesive. *Int. J. Adhes. Adhes.*, 27: 330–337.

Pasternak, E., Shufrin, I., Dyskin, A.V. 2015. Thermal stresses in hybrid materials with auxetic inclusions. The University of Western Australia, viewed 05 October 2020, Research article.

Tawfik, B., Leheta, H., Elhewy, A., and Elsayed, T. 2016, "Weight reduction and strengthening of marine hatch covers by using composite materials", Volume 9, International Journal of Naval Architecture and Ocean Engineering.

Unknown author and date. Technical data of Carbon fibers and other materials. Nippon Graphite Fiber Coorporation, Data Sheet. viewed 11 October 2020, http://www.ngfworld.com/en/en_fiber/en_low_thermal_expansion.html

Unknown, 2002, "Titanium Alloys – Ti6Al4 Grade 5" U.S. Titanium Industry Inc. Editorial Feature, viewed 11 October 2020, https://www.azom.com/properties.aspx?ArticleID=1547

Wang, X.L., Hoffmann, C.M., Hsueh, C.H., Sarma, G., Hubbard, C.R. and Keiser, J.R., 1999, 'Influence of residual stress on thermal expansion behaviour', Applied Physics Letters, Volume 75, Issue 21.

Hyeon-Seok, C., Byeong-Su, K., Seong-Min, P., Viet-Hoai, T., Young-Woo, N. and Jin-Hwe, K., 2020, 'Tensile strength of composite bonded scarf joint in various thermal environmental conditions', Advanced Composite Materials, Volume 29, Issue 3 pp 285-300.

9. Appendices

ENG4111/4112 Research Project
Project Specification

For: Nicholas Wall

Title: Tailored Composite Scarf Repair with Additive Manufacturing

Major: Mechanical Engineering

Supervisors: Xuesen Zeng

Enrolment: ENG4111 – ONC S1, 2020
ENG4112 – ONC S2, 2020

Project Aim: To develop an initial manufacture and bonding process for 3D printed titanium components used in scarf ribbon repairs and qualitatively analyse the materials mechanical properties when bonded with a composite material.

Programme: Version 1, 18th March 2020

1. Review existing literature on adhesive methods, porosity effect and mechanical properties of 3D printed titanium.

2. Design of experiment, identifying parameters of the study from the literature review. (This includes developing a method for sample manufacture and adhesion)

3. Determine most desirable material properties to be evaluated including material microscopy, failure properties and comparison between the test sample design and manufactured geometry.

4. Review currently available facilities for conduct of experiment and data collection and select accordingly. (This is to include use of digital image correlation)

5. Design experiment detailing test equipment selection to appropriately address desired material properties. Ensure compatibility of manufacture method and experiment.

6. Liaise with project supervisor to ensure final experiment design is appropriate and achieves project objectives.

7. Demonstrate effective production of test samples, consistent adhesion and effective use of testing equipment in laboratory conditions.

If time and resources permit:

8. Compare and contrast results from experiment with results from previously conducted composite-composite bonded experiments.

9. Conduct additional tests using an embedded sensor in adhesive layer for more accurate and insightful results using an alternate method of data collection.

10. Make recommendations on further studies in composite scarf ribbon components.

Project Schedule - Original

Activity	Semester 1 (week 1 beginning 24 Feb)																	Recess			Semester 2													
	1	2	3	4	5	6	7	8	9	10	11	12	13	14	15	16	17	18	19	20	21	22	23	24	25	26	27	28	29	30	31	32	33	34
Supervisor Meetings				▓			▓	▓	▓	▓	▓	▓	▓	▓	▓	▓	▓	▓			▓		▓		▓		▓	▓		▓		▓	▓	
Phase 1 - Prework																																		
Resource Allocation and Checks				▓	▓																													
Phase 2 - Research																																		
Literature Review				▓	▓	▓	▓																											
Design of Experiment							▓	▓																										
Design of Fabrication							▓	▓																										
Results Expectation					▓	▓	▓																											
Phase 3 - Fab'																																		
Fabrication - Parent								▓	▓	▓	▓																							
Fab' - Titanium								▓	▓																									
Sample Analysis and Comparison											▓																							
Adhesion of Components											▓																							
Analysis of Bonding Morphology											▓	▓																						
Phase 4 - Testing																																		
Conduct of Tensile/Failure Mode Experiments (DIC)											▓	▓	▓	▓	▓	▓	▓	▓																
Material Morphology Record											▓	▓	▓	▓	▓	▓	▓	▓																
Analyse and Compare Results																		▓	▓	▓	▓	▓	▓	▓										
Identify and Interpret Trends																			▓	▓	▓	▓	▓	▓										
Phase 5 - Writing																																		
Prepare Draft Dissertation				▓	▓	▓	▓	▓	▓	▓	▓	▓	▓	▓	▓	▓	▓	▓	▓	▓	▓	▓	▓	▓	▓	▓	▓	▓	▓					
Feedback																														▓	▓			
Present - Prof' Prac 2																																▓		
Final Dissertation																														▓	▓	▓	▓	

Appendix C: FM300-2 Technical data sheet

FM® 300-2

FM® 300-2 film adhesive is a 250°F (121°C) cure version of Solvay's widely used FM® 300 film adhesive. It delivers the same superior high temperature performance, toughness and stress/strain properties of FM® 300 film adhesive without requiring a 350°F (177°C) cure cycle. In addition, FM® 300-2 film adhesive's processing window includes temperatures up to 300°F (149°C) providing a unique level of flexibility from one adhesive product.

FM® 300-2 adhesive was developed specifically for co-cure and secondary composite bonding applications. Through innovative curative technology, the required cure temperature is reduced allowing for secondary bonding of structure far below the composite's glass transition point. FM® 300-2 film adhesive also offers optimum flow control desirable for co-cure composite bonding.

In metal bond applications, FM® 300-2 film adhesive provides excellent moisture and corrosion resistance in high humidity environments with a minimal reduction in mechanical properties. To achieve consistent mechanical performance as well as maximum environmental resistance in bonding metallic details, the use of pre-cured BR® 127 corrosion inhibiting primer is recommended.

FM® 300-2 adhesive is available as an unsupported or supported film employing both knit and random mat carriers. A low-flow version of FM® 300-2 film adhesive for composite interleaving, designated FM® 300-2 interleaf adhesive, is also available.

Typical applications for FM® 300-2 include co-cure composite bonding, secondary composite bonding and vacuum-only processing common in repairs.

Features and Benefits

- 250°F (121°C) cure version of FM® 300 film adhesive
- Offers service temperatures from -67°F to 300°F (-55°C to 149°C)
- Excellent moisture and corrosion resistance in high humidity environments with no significant reduction in mechanical properties
- Over 25 years of flight history

- Displays similar stress/strain properties to FM® 300 film adhesive under both dry and wet conditions through 220°F (104°C)
- Ideal for co-cure and secondary composite bonding applications. Compatible with most thermoset and thermoplastic composite systems
- Recommended use with products BR® 127 Primer and FM® 410-1 Foaming Adhesive

CHARACTERISTICS

Table 1 | Physical Properties

Shelf Life	12 months at or below 0°F (-18°C) from date of shipment for supported form 6 months at or below 40°F (4°C) from date of shipment for unsupported form
Shop Life	20 days at or below 75°F (24°C)
Volatiles ASTM D 3530	1.0% maximum 250°F (121°C)
Outgassing Properties[1] (after complete cure) ASTM E 595	TWL - 1.35% CVCM - 0.08% WVR – 0.49%

[1] Properties based on FM 300-2K cured at 250°F (121°C) for 60 minutes.

Table 2 | Product Availability

Property	Film Adhesive	Nominal Weight[1] psf (gsm)	Nominal Thickness in (mm)	Color	Carrier
Product Forms	FM® 300-2K	0.100 (489)	0.016 (0.41)	Red	Knit
	FM® 300-2K	0.080 (391)	0.013 (0.33)	Red	Knit
	FM® 300-2M	0.050 (244)	0.008 (0.20)	Red	Random Mat
	FM® 300-2M	0.060 (293)	0.010 (0.25)	Red	Random Mat
	FM® 300-2M	0.030 (146)	0.005 (0.13)	Red	Random Mat
	FM® 300-2U	0.030 (146)	0.005 (0.13)	Red	Unsupported
Roll With	36, 48, & 50 in (91, 122, & 127 cm)				
Roll Length	60 yds (55 m)				

[1] Weight tolerance equals nominal weight ± 0.005 psf (± 24 gsm)

Table 3 | Physical Proerties: BR® 127 Corrosion Inhibiting Primer

Shelf Life	12 months at or below 40°F to 55°F (4°C to 13°C) from date of shipment
Shop Life	10 days at 90°F (32°C)
Color	Yellow
Solids	10% ± 1%
Density	7.30 lbs/gal (875 g/L)
Recommended Primer Thickness	0.10 – 0.30 mil (.0025 - .0076 mm)
Recommended Cure	Airy dry 30 minutes in ambient conditions Cure 30 minutes at 250°F (121°C)

PROPERTIES

Metal Bonding

Table 4 | Mechanical Performance: FM® 300-2 Film Adhesive with BR® 127 Primer[1]

Property	Test Temperature	FM 300-2K 0.10 psf (489 gsm)	FM 300-2K 0.08 psf (391 gsm)	FM 300-2M 0.05 psf (244 gsm)	FM 300-2M 0.03 psf (146 gsm)	Substrate
Lap Shear ASTM D 1002	°F (°C)	psi (MPa)				0.063 in (1.60 mm) 2024-T3 Aluminum
	-67 (-55)	4280 (29.5)	4580 (31.6)	4330 (29.8)	4000 (27.6)	
	75 (24)	5410 (37.3)	5900 (40.7)	4850 (33.5)	-	
	180 (82)	5200 (35.9)	5300 (36.6)	5150 (35.5)	-	
	250 (121)	3750 (25.9)	3730 (25.7)	3800 (26.2)	4040 (27.9)	
	300 (149)	-	2300 (15.8)	-	2960 (20.4)	
Metal-to-Metal Climbing Drum Peel ASTM D 1781	°F (°C)	in-lb/in (Nm/m)				0.020 in (0.51 mm) and 0.064 in (1.63 mm) 2024-T3 Aluminum
	-67 (-55)	17 (76)	18 (80)	20 (89)	23 (102)	
	75 (24)	33 (147)	35 (156)	31 (138)	30 (133)	
	180 (82)	39 (173)	40 (178)	35 (156)	33 (147)	
	250 (121)	39 (173)	38 (169)	35 (156)	31 (138)	
	300 (149)	-	40 (178)	-	33 (147)	
Honeycomb Sandwich Peel ASTM D 1781	°F (°C)	in-lb/3 in (Nm/m)				Skin: 0.020 in (0.51 mm) 2024-T3 Aluminum Core: 0.004 in (0.102 mm) NP 5052 DURACORE® II honey comb, 0.25 in (6.35 mm) cell, 7.9 pcf (0.127 g/cc) density, 0.50 in (12.7 mm) thick
	-67 (-55)	36 (53)	34 (50)	15 (22)	14 (21)	
	75 (24)	50 (74)	45 (67)	21 (31)	17 (25)	
	250 (121)	50 (74)	44 (65)	22 (33)	16 (24)	
	300 (149)	-	33 (48)	-	13 (19)	
Flatwise Tensile ASTM C 297	°F (°C)	psi (MPa)				Skin: 0.020 in (0.51 mm) 2024-T3 Aluminum Core: 0.004 in (0.010 cm) NP 5052 DURACORE® II honey comb, 0.25 in (6.35 mm) cell, 7.9 pcf (0.127 g/cc) density, 0.50 in (12.7 mm) thick
	-67 (-55)	1230 (8.5)	1080 (7.5)	950 (6.6)	612 (4.2)	
	75 (24)	1240 (8.6)	1120 (7.7)	892 (6.2)	592 (4.1)	
	180 (82)	1000 (6.9)	961 (6.6)	760 (5.2)	496 (3.4)	
	250 (121)	700 (4.8)	685 (4.7)	534 (3.7)	460 (3.2)	
	300 (149)	-	325 (2.2)	-	160 (1.1)	

[1] Primer: BR® 127 corrosion inhibiting primer, 0.0002 inch (0.005 mm) thick, cured 60 minutes at 250°F (121°C)

Metal Surface Preparation: FPL Etched

Cure Cycle: Heat to 250°F (121°C) at 3°F (1.7°C)/minute, hold at 250°F (121°C) for 90 minutes, 40 psi (0.28 MPa)
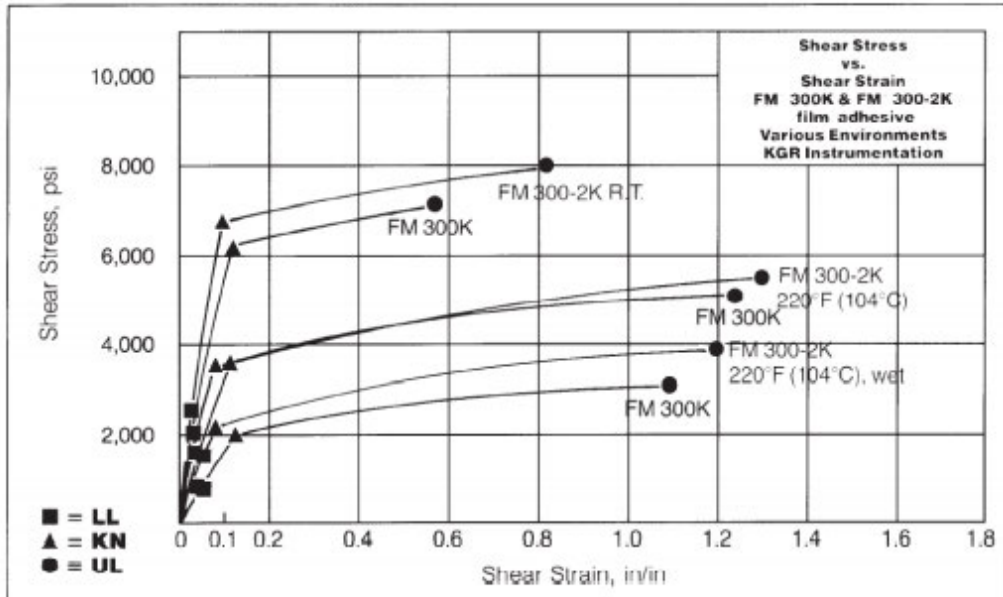
Figure 1 | KGR-1 Stress Strain Data for FM® 300 K vs. F M® 300-2K, 0.06 psf (293 gsm) with BR® 127 Primer

PROCESSING

Recommended Cure Cycle

Autoclave Cure Cycle   Apply full vacuum, 24 in Hg (0.081 MPa) minimum.
Apply 40 psi (0.28 MPa) pressure, vent vacuum at 20 psi (0.14 MPa).
Heat from 75°F (24°C) to 250°F (121°C) at 2°F - 5°F (1°C - 3°C)/minute.
Hold at 250°F (121°C) for 90 minutes.
Cool under pressure below 140°F (60°C) at 2°F - 5°F (1°C - 3°C)/minute.

FM® 300-2 film adhesive may also be bonded at pressures ranging from 15 psi – 100 psi (0.10 MPa – 0.69 MPa) depending upon the application.

Surface Preparation

Non-Metallic Cured Substrates

Most high performance composites employ a removable peel ply of nylon or Dacron® fabric. Remove the peel ply and bond immediately. For surfaces without peel ply:

1. Lightly sand the surface to be bonded using 240 grit – 280 grit sandpaper.

2. Clean the surface using clean cotton (lint free) cloth and MEK or acetone.

3. Dry thoroughly at 160ºF ± 10ºF (71°C ± 6°C) for 1 hour - 2 hours.

Aluminum Skins

A clean, dry, grease-free surface is required for bonding. FM® 300-2 is used with standard cleaning techniques involving a four step procedure of solvent degreasing, alkaline cleaning, chemical deoxidizing (etching), and phosphoric acid anodizing*. General guidance for etching and phosphoric acid anodizing can be found in ASTM 2651 and ASTM 3433, respectively. Best results for aluminum feature priming after appropiate surface preparation, with BR® 6747-1, BR® 6747-1 NC or BR® 127 primer.

*Boeing patent 4,085,012. April 1978. Phophoric acid anodizing is now being used by a large number of aircraft manufacturers due to the improved surface bond durability it provides.

Primer Application

Although not mandatory, BR® 127 corrosion inhibiting primer is recommended for use with FM® 300-2 adhesive in the bonding of aluminum details. BR® 127 primer offers superior durability and resistance to hostile environments within the bond line and also may be used as a protective coating outside the bonded areas. Apply BR® 127 as follows:

1. Allow BR® 127 material to warm to room temperature, 75°F (24°C), prior to opening container

2. Thoroughly mix before application and agitate during application

3. Spray or brush coat to a dry primer thickness of 0.0001 in (0.0025 mm) nominal with a 0.0003 in (0.0076 mm) maximum thickness.[1]

4. Air dry 30 minutes minimum prior to using

5. Oven dry 30 minutes at 250°F ± 10°F (121°C ± 6°C)

[1]For protective coating applications, increase primer thickness to 0.0004 in to 0.0010 in (0.010 mm to 0.025 mm)

LAY-UP PROCEDURE

1. When FM® 300-2 is removed from refrigerator storage, the adhesive must be allowed to reach room temperature [75°F (24°C)] before the roll is unpackaged. Note that the adhesive film is sandwiched between release paper and polyliner.

2. Remove either of the interliners and place the adhesive against the surface to be bonded. Care should be taken to prevent air entrapment between the film adhesive and substrate, especially in large area bonds.

3. If additional tack is desired, the adhesive may be heated to as high as 140°F (60°C) for up to 30 minutes without altering the adhesive properties. Before heat tacking, ensure the film is properly positioned, otherwise removal will be difficult.

4. Complete the assembly after removing the other interliner.

HEALTH & SAFETY

Please refer to the product SDS for safe handling, personal protective equipment recommendations and disposal considerations.

SOLVAY
asking more from chemistry®

University of Southern Queensland

Print View

USQ Safety Risk Management System

Version 2.0

Safety Risk Management Plan

Risk Management Plan ID: RMP_2020_4550	Status: Approve	Current User: i:0#.w|usq\u1039672	Author: i:0#.w|usq\u1039672	Supervisor: i:0#.w|usq\u8007520	Approver: i:0#.w|usq\u8007520

Assessment Title:	ENG4111/ENG4112 - Final Year Project	Assessment Date:	6/08/2020
Workplace (Division/Faculty/Section):	204010 - Faculty of Health, Engineering and Sciences	Review Date:	(5 years maximum)

Approver: Xuesen Zeng	Supervisor: (for notification of Risk Assessment only) Xuesen Zeng

Context

DESCRIPTION:

What is the task/event/purchase/project/procedure?	Single vacuum bag debulking, hot adhesive bonding and tensile testing of prepared samples with data collection.
Why is it being conducted?	In fulfilment of ENG4111/ENG4112 to contribute to the research topic in conjunction with Xuesen Zeng.
Where is it being conducted?	Lab building P11, USQ Toowoomba.
Course code (if applicable)	ENG4111/ENG4112

Chemical Name (if applicable)	FM 300-2 (film adhesive)

WHAT ARE THE NOMINAL CONDITIONS?

Personnel involved	Student - Nicholas Wall, Supervisor - Xuesen Zeng, Lab Contact - Brian Lenske.
Equipment	MTS 10kN testing machine, MTS 100kN testing machine, SANS compression machine, vacuum sealing machine, thermal heating pad with control sensors.
Environment	Laboratory conditions (P11)
Other	
Briefly explain the procedure/process	Using FM 300-2 film adhesive, scarf panels of 3D-printed titanium and composite material will be sanded and the surface prepared before being bonded using a single vacuum bag debulking hot bonding process. This will involve use of the vacuum sealing machine and thermal heating pad with control sensors for a period of around 3 hours.
	Following this the panels will be water-jet cut into appropriate sized samples by the engineering workshop.
	These samples will then be tensile and compressive tested using the aforementioned equipment and data recorded with the addition of digital image correlation for further data collection and behaviour analysis.

Assessment Team - who is conducting the assessment?

Assessor(s):	Xuesen Zeng
Others consulted: (eg elected health and safety representative, other personnel exposed to risks)	

Risk Register and Analysis

	Step 1	Step 2	Step 2a	Step 2b	Step 3			Step 4				
	Hazards: From step 1 or more if identified	**The Risk:** What can happen if exposed to the hazard without existing controls in place?	**Consequence:** What is the harm that can be caused by the hazard without existing controls in place?	**Existing Controls:** What are the existing controls that are already in place?	**Risk Assessment:** Consequence x Probability = Risk Level			**Additional Controls:** Enter additional controls if required to reduce the risk level	**Risk assessment with additional controls:** Has the consequence or probability changed?			
					Probability	Risk Level	ALARP		Consequence	Probability	Risk Level	ALARP
	Example											
	Working in temperatures over 35°C	*Heat stress/heat stroke/exhaustion leading to serious personal injury/death*	*catastrophic*	*Regular breaks, chilled water available, loose clothing, fatigue management policy.*	*possible*	*high*	*No*	*temporary shade shelters, essential tasks only, close supervision, buddy system*	*catastrophic*	*unlikely*	*mod*	*Yes*
1	Fracture frag...	High energy failure of sample can cause injury to members eyes or skin.	Moderate	Use of PPE (safety glasses, lab coats), guards on testing equipment, equipment tested and tagged in acordance with WHS requirements, supervisor on site at all times.	Rare	Low	☐					☑
2	Chemical exp...	Fume inhalation, exposure to skin.	Minor	Ventilated area, PPE (mask, safety glasses, lab coat, gloves), emergency wash down station nearby (prepped and tested by lab), accompanied by supervisor.	Unlikely	Low	☐					☑
3	Use of cuttin...	Unsafe use can result in personnel injury.	Minor	Appropriate supervision and PPE to be worn. Guards on equipment where possible and correct training/guidance provided.	Unlikely	Low	☐					☑
4	Exposure to s...	Skin burn, damage to material left nearby.	Minor	Designated area away from equipment, area is contained with a room to limit interaction, supervision of equipment during operation.	Unlikely	Low	☐					☑
5	Exposure to ...	Damage to hearing of personnel involved.	Minor	Appropriate use of PPE (hearing protection), ensuring machinery is serviceable, monitoring of equipment during use.	Rare	Low	☐					☑

Step 5 - Action Plan (for controls not already in place)

	Additional Controls:	Exclude from Action Plan: (repeated control)	Resources:	Persons Responsible:	Proposed Implementation Date:

Appendix E: Tensile Test Results

Sample	Cross-Sectional Area (m²)	Force (N)	Tensile Strength (MPa)	Average (Tensile)	Std Dev (Tensile)	Elongation @ Failure (mm)	Strain (%)	Shear Strength (MPa)	Average (Shear)	Std Dev (Shear)
1	0.000156	28150.28	180.049			3.0988	2.331	10.389		
2	0.000156	26476.35	169.249			3.1754	2.388	9.766		
3	0.000157	25324.06	161.349			2.8232	2.123	9.310		
4	0.000158	25044.01	158.896			3.0596	2.301	9.168		
5	0.000157	21913.96	139.443	161.7972	14.97486	2.525	1.899	8.046	9.336	0.864
6	0.000155	13753.03	88.615			1.5173	1.141	5.113		
7	0.000155	14938.82	96.148			1.6587	1.248	5.548		
8	0.000155	18273.34	117.851			2.1797	1.639	6.800		
9	0.000156	16924.88	108.526			1.9952	1.501	6.262		
10	0.000155	12990.56	83.797	98.9874	14.08206	1.3289	0.999	4.835	5.712	0.813
12	0.000154	16912.41	109.522			1.6735	1.259	6.319		
13	0.000156	19388.73	124.482			2.4082	1.811	7.183		
14	0.000156	20734.03	132.576			2.4231	1.822	7.650		
15	0.000158	19794.43	125.66	123.06	9.705905	1.9983	1.503	7.250	7.100	0.560

Appendix F: Microscopy Pre-Experiment Images

Sample 1 - Side 1
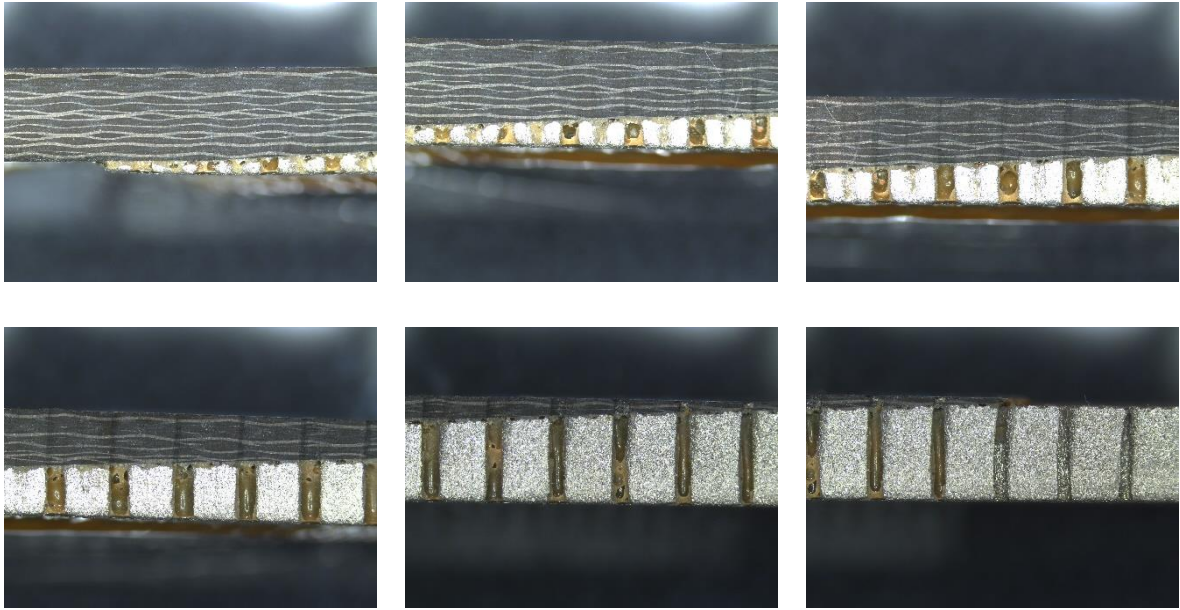
Sample 1 - Side 2
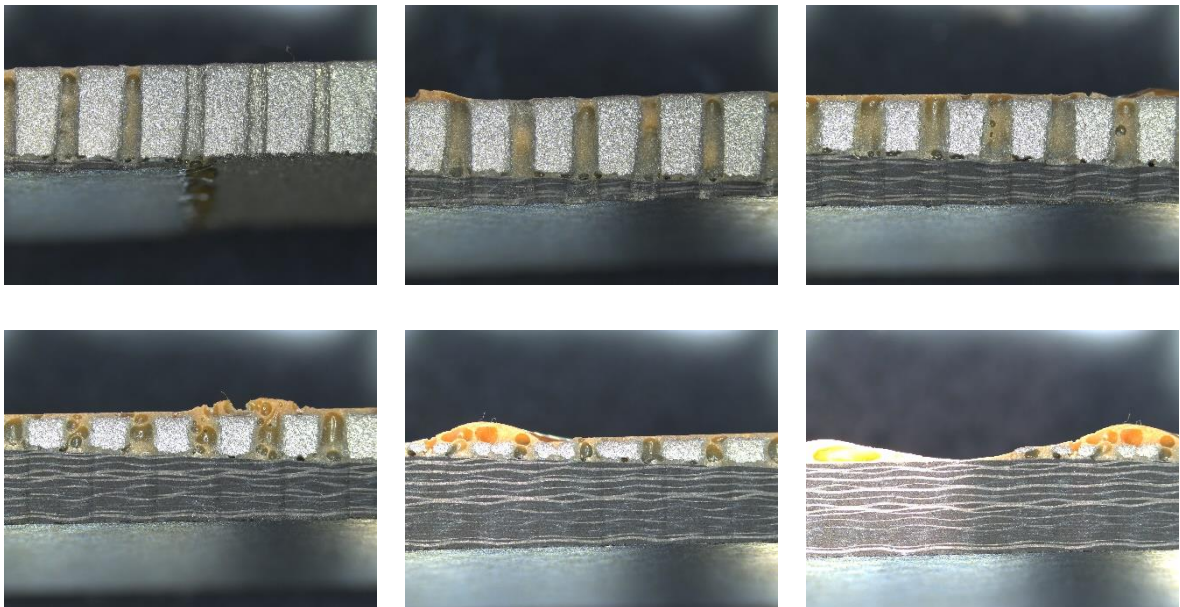
Sample 2 - Side 1
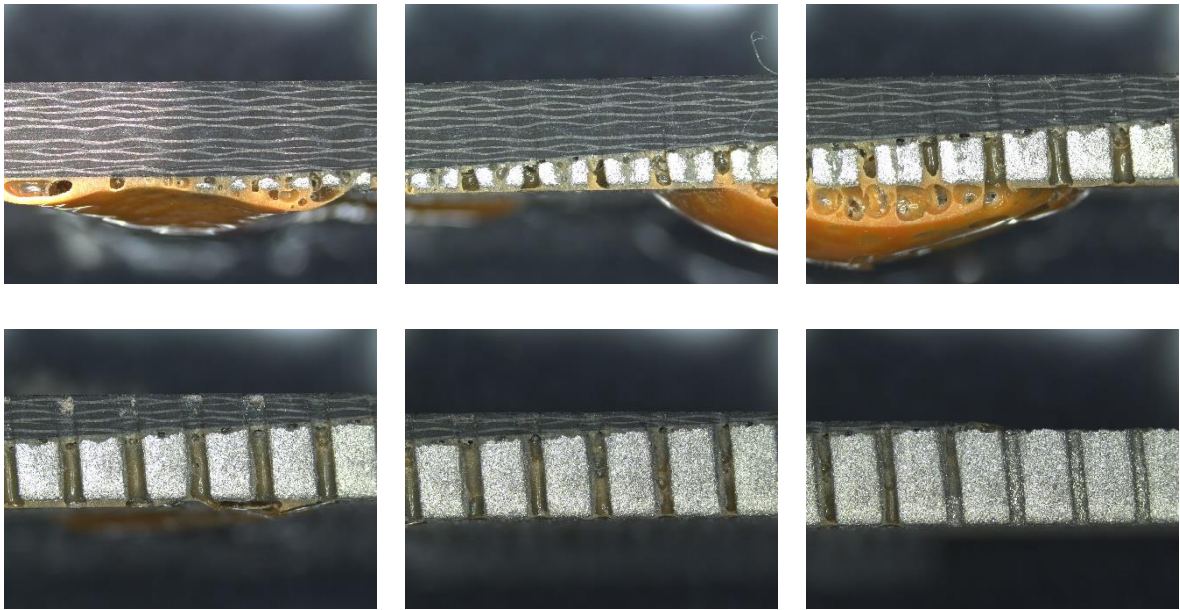
Sample 2 - Side 2
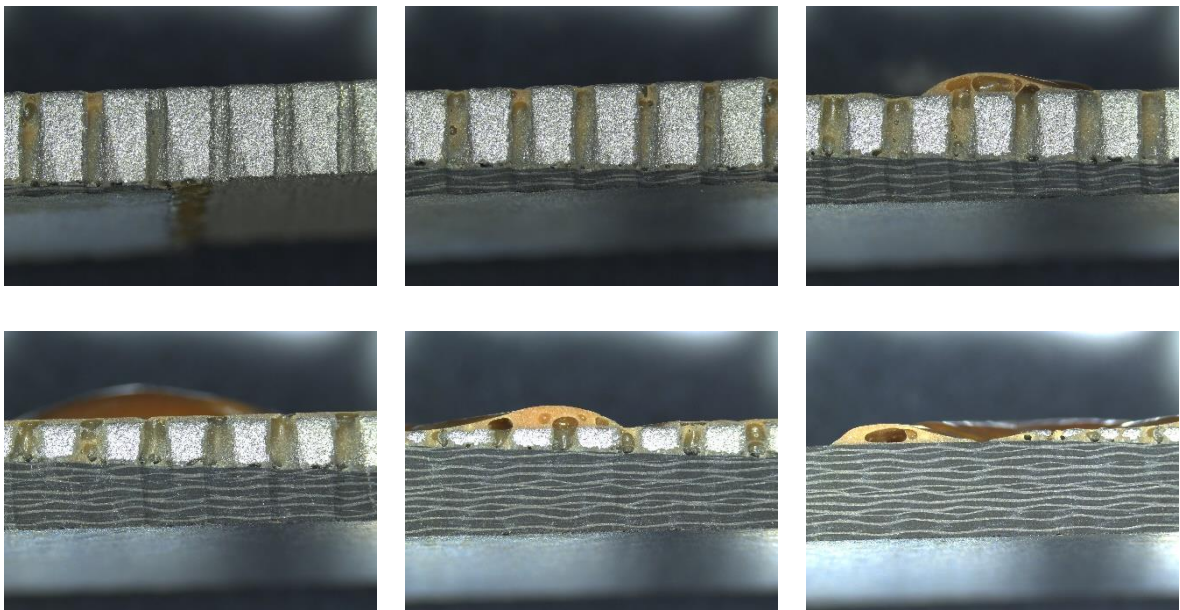
Sample 3 - Side 1
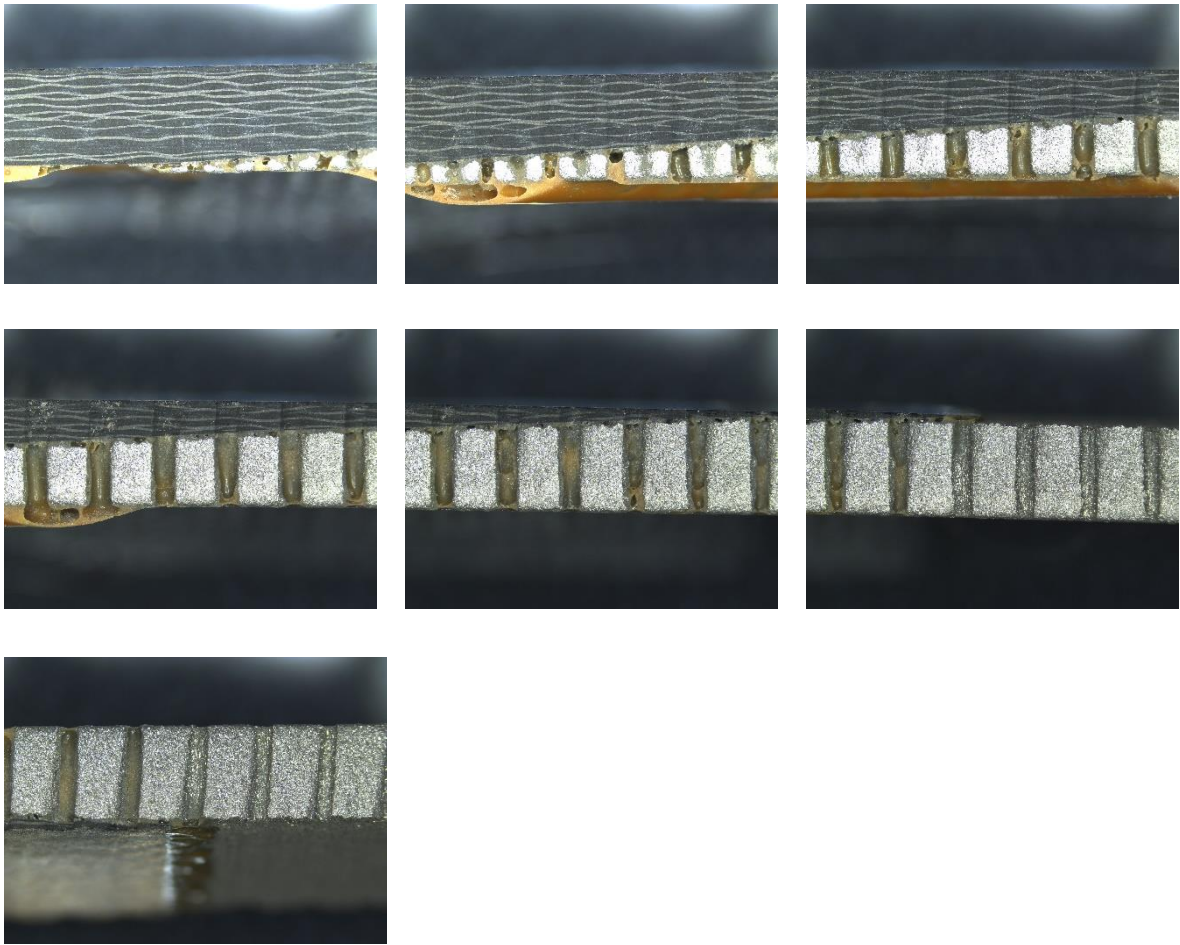
Sample 3 - Side 2
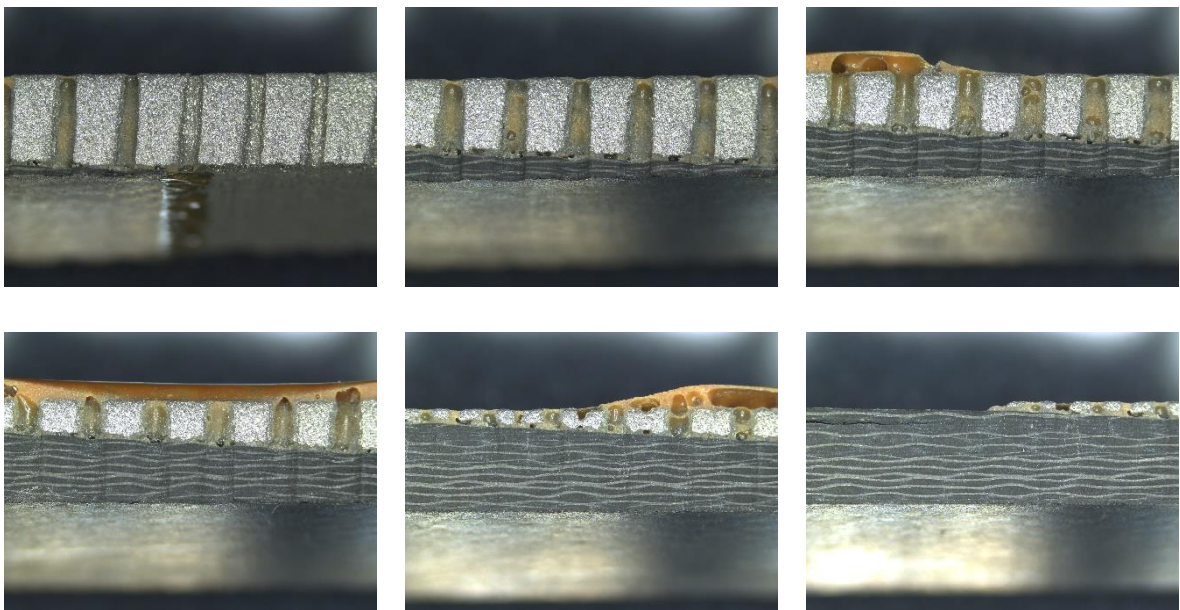
Sample 4 - Side 1
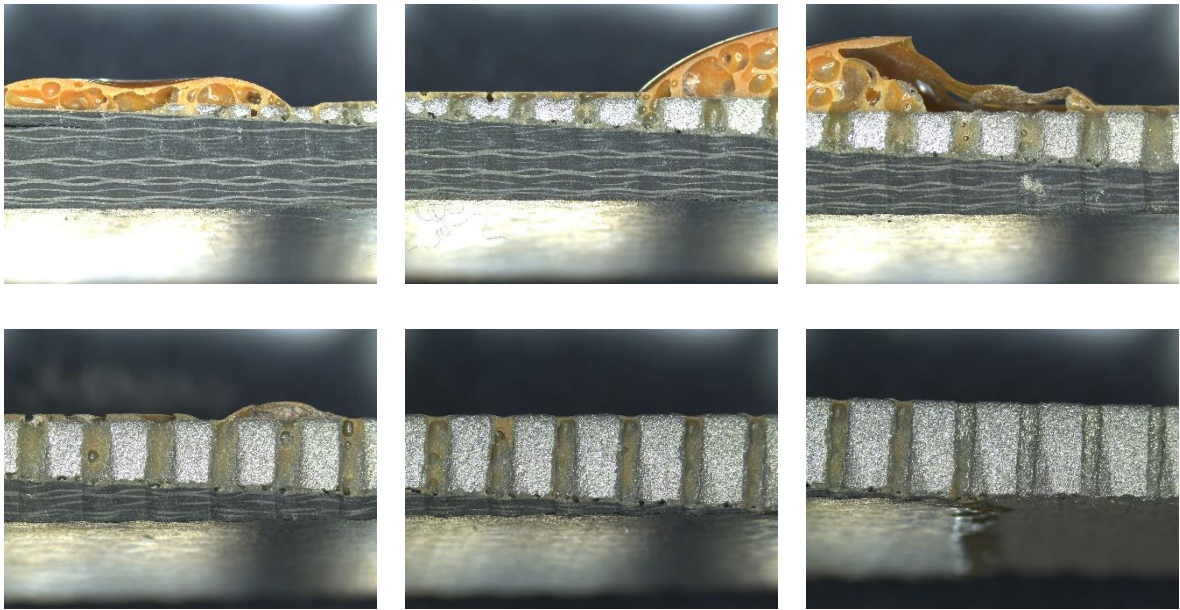
Sample 4 - Side 2
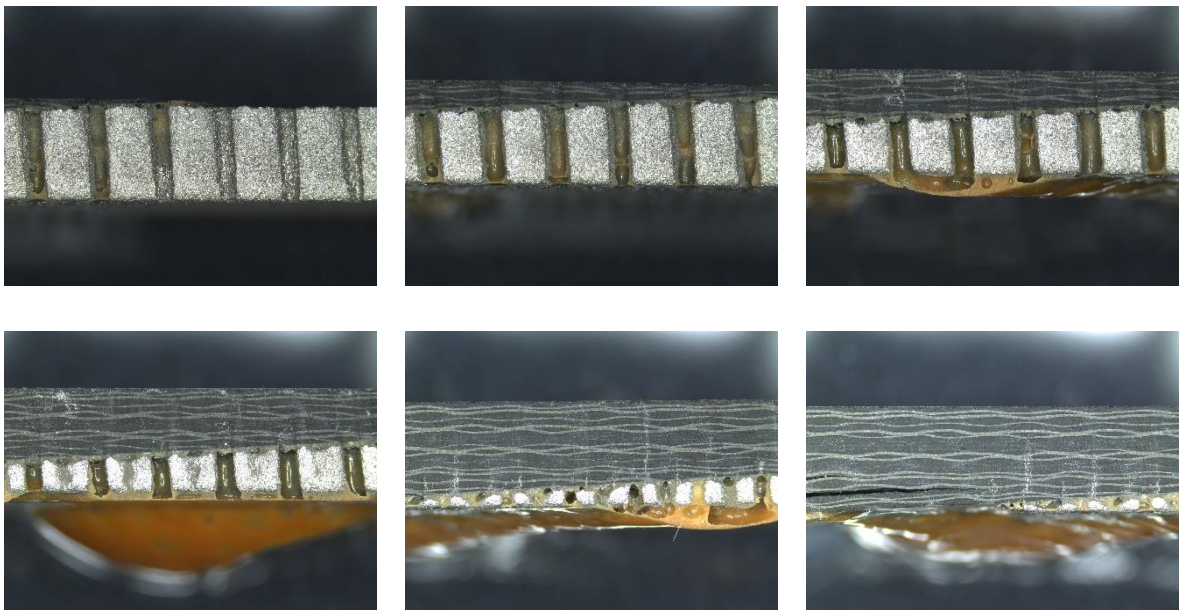
Sample 5 - Side 1
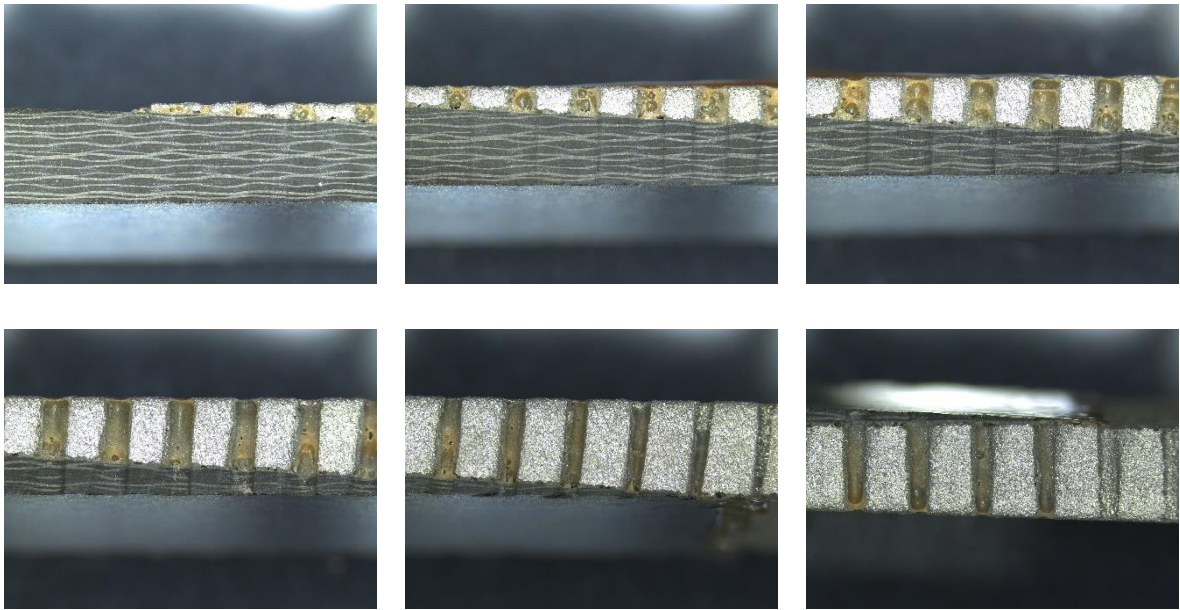
Sample 5 - Side 2
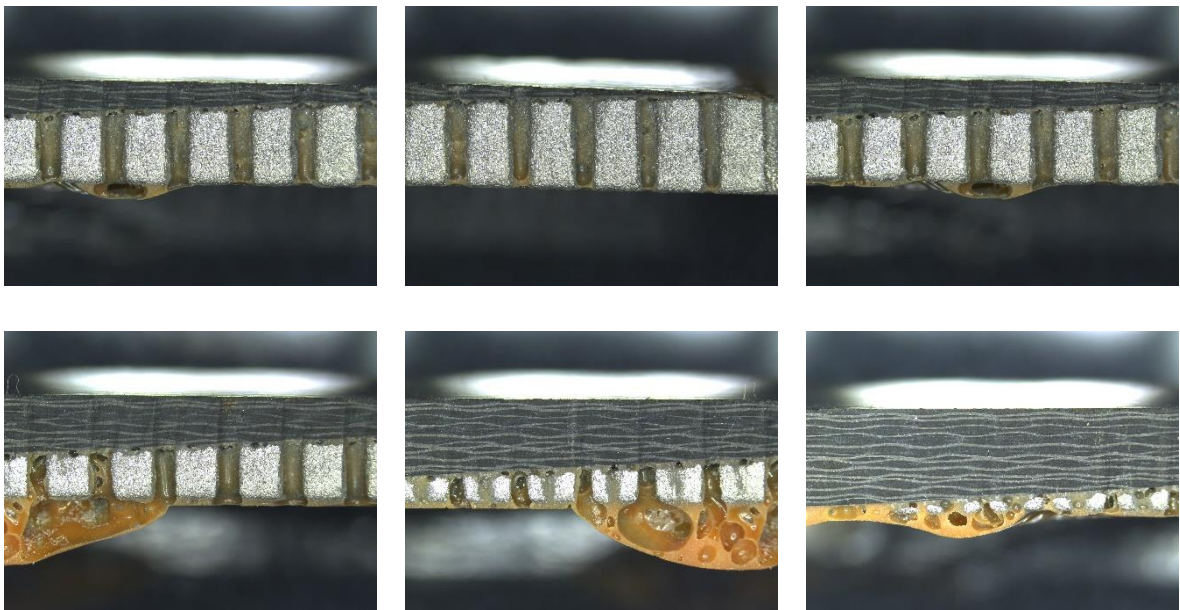
Sample 6 - Side 1
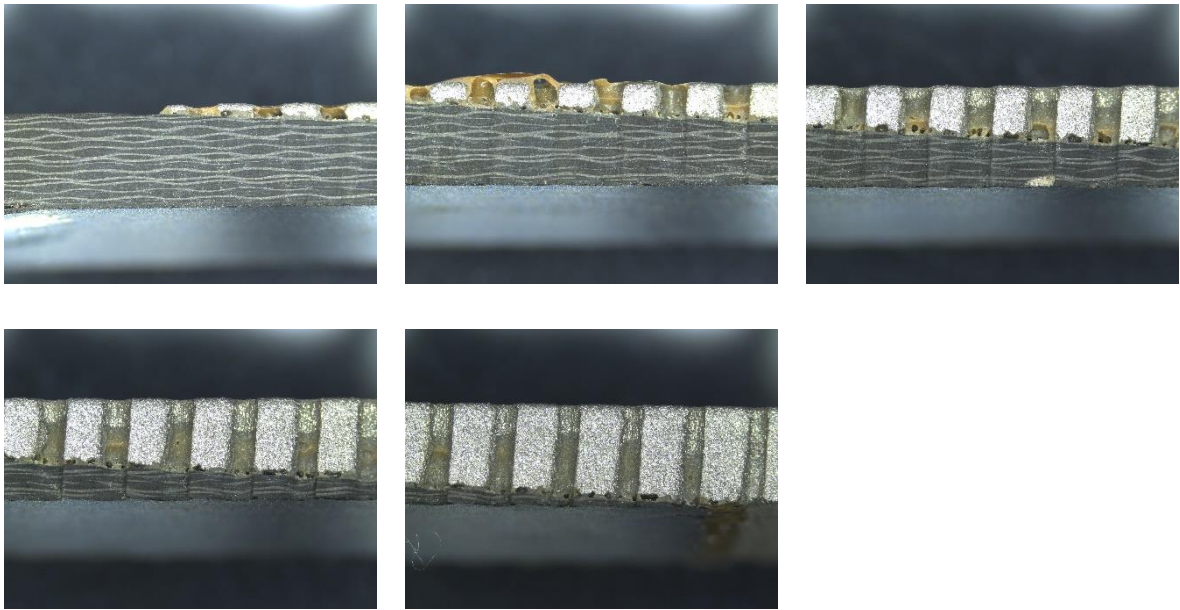
Sample 6 - Side 2
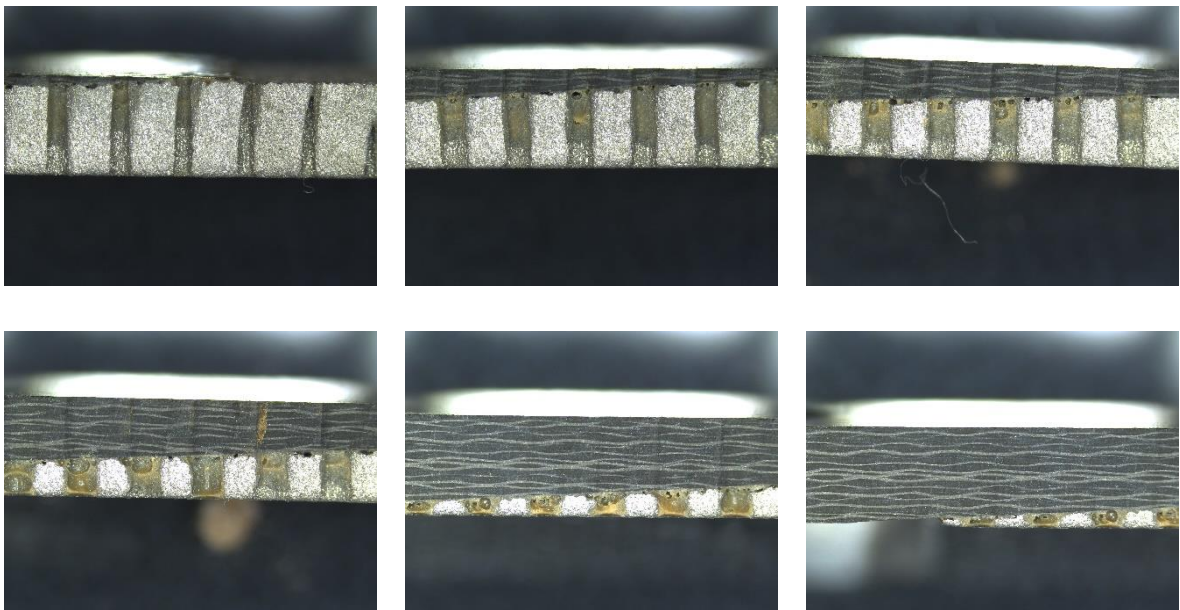
Sample 7 - Side 1
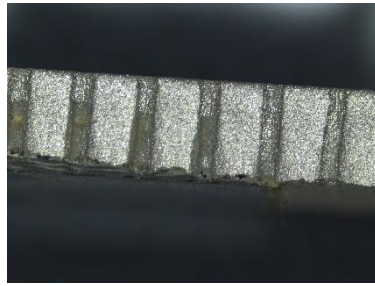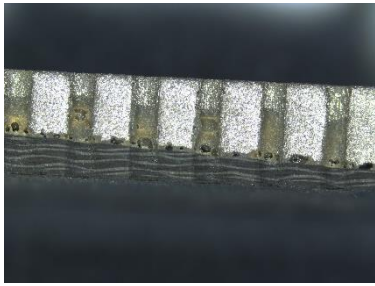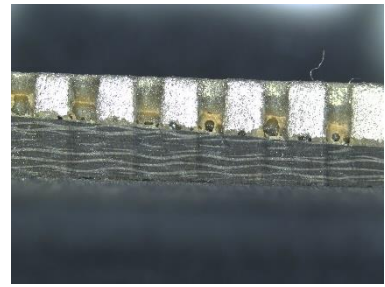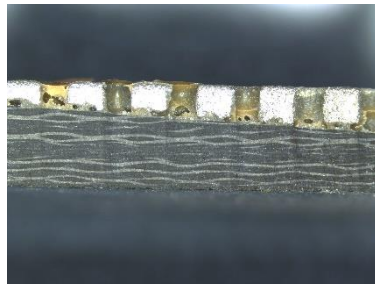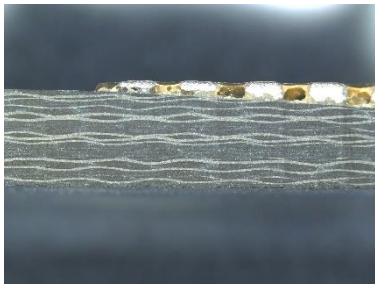
Sample 7 - Side 2
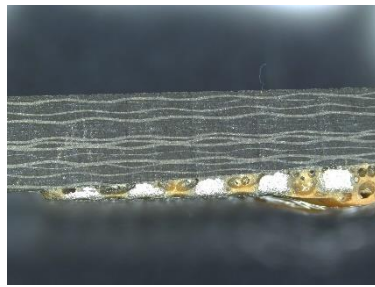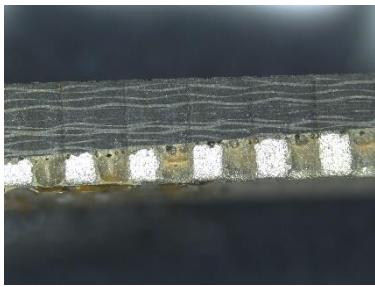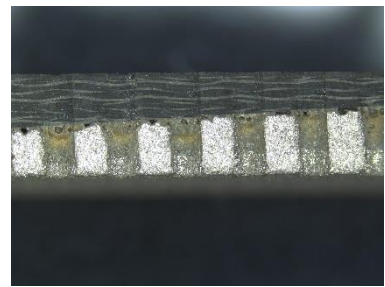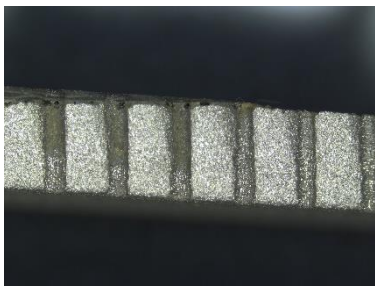
Sample 8 - Side 1
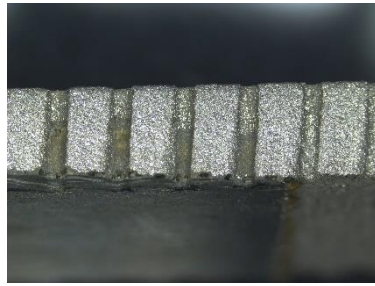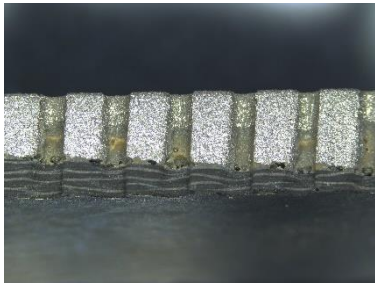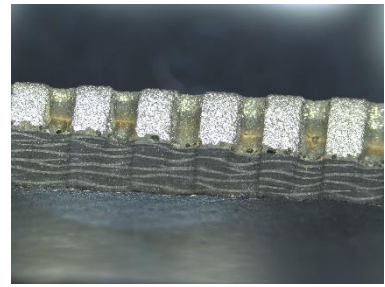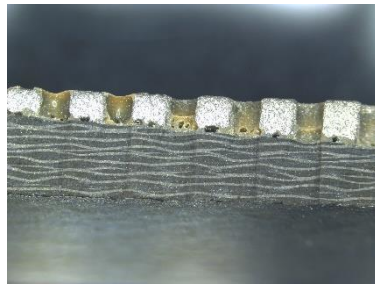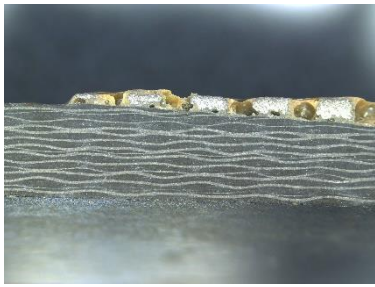
Sample 8 - Side 2
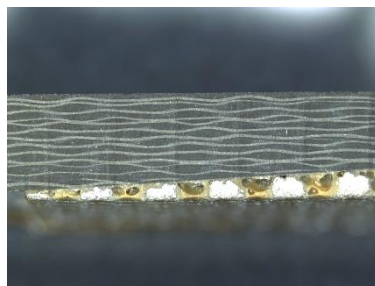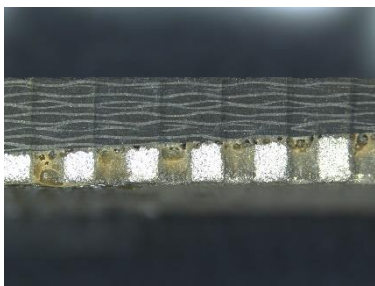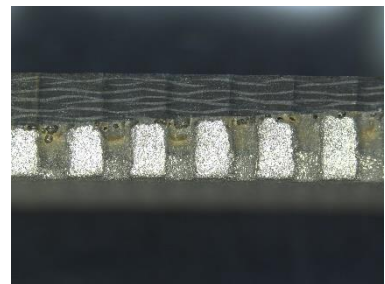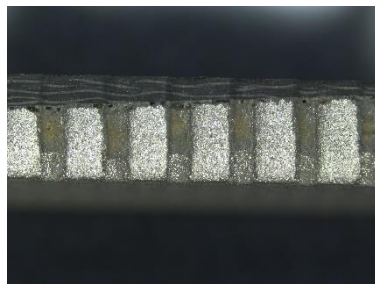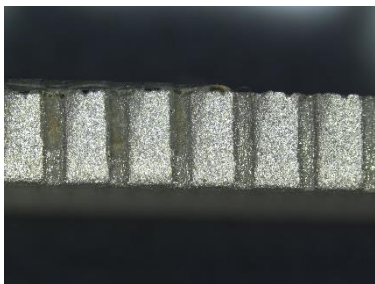
Sample 9 - Side 1
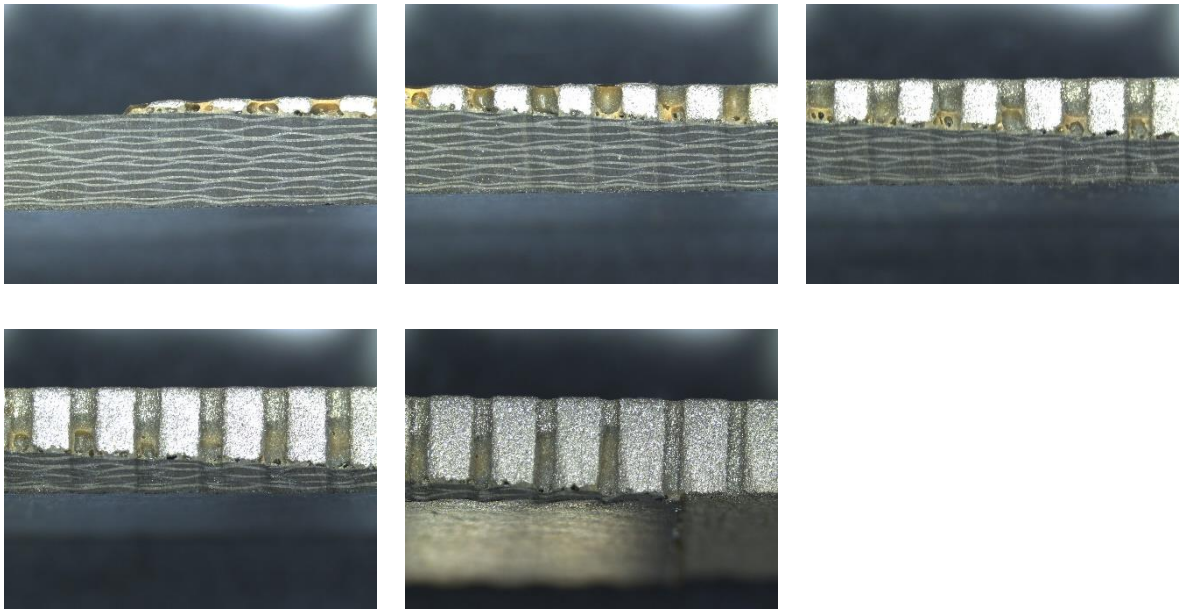
Sample 9 - Side 2
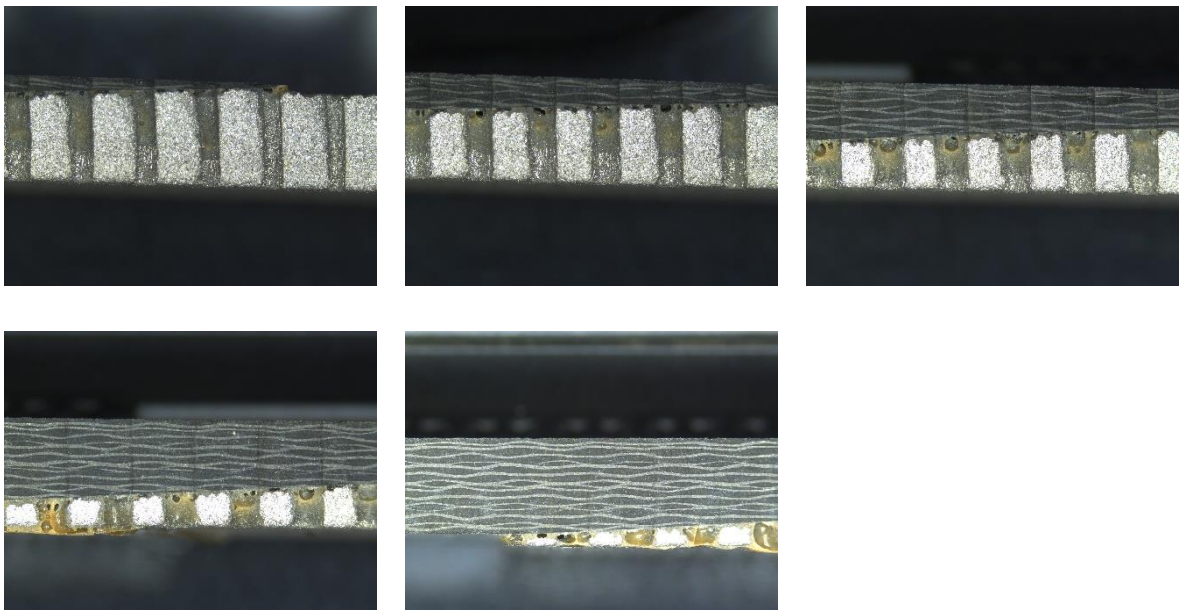
Sample 10 - Side 1
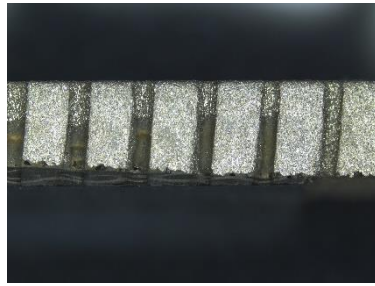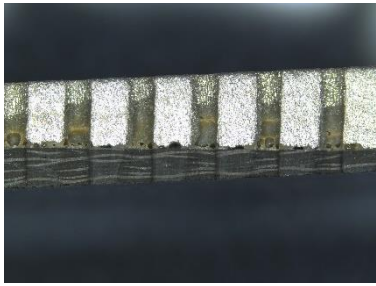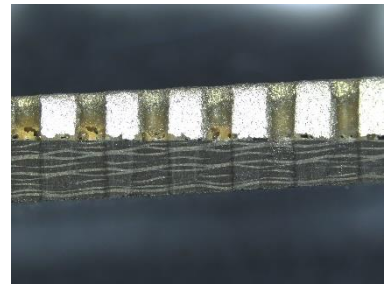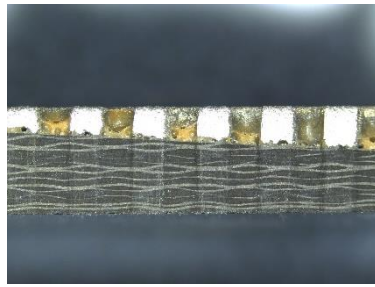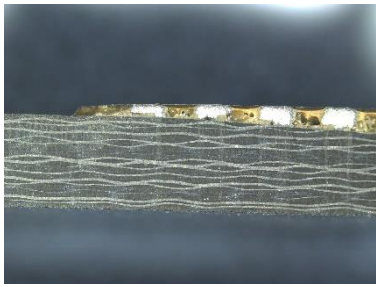
Sample 10 - Side 2
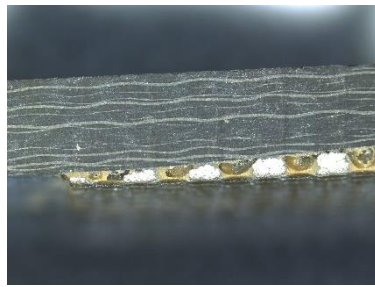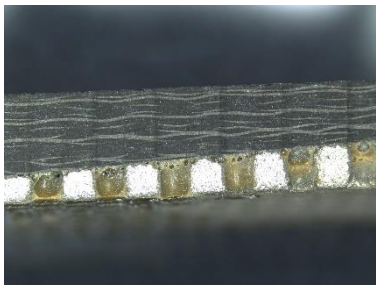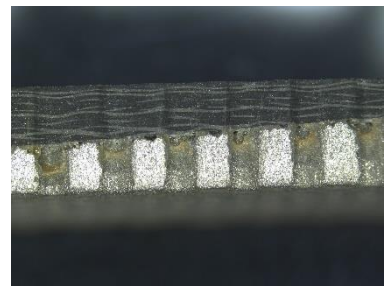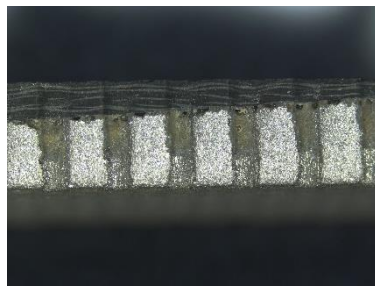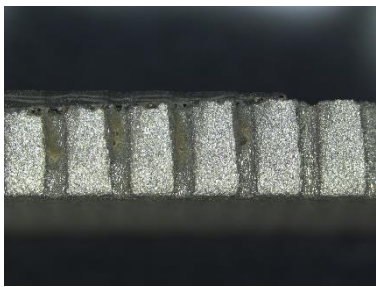
Sample 11 - Side 1
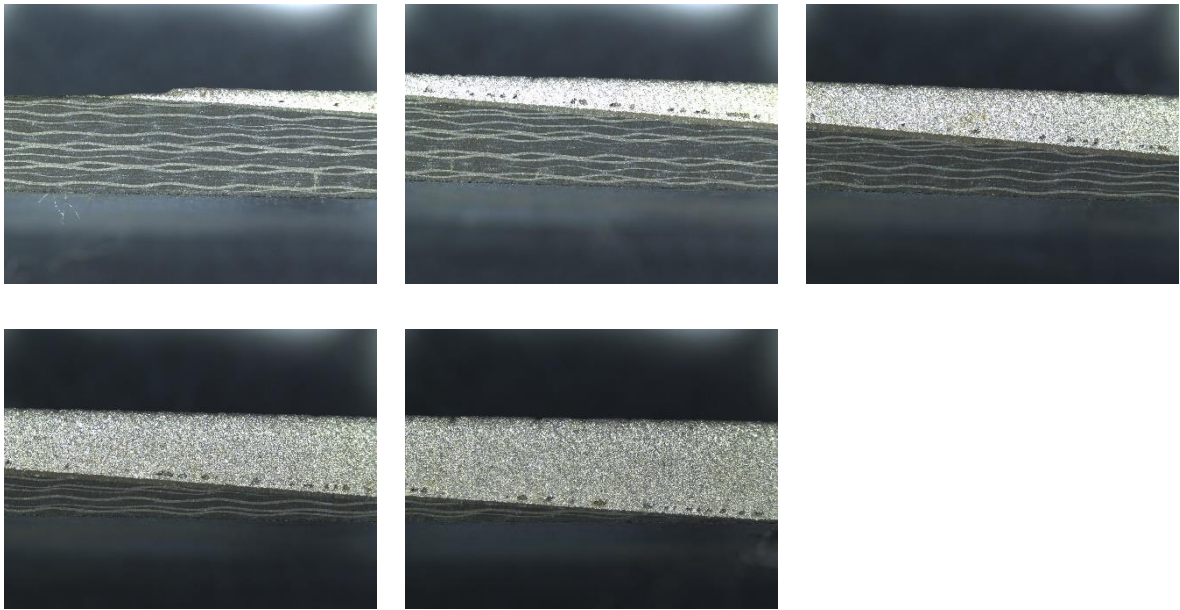
Sample 11 - Side 2
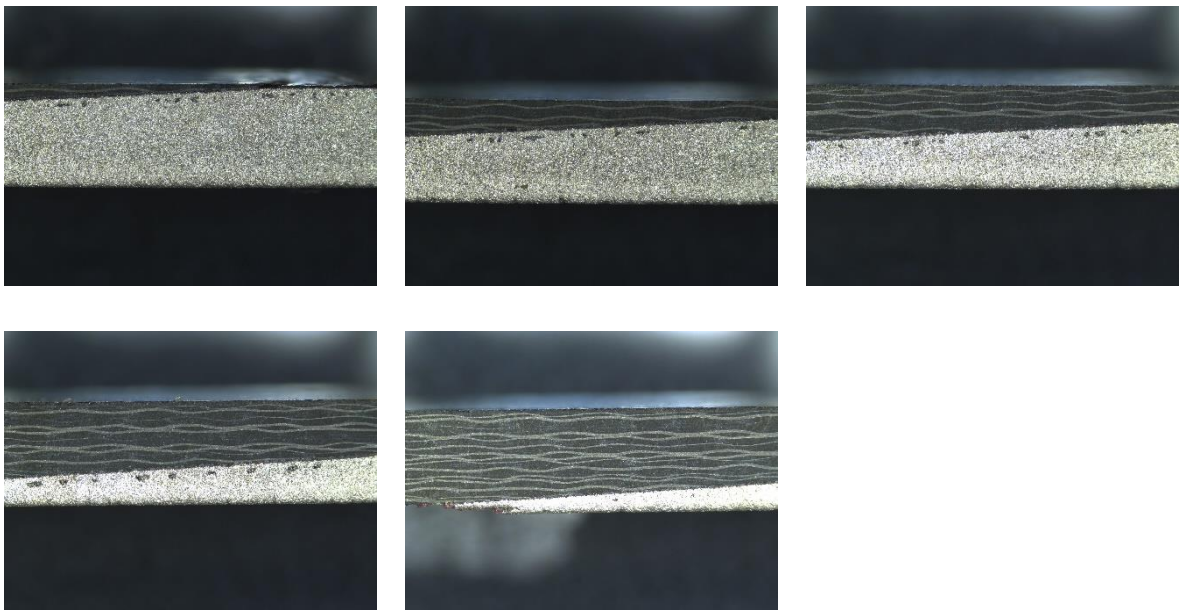
Sample 12 - Side 1
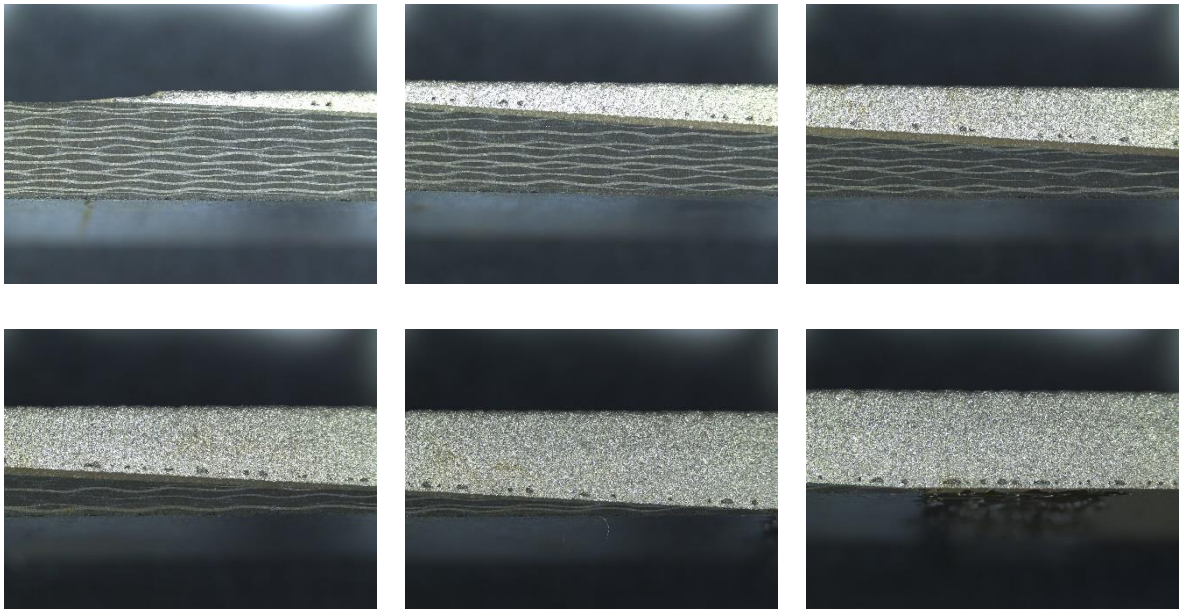
Sample 12 - Side 2
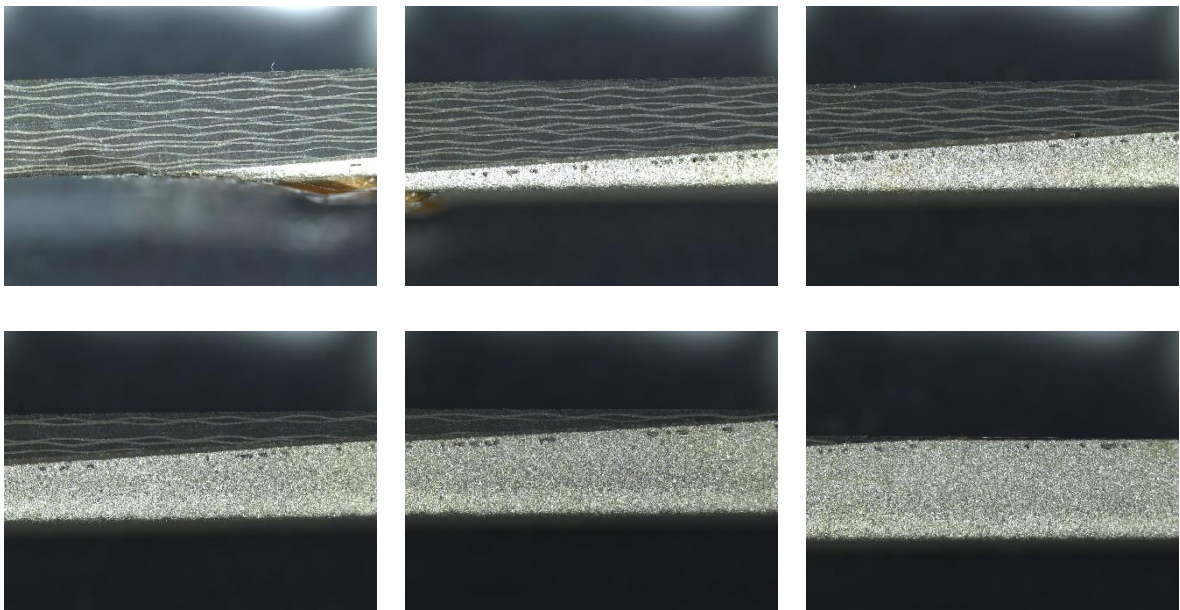
Sample 13 - Side 1
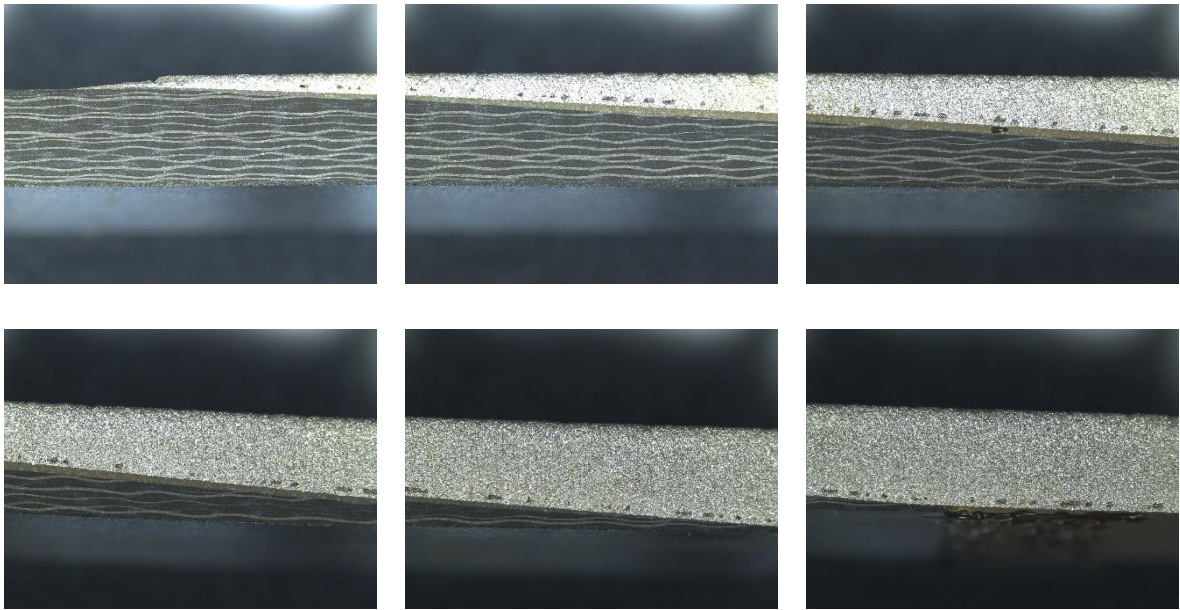
Sample 13 - Side 2
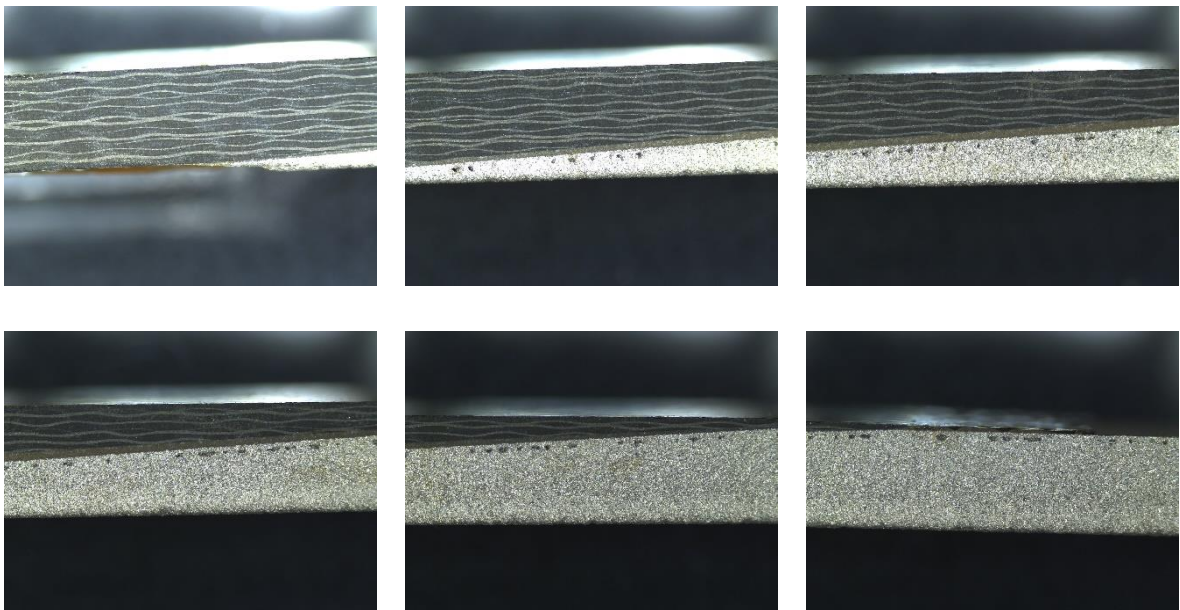
Sample 14 - Side 1
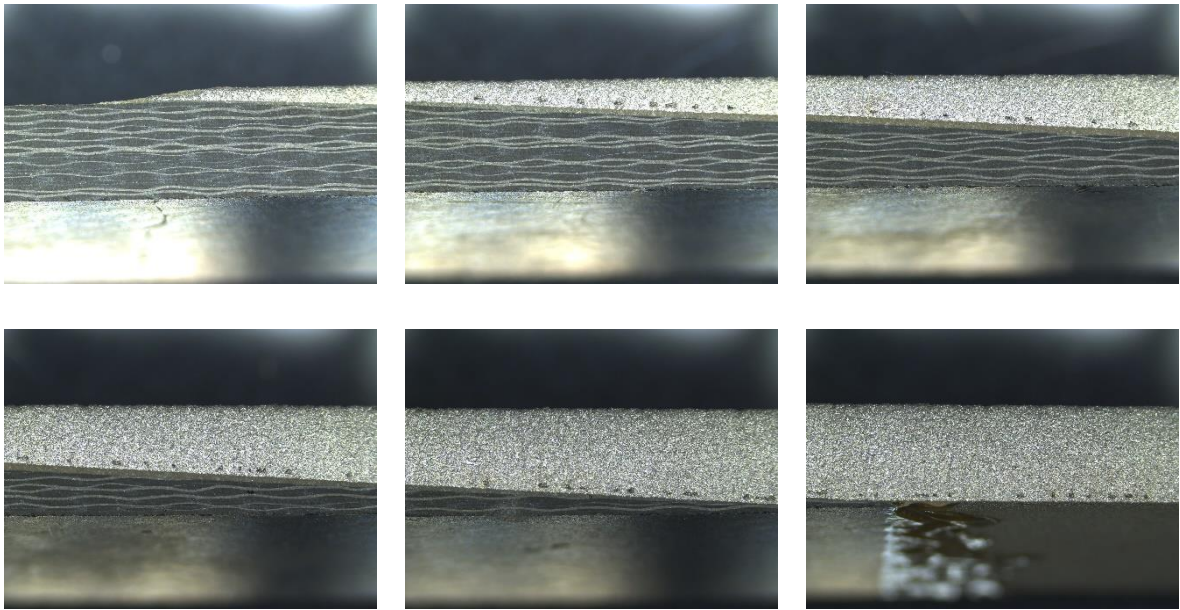
Sample 14 - Side 2
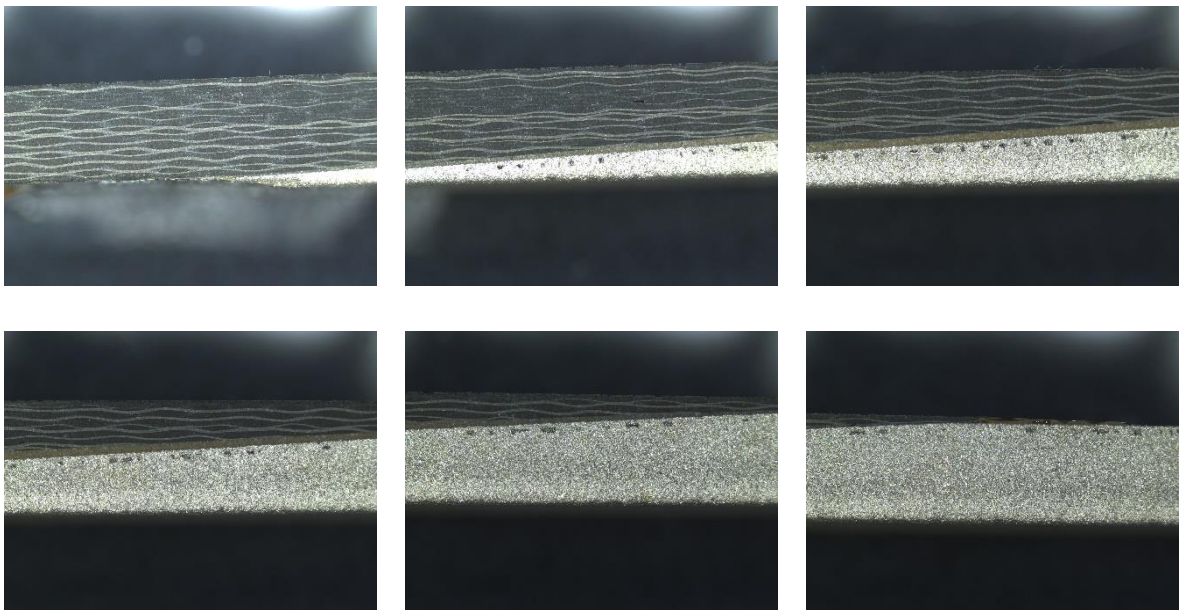
Sample 15 - Side 1
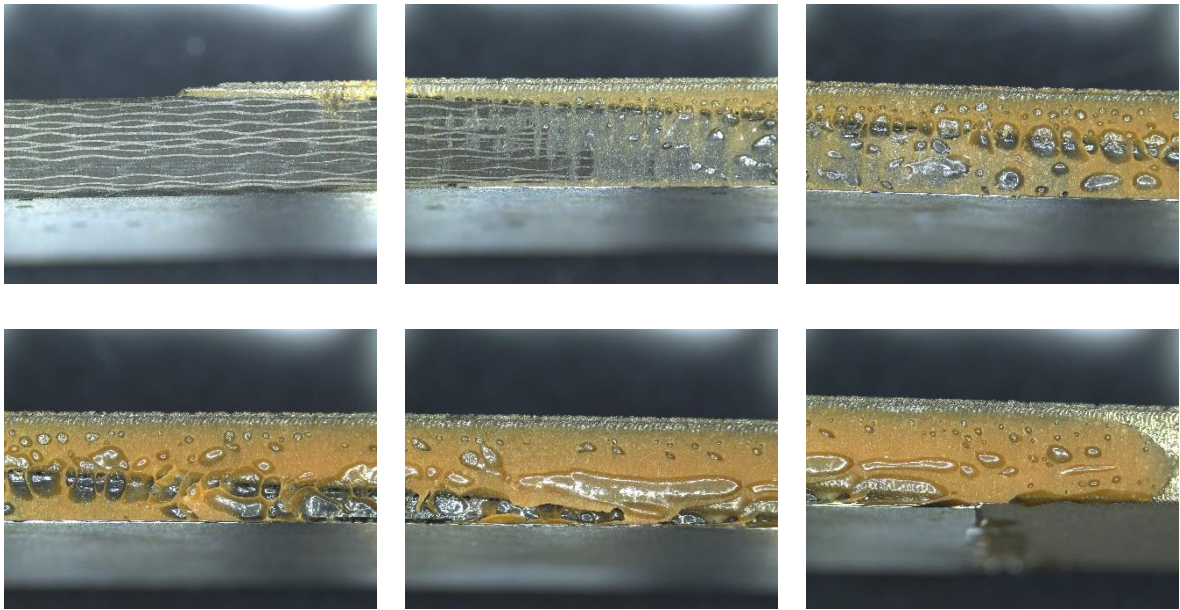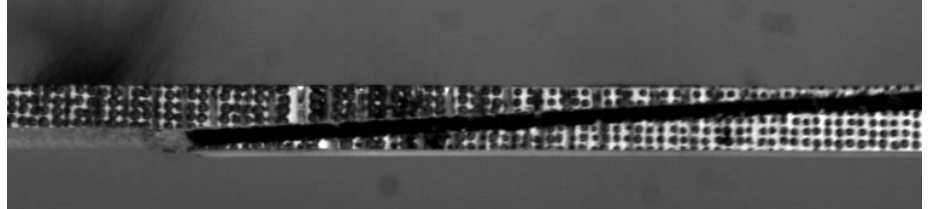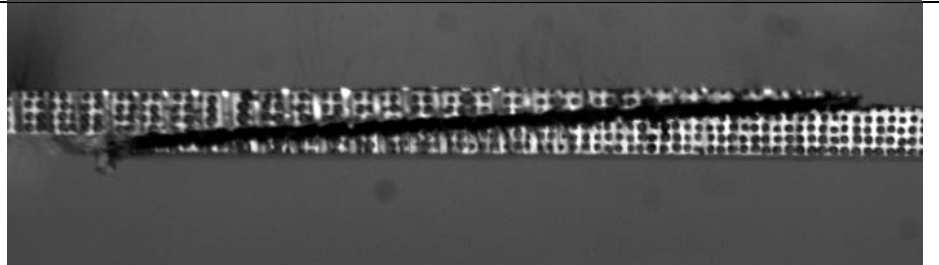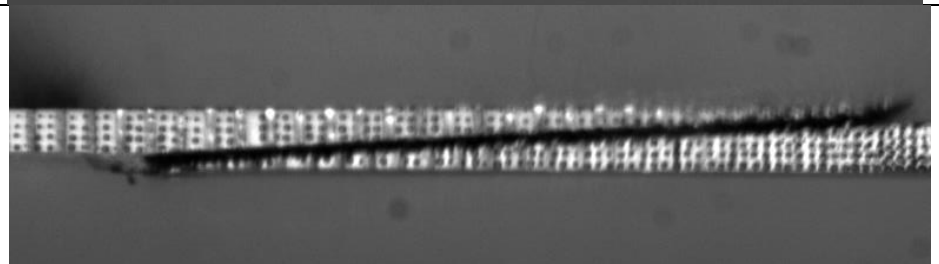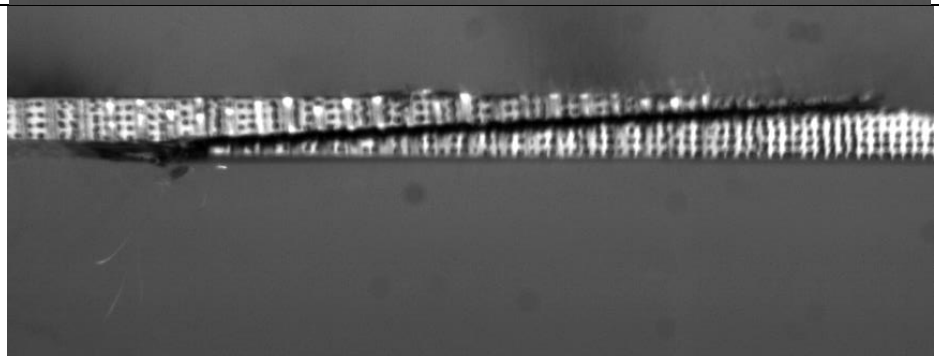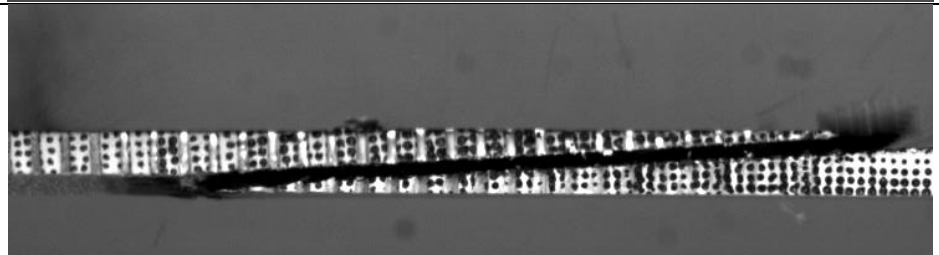
Sample 15 - Side 2
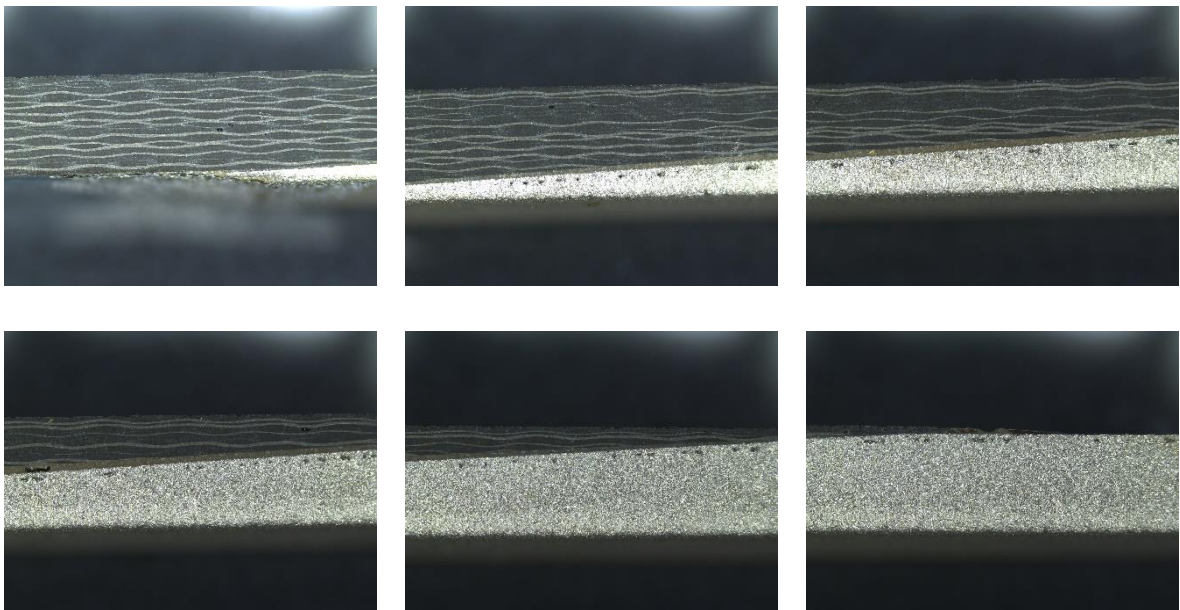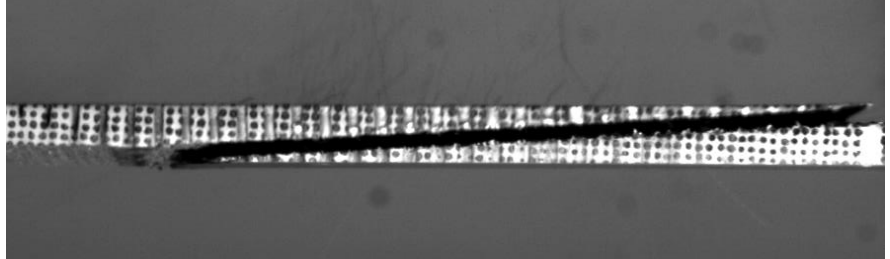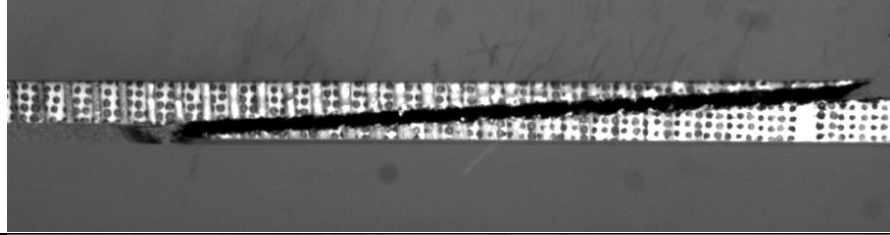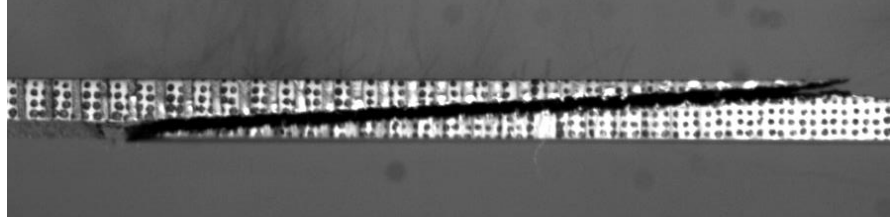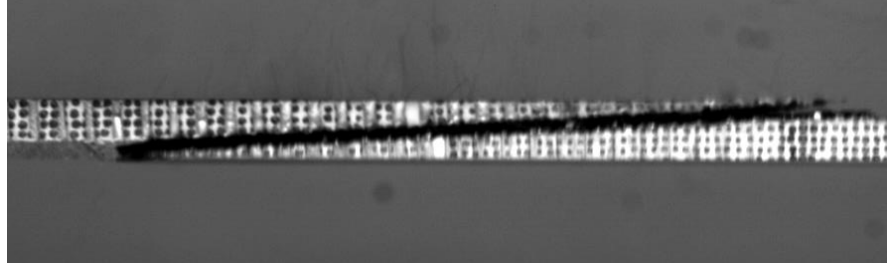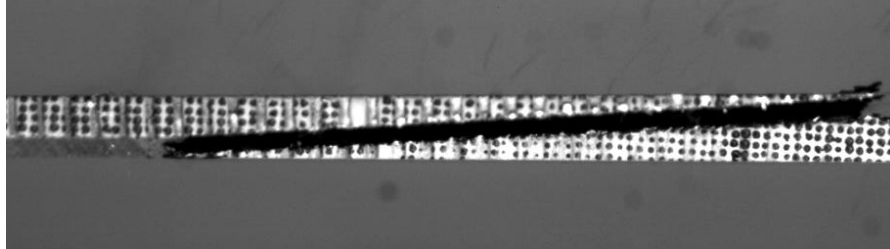
Appendix G: DIC Feature Frame Images
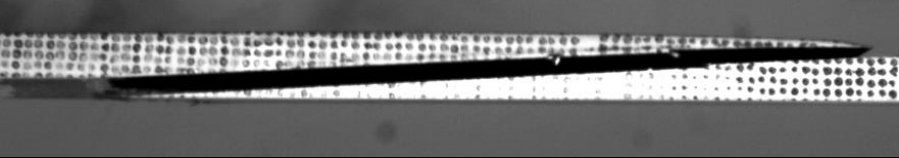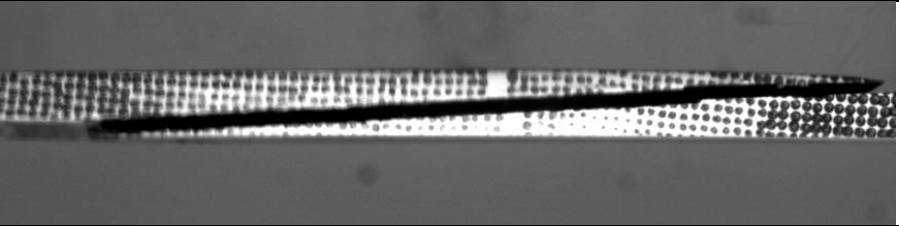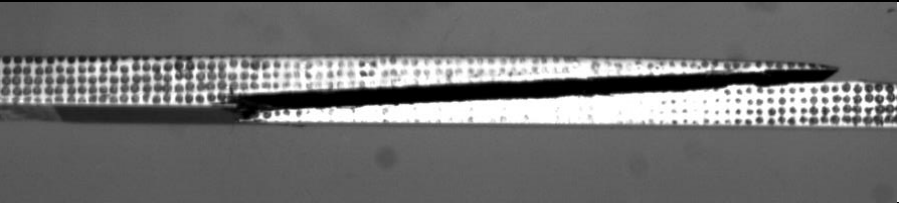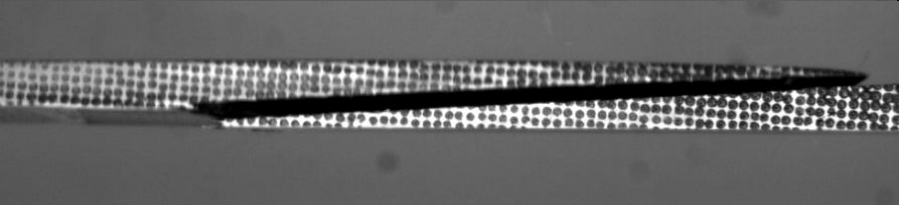
Double Film Adhesive Honeycomb Lattice Scarf Samples

Sample 1	
Sample 2	
Sample 3	
Sample 4	
Sample 5	

Single Film Adhesive Honeycomb Lattice Scarf Samples
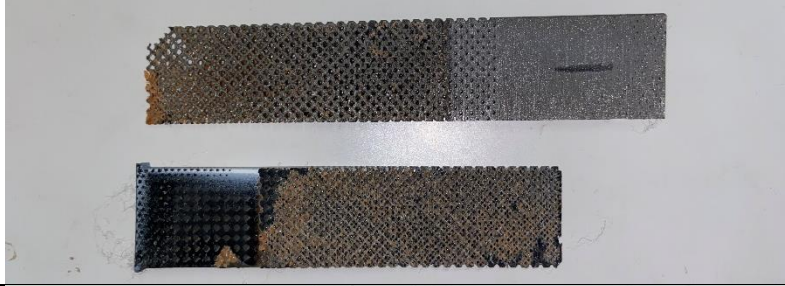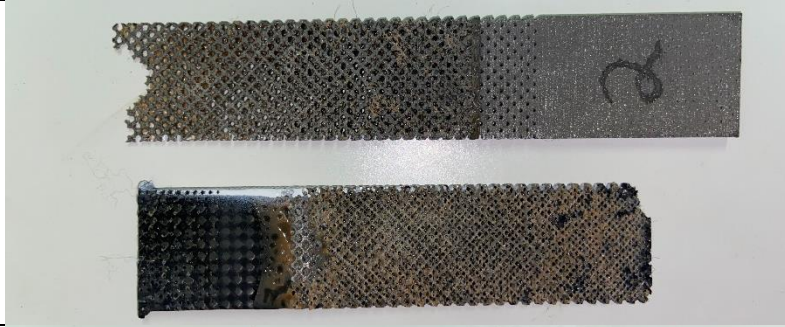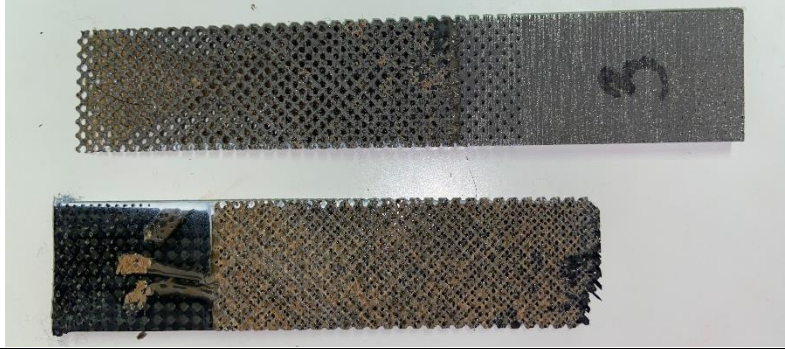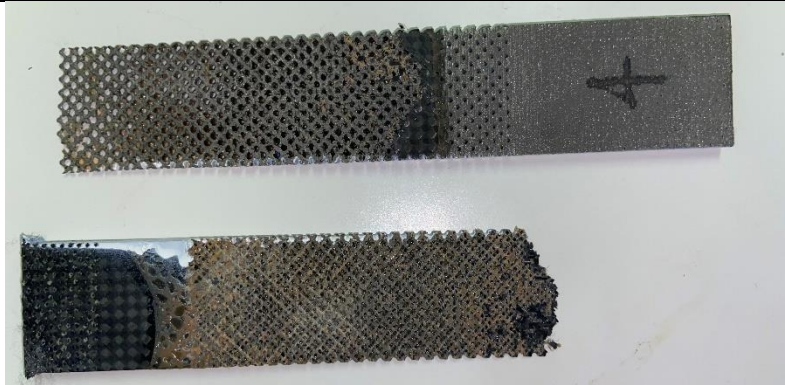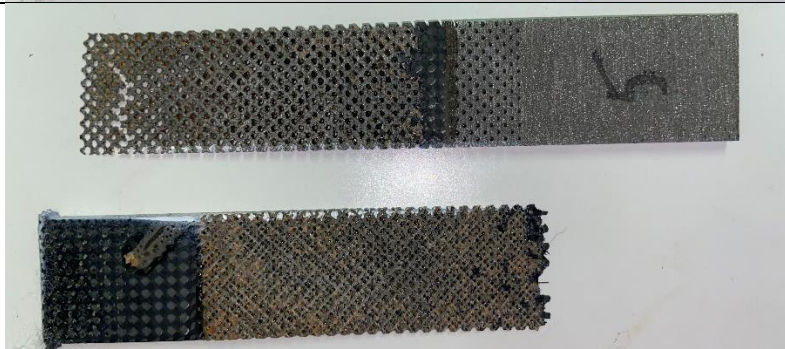
Sample 6	
Sample 7	
Sample 8	
Sample 9	
Sample 10	

Single Film Adhesive Solid Scarf Samples
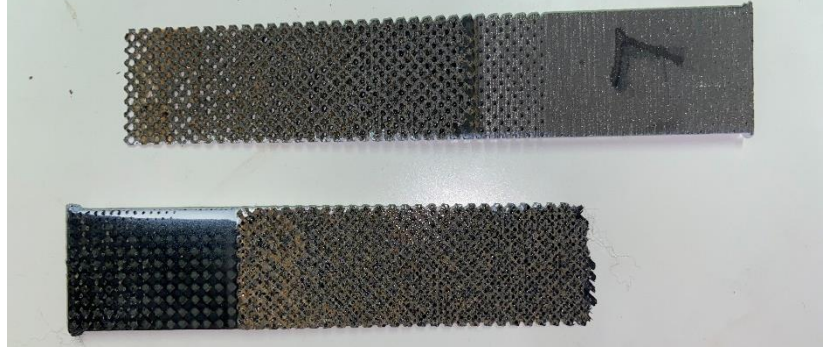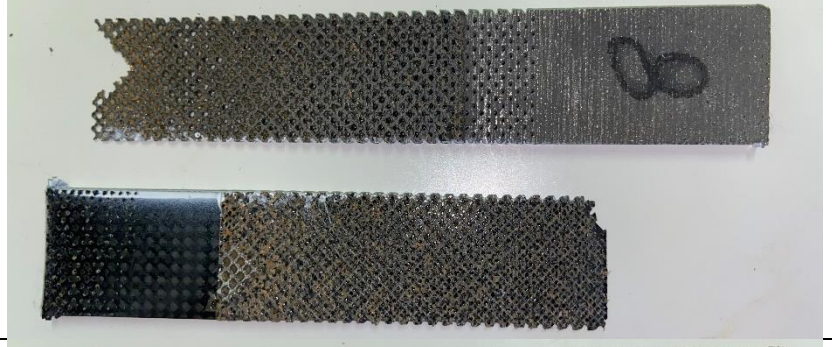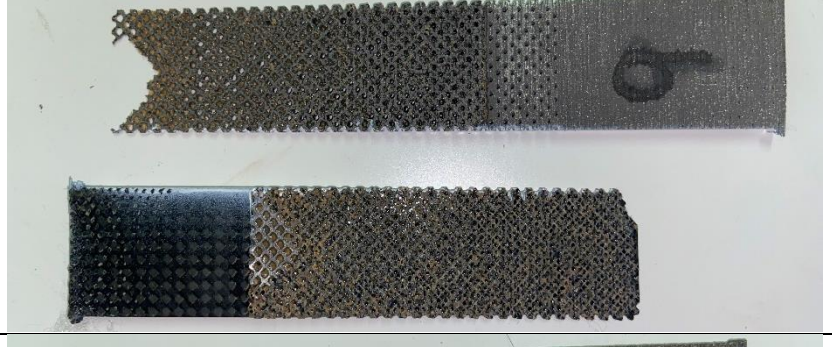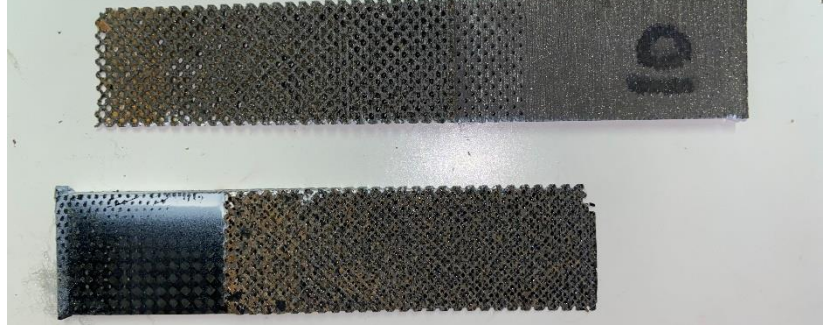
Sample 11	Premature Failure
Sample 12	
Sample 13	
Sample 14	
Sample 15	

Appendix H: Failure Mechanisms Images
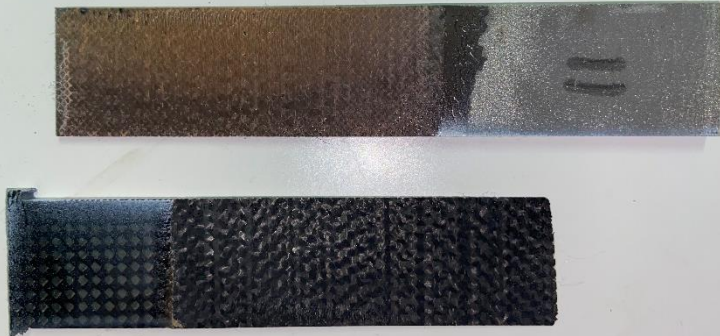
Double Film Adhesive Honeycomb Lattice Scarf Samples

Sample 1	
Sample 2	
Sample 3	
Sample 4	
Sample 5	

Single Film Adhesive Honeycomb Lattice Scarf Samples

Sample 6	
Sample 7	
Sample 8	
Sample 9	
Sample 10	

Single Film Adhesive Solid Scarf Samples

Sample 11	
Sample 12	
Sample 13	
Sample 14	
Sample 15	

Appendix I: Superfluous Workspace Images